Universidade de Aveiro
Ano 2017
Departamento de Química

CLÁUDIA FILIPA DE OLIVEIRA GOMES

Implementação de métodos biomoleculares para explorar o modo de ação do Exo-Wound *in vitro*

Implementation of biomolecular methods to explore the mode of action of Exo-Wound *in vitro*

Universidade de Aveiro
Ano 2017

Departamento de Química

CLÁUDIA FILIPA DE OLIVEIRA GOMES

Implementação de métodos biomoleculares para explorar o modo de ação do Exo-Wound *in vitro*

Implementation of biomolecular methods to explore the mode of action of Exo-Wound *in vitro*

Dissertação apresentada à Universidade de Aveiro para cumprimento dos requisitos necessários à obtenção do grau de Mestre em Bioquímica, ramo de Métodos Biomoleculares, realizada sob a orientação científica da Doutora Joana Rita Simões Correia, Administradora e Coordenadora Científica da empresa *Exogenus Therapeutics*, e do Doutor Valdemar Inocêncio Esteves, Professor do Departamento de Química da Universidade de Aveiro

“It always seems impossible until it’s done.”
Nelson Mandela

o júri

Presidente

Prof. Doutor Pedro Miguel Dimas Neves Domingues
Professor auxiliar com agregação do Departamento de Química da Universidade de Aveiro

Doutora Joana Rita Simões Correia
Administradora e Coordenadora Científica da empresa Exogenus Therapeutics

Doutor Mário Martins Rodrigues Grãos
Investigador do Centro de Neurociências e Biologia Celular da Universidade de Coimbra

Agradecimentos

À minha orientadora, Doutora Joana Correia, pela confiança depositada em mim que possibilitou não só o desenvolvimento deste trabalho, mas também a aquisição de experiências verdadeiramente enriquecedoras. Agradecer principalmente pela disponibilidade e motivação, pelo olhar crítico e interessado, e por todos os conhecimentos transmitidos, que irão certamente acompanhar-me ao longo desta minha caminhada.

Ao meu orientador, Doutor Valdemar Esteves, por ter aceite este desafio e por ter demostrado um constante interesse no trabalho desenvolvido e disponibilidade para solucionar qualquer problema.

Ao Filipe Duarte, por todo o conhecimento partilhado durante este ano e principalmente pela paciência, motivação e conselhos transmitidos.

Ao Renato Cardoso, pelas críticas construtivas e por todo o incentivo demostrado.

À Sílvia Rodrigues, por ter acompanhado de perto esta jornada, pelo incansável apoio, e pela constante partilha de opiniões, mostrando sempre uma visão positiva.

À Inês Coelho, pelo constante apoio, ânimo e carinho demostrados ao longo desta jornada.

Ao grupo Exo-Lab pela imensa boa disposição e pelo ótimo ambiente de trabalho, transformando frustrações em aprendizagens, que certamente não esquecerei.

À Luísa Marques, pela oportunidade, pelo interesse e incentivo transmitidos durante a realização deste trabalho.

À Inês Caramelo, pela amizade, pelos desabafos e pelas viagens partilhadas entre Aveiro e Cantanhede.

À Família Grega, à Diana, à Bárbara, à Elisabeth, à Raquel, à Luísa, à Rosa, ao Fábio e à Sofia, pela companhia, brincadeira e amizade que coloriram as chegadas a casa depois de dias intensos e cansativos.

À Bárbara Macedo, por me ter acompanhado durante todo o percurso académico, por todo o apoio e pela amizade sincera.

À Beatriz Ribau, pelas brincadeiras e parvoíces, pelos momentos sérios e sobretudo pelo ombro amigo.

À Catarina Ferreira, por ter incentivado grande parte das aventuras vividas nestes cinco anos, pela amizade e pelas experiências partilhadas.

À Sara Moura, pelas viagens e concelhos partilhados, por todo apoio, motivação e pela amizade incondicional.

Ao Bruno Silva, pela imensa paciência, pela colaboração na elaboração das imagens deste trabalho, por me ter incentivado nos momentos mais difíceis, e por estar sempre pronto para celebrar mais uma vitória.

À Exogenus Therapeutics, pela oportunidade e por proporcionar as condições necessárias à realização deste trabalho.

À cidade e à Universidade de Aveiro, por me terem acolhido nestes cinco anos de vida académica.

A todos os meus familiares, pelo constante apoio e interesse.

Ao meu irmão, pelas palermices, brincadeiras e conversas sérias, e por me mostrar que tudo é possível.

Aos meus pais, por me terem acompanhado desde sempre, por me terem apoiado incondicionalmente, pela enorme paciência, e por serem os principais impulsionadores de todas as conquistas alcançadas ao longo de todas as jornadas.

A todos, um enorme e sincero Obrigada!

palavras-chave

Cicatrização; Fatores de Crescimento; Feridas da pele; Imunocitoquímica; Matriz Extracelular; Modo de Ação; PCR quantitativo; *Western Blot*.

Resumo

Este trabalho descreve e apoia cientificamente as atividades realizadas durante o estágio de mestrado na *Exogenus Therapeutics*. Esta empresa portuguesa possui um produto biológico em desenvolvimento, *Exo-Wound*, que mostrou acelerar o processo de cicatrização de feridas, estimulando a regeneração da pele. Porém, os mecanismos implícitos aos efeitos benéficos exercidos pela sua substância ativa permanecem parcialmente desconhecidos. Neste contexto, uma das hipóteses de seu modo de ação está relacionada com a modulação da produção de proteínas de matriz extracelular e produção de fatores de crescimento por células da pele, como fibroblastos e queratinócitos. Assim, a implementação e validação de métodos analíticos que permitam a avaliação da expressão e produção destas ou de outras biomoléculas é crucial para compreender o modo de ação deste produto. Esta dissertação de mestrado apresenta os passos realizados necessários à implementação e otimização de métodos biomoleculares, nomeadamente *Western Blot*, *Reverse Transcription Real-time Polymerase Chain Reaction* e Imunocitoquímica, no laboratório da *Exogenus Therapeutics.* Além disso, os resultados aqui apresentados mostram a validação preliminar destas metodologias para a avaliação da expressão e produção de proteínas da matriz extracelular e da expressão de fatores de crescimento por linhas celulares da pele, como fibroblastos e queratinócitos cultivados *in vitro*.

keywords

Wound Healing; Growth factors; Skin wounds; Immunocytochemistry, Extracellular Matrix; Mode of Action, Quantitative PCR; Western Blot

abstract

This work describes and scientifically supports the activities carried out during the master's degree at Exogenus Therapeutics. This Portuguese company has a biological product in development, Exo-Wound, which has shown to accelerate the healing process of wounds, stimulating the regeneration of the skin. However, the mechanisms governing skin regeneration and wound healing acceleration remain partially unknown. In this context, one of the hypotheses of its mode of action is related to the modulation of the production of extracellular matrix proteins and the production of growth factors by skin cells, such as fibroblasts and keratinocytes. Thus, the implementation and validation of analytical methods that allow the evaluation of the expression and production of these biomolecules or others is crucial to understanding the mode of action of this product. This master's thesis presents the steps required to implement and optimize biomolecular methods, namely Western Blot, Reverse Transcription Real-time Polymerase Chain Reaction and Immunocytochemistry, in the laboratory of Exogenus Therapeutics. In addition, the results presented here show the preliminary validation of these methodologies for the evaluation of the expression and production of extracellular matrix proteins and the expression of growth factors by skin cell lines, such as fibroblasts and keratinocytes cultured *in vitro*.

Index

Index of Figures

Index of Tables

List of acronyms and abbreviations

A	APS	Ammonium Persulfate
B	BSA	Bovine Serum Albumin
C	C1	Exo-101 Concentration of $2.5x10^9$ part/ml
	C2	Exo-101 Concentration of $5x10^9$ part/ml
	CM	Conditioned Medium
	Col1	Collagen I
	Col1a1	Collagen I α1-chain
	COL1A1	Gene to Collagen I α1-chain
	Col1a2	Collagen I α2-chain
	COL1A2	Gene to Collagen I α2-chain
	Col3	Collagen III
	Col3a1	Collagen III α1-chain
	COL3A1	Gene to Collagen III α1-chain
	C^T or C^q	Threshold Cycle or Quantification Cycle
D	DAPI	4',6-Diamidino-2-Phenylindole, Dihydrochloride
	DMEM	Dulbecco's Modified Eagle Medium
E	ECL	Enhanced Chemiluminescence Luminol
	ECM	Extracellular Matrix
	EGF	Epidermal Growth Factor
	EGFR	Epidermal Growth Factor Receptor
	ELISA	Enzyme-Linked Immunosorbent Assay
F	FBS	Fetal Bovine Serum
	FGF	Fibroblast Growth Factor
	Fn	Fibronectin
	FNI	Fibronectin type I repeat
	FNII	Fibronectin type II repeat
	FNIII	Fibronectin type III repeat
G	GAG	Glycosaminoglycan
	GF	Growth Factor
H	HA	Hyaluronic Acid
	HRP	Horseradish Peroxidase

I	ICC	Immunocytochemistry
	IGF	Insulin-like Growth Factor
	IL	Interleukin
	IL-R	Interleukin Receptor
K	KGF	Keratinocyte Growth Factor
M	MFI	Mean Fluorescence Intensity
	MMP	Matrix Metalloproteinases
	MW	Molecular Weight
N	NHDF	Normal Human Dermal Fibroblasts
	NHEK	Normal Human Epidermal Keratinocytes
P	PBS	Phosphate-buffered Saline
	PDGF	Platelet-derived Growth Factor
	PFA	Paraformaldehyde
	PG	Proteoglycan
	PVDF	Polyvinylidene Fluoride
R	RD1	Repeated Dose for 1 day
	RD2	Repeated Dose for 2 days
	RD3	Repeated Dose for 3 days
	RIPA	Radioimmunoprecipitation Assay
	RT-qPCR	Reverse Transcription Real-time Polymerase Chain Reaction
	RFU	Relative Fluorescent Units
S	SEM	Standard Error Mean
	SD	Single Dose
	SDS	Sodium Dodecyl Sulfate
	SDS-PAGE	Sodium Dodecyl Sulfate Polyacrylamide Gel Electrophoresis
	SMA	Smooth Muscle Actin
T	T_a	Annealing Temperature
	TBS	Tris-buffered Saline
	TEMED	Tetramethylethylenediamine
	TGF	Transforming Growth Factor
	TGF-βR	Transforming Growth Factor-β Receptor
	TNF	Tumor Necrosis Factor
U	UCB	Umbilical Cord Blood
V	VEGF	Vascular Endothelial Growth Factor
	VEGFR	Vascular Endothelial Growth Factor Receptor

Chapter 1: Introduction

1. Introduction

This work describes, explains, and scientifically supports the activities carried out during the master's internship at Exogenus Therapeutics. This Portuguese company has been researching and developing a biological product, Exo-Wound, for wound healing. This product consists of a hydrogel containing an active substance, Exo-101, which are exosomes derived from Umbilical Cord Blood (UCB) cells. Exosomes are nano-sized vesicles, enclosing lipids, proteins and RNA, which are fine-tuned by the secreting cells. Exosome-based technologies are a cell-free approaches and as such have several advantages compared to cellular therapies. Using cells transplantation directly as therapy can potentially trigger innate and adaptive immune responses to allografts [1,2]. Cell-free therapies can be stored for a longer time periods than freshly prepared cells and the heterologous use of the exosomes-based therapies allows the fast and immediate treatment possible [3]. Thus, Exo-101 is able to avoid the main disadvantages of using cell therapy, but at the same time it can induce beneficial effects associated with the use of biological components.

Recently, Exogenus Therapeutics' team has been developing this innovative product and has achieved promising results *in vitro* and *in vivo*, demonstrating shortened healing time and improvement of processes related to wound healing. Due to its origin, Exo-Wound is considered a biological pharmaceutical product and it can be classified, in the future, as a therapeutic advanced product for the treatment of chronic wounds. The pharmaceutical development of a biological product depends on the identification and understanding of the effects and mechanisms of action *in vitro.* This knowledge is crucial to facilitate future regulatory approval and accelerate the product development. Exo-Wound is at an early stage of development but with the forthcoming goal of soon advancing to clinical trials. In this perspective, the primary goal of Exogenus Therapeutics is to explore the mode of action of Exo-101 to facilitate future regulatory approval, and to increase the value of the product.

The Exo-Wound product has the ultimate goal of improving and accelerating the wound healing process of chronic wounds. A wound is a disturbance of normal functional skin and anatomic structure or other adjacent structures [4]. Skin healing process is a complex and extremely coordinated process [5]. This biologic process in adult organism can be divided into four major phases: hemostasis, inflammation, proliferation and remodelling [6]. When wound proceeds through a normal reparative process in an orderly and timely manner that results in continued repair of anatomic and functional integrity. For the healing process to succeed, the four phases of this process must be achieved and completed. Some wounds fail this continuous process and stay

trapped between the inflammatory and proliferative phases, resulting in chronic or non-healing wounds [4,7]. These wounds can affect different types of tissues as skin, muscle or bone, however, skin is the most common organ affected by this health problem.

Chronic wounds are considered a co-morbidity because they are very often associated to diabetes, obesity, compromised vascular circulation, arterial insufficiency, burns and vasculitis [8,9]. With the aging of the population and due to the increase in the prevalence of diabetes and obesity, the incidence and prevalence of chronic wounds tends to increase [10,11]. It is estimated that the prevalence of chronic wounds worldwide reaches 50 million cases, and this number is forecasted to increase in the next few years [10]. There is a significant percentage of patients that, despite receiving standard treatments, do not achieve complete healing of the wounds within months. With this purpose, advanced care technologies, namely biological therapies, are being developed in order to achieve complete healing of critical wounds [12,13]. Nevertheless, there is still a huge need for new approaches to improve the progress of chronic wounds healing. Exogenus Therapeutics have the goal of to fill this world health need with Exo-Wound.

Currently, there are several hypotheses to mode of action of Exo-101. One of these hypotheses is related to the stimulation of proliferative phase of wound healing process. This effect can be due to modulation of extracellular matrix (ECM) components and growth factors (GFs) production by skin cells, such as fibroblasts and keratinocytes. The secretion of this molecules are integrant part of maintenance of skin structure and biology, and of progress wound healing. Thus, it is important to Exogenus Therapeutics the evaluation of secretion of ECM components and GFs by skin cells after treatment with Exo-101, *in vitro*. Reasonably, this evaluation must be based on analytical methods which allow the assess to their expression and secretion. Thus, it is important the implementation and optimization of analytical methods to evaluate the ECM components and GFs secretion by skin cells after Exo-101 treatment in Exogenus Therapeutics' laboratory.

Thus, the following chapter provides a brief overview of essential concepts regarding skin structure and function, wound healing process, the role of the ECM and GF in its success. In addition, some concepts about the laboratorial techniques implemented in Exogenus Therapeutics' laboratory will be introduced, in order to assess the expression and production of ECM components and GFs by skin cells *in vitro*.

1.1 Skin Function and Structure

The Exo-Wound is a biological product which is intended to be used for skin lesions, but it has the ultimate goal of improving and accelerate the wound healing process of chronic wounds. Chronic wounds can affect different tissues such as skin, muscle or bone. However, skin is the major organ affected by chronic wounds. The skin can be defined as a thin layer of tissue that forms the natural outer covering of the body and it has critical functions, such as physical protection and homeostasis [6,14]. This organ protects the organism against harmful environmental agents, such as abrasion and ultraviolet light, and it also keeps the body free of microorganisms. In addition, the skin reduces water loss and thus prevents dehydration. The body temperature is regulated by the activity of sweat glands and by the amount of blood flow through the skin. In the skin, there are also nerve endings that are responsible for sensation. Moreover, an important regulator of calcium homeostasis, vitamin D, is a product of the exposure of skin to ultraviolet light, being essential to the maintenance of homeostasis. Finally, this organ is also essential to the excretion of small amounts of waste products. Thus, any damage on the integrity of the skin may weaken the individual, leading to some pathological conditions, such as loss of fluid, electrolyte imbalance and infections [6,15].

Structurally, the skin is compose by three layers: the hypodermis, the dermis and the epidermis (Figure 1) [6,14,16]. Hypodermis, or subcutaneous tissue, is found beneath the dermis and above the muscle and it is composed mostly by adipocytes. This layer of loose connective tissue, connects the skin to underlying muscle or bone. Above hypodermis lies dermis. This layer is responsible for the structural strength and elasticity of skin through ECM. Dermis supports the blood vessels and nerve endings of skin. This layer serves as a basis for epidermis. Epidermis is the outmost layer of skin. It is an epithelial tissue primarily constituted by keratinocytes and form the body's first protective barrier against pathogens and dehydration. The dermis and the epidermis are the main layers of skin and they represent the most part of skin functions.

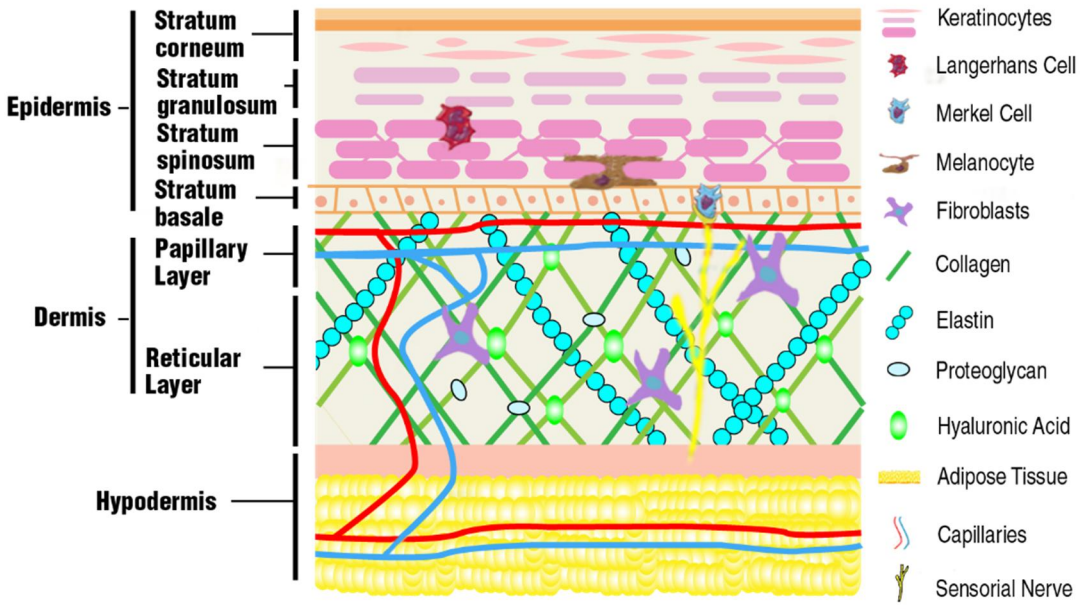

Figure 1 - Schematic representation of the structure of the skin.
The main layers of the skin are depicted - hypodermis, dermis and epidermis – as well as its main cellular and molecular constituents [6,14,16]. The deepest layer of skin, hypodermis, is composed mainly by adipocytes and connects the skin to underlying muscle or bone. The dermis is responsible for the structural strength of skin, given support to cells and biological structures. The most superficial layer of skin, epidermis, have keratinocytes as principal constituent and forms a primary barrier of human body.

The dermis consists of connective tissue that presents in its general composition fibroblasts, a scarce amount of adipocytes and macrophages [6,16]. Dermal fibroblasts are the most prevalent cell type in human dermis. They are the main conductors of maintenance of structure and function of dermis, having important roles in cutaneous wound healing. Dermal fibroblasts are responsible for the production and conservation of ECM, which is an essential component of skin [6]. The ECM present in dermis is composed by a network of multiple biomolecules which serves as scaffold to cells and other structures. The ECM consists of two major classes of biomolecules: fibrous proteins and glycosaminoglycans (GAGs), which are usually linked to protein forming the proteoglycans (PGs) [16]. The fibrous proteins can be structural proteins, such as collagen and elastin, or specialized proteins, which include fibronectin or laminin. These last ones connect the matrix elements one to another and to cells. The GAGs, such as hyaluronic acid (HA) and proteoglycans, permit elasticity and lubrication. The ECM provide structural support to some hair follicles, nerve endings, glands and other structures [6,14]. The dermis can be divided in two distinct layers: the reticular layer and the papillary layer. The reticular layer is the deeper and the main layer of the dermis. This layer is composed of dense irregular connective tissue and is continuous with the subcutaneous tissue. The ECM in this layer of dermis forms a network of irregularly arranged fibres that are resistant to stretching. The papillary layer is loose connective tissue which has projections, that are extended towards to the epidermis. The ECM in papillary layer has thin fibres that are

rather loosely organised. In its composition it is possible to detect blood vessels that supply the covering epidermis with nutrients and oxygen, remove waste products, and aid in regulating body temperature [14].

The epidermis is the superficial layer of the skin and it is divided into four typical cell layers: *stratum basale*, *stratum spinosum*, *stratum granulosum* and *stratum corneum*, from the deepest to the most superficial [6,14]. Only in thick skin, there is still a fifth layer, found between the *stratum corneum* and *stratum granulosum*: the *stratum lucidum*. The epidermis is composed of several types of cells, such as melanocytes, Langerhans cells, Merkel cells and keratinocytes [6]. Melanocytes produce melanin that contributes to skin colour, while Langerhans cells contribute to immune protection [17,18]. Merkel cells are associated with the nerve endings, which are responsible for detecting superficial pressure and light [19]. Keratinocytes are the main cellular type of the epidermis [14]. These cells, which are responsible for production of keratin, give the epidermis its ability to resist abrasion and reduce water loss [6]. Additionally, keratinocytes participate in an important process of renewal of epidermis, named keratinization. This process of continuous cytodifferentiation, begins in the deepest layer of the epidermis, where keratinocyte stem cells undergo mitosis and new keratinocytes are produced [6,14,20]. During the process of keratinization, they migrate up from the basement membrane toward the *stratum corneum*. As they move from the deeper epidermal layers to the surface, the keratinocytes mature, change shape and accumulate keratin. Thus, these different stages are responsible for the five layers that constitute epidermis. When these cells reach the *stratum corneum* the cells eventually die and produce an outer layer of dead cells that resists abrasion and forms a permeability barrier [6]. Then, they are either sloughed off or rubbed off by friction in a process called desquamation [14].

In summary, the skin plays a crucial role in the sustenance of life through its numerous functions, such as protection, regulation of water and electrolytes balance or thermoregulation. When this barrier is disrupted these functions are no longer adequately performed, and it becomes vital to rapidly restore its healthy state. Each layer of the skin is important to perform these functions. At functional level, keratinocytes and dermal fibroblasts are cells specific of skin and they play an important role in wound healing process.

1.2 Wound healing process

As already mentioned, the skin protects the organism and is essential in the maintenance of homeostasis [6,21]. Any damage on the integrity of the skin may initiate a process of wound healing and regeneration to restore proper skin function [6,15]. This process is a complex and extremely coordinated process and involve a multitude of cellular and molecular components [5]. For the general well-being of patients, the wound healing process should be efficient and complete [14]. Abnormalities in this process often lead to some disorders of skin such as chronic wounding. Wound healing is the physiological process target to Exo-Wound, and its mode of action may be related to the induction of the proliferative phase. Thus, an understanding of normal wound healing provides additional insight into biology of the skin and potentiate the knowledge of the presumed effects of Exo-Wound.

The process of skin repair in adult organism can be divided into four major phases: hemostasis, inflammation, proliferation and remodelling (Figure 2) [5,6,15,22]. This complex and well-regulated process requires the participation of multiple cellular type such as platelets, inflammatory cells, fibroblasts, keratinocytes and endothelial cells. GFs, cytokines and components of ECM are essential regulators of the wound healing process, and their contribution to the different phases of this complex biological process will be detailed bellow [6,15].

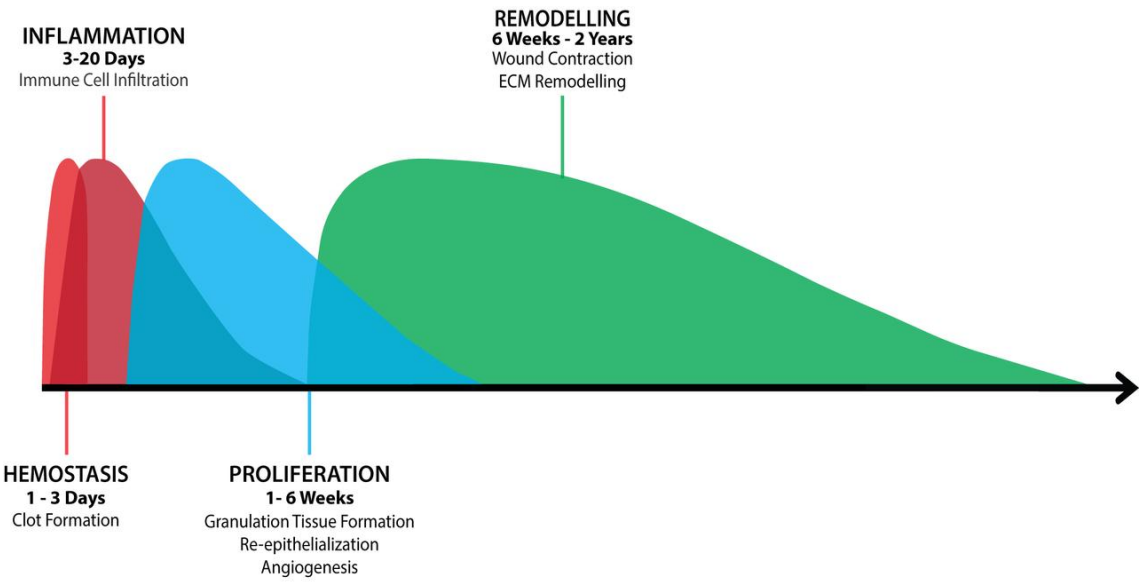

Figure 2 - Graphic representation of normal wound healing process through the timeline.
The normal healing process begins with hemostasis. The chemotaxis resulting from this phase leads to immune cell infiltration. Then follows attraction and proliferation of fibroblasts, endothelial cells and keratinocytes. In the remodelling phase, the main features are the wound contraction and ECM remodelling. *Adapted from: http://www.enluxtrawoundcare.com/non-healing-wounds.html* [22].

- **Hemostasis**

Hemostasis is the first phase of wound healing and it takes place immediately after the occurrence of injury [21]. The most important mediators of hemostasis are blood vessels, fibrin and platelets. Blood vessels are induced to vasoconstriction, which persists for 10 to 15 minutes after injury [6,15]. Fibrin and platelets are responsible for clot formation, platelet aggregation and degranulation of vesicles. Successful hemostasis will produce a fibrin clot to stop any bleeding. The fibrin clot is an essential structure which serve as a provisional matrix for inflammatory cells, fibroblasts, and GFs [15,23,24]. The clot stabilization depends on factor XIII. When the factor XIII binds fibrins to plasma fibronectin, a fibrin–fibronectin clot is formed.

- **Inflammation**

The main goal of the inflammatory phase is to create an immune barrier, by initiating a series of molecular events that protect the individual against invading micro-organisms [21]. The inflammatory phase is characterized by physiologic changes, such as capillary vasodilation and increased permeability, that facilitate arrival of serum proteins into the wound [6,15]. The cellular phase of inflammation follows, and is evidenced by the migration of phagocyte white blood cells. The main inflammatory cells involved are neutrophils, monocytes and arising macrophages.

Although in the literature the separation of hemostasis and inflammatory phases is documented, they occur almost at the same time. The first signal of skin damage comes from epidermal barrier. Keratinocytes secrete interleukin (IL)-1 immediately after injury, alerting surrounding cells [25]. IL-1 will induce chemotaxis, attracting inflammatory cells, such as neutrophils and monocytes. In addition, platelets release GFs and cytokines, such as transforming growth factor (TGF)-β, platelet-derived growth factor (PDGF) and epidermal growth factor (EGF) [5,26,27]. These molecules provide a chemotactic stimulus for neutrophils and monocytes.

Neutrophils are the first inflammatory cells to arrive at the wound site. They are early responders to numerous cytokines and GFs [5,15,21,27]. Neutrophils are responsible for phagocytosis of cellular debris, foreign particles and bacteria [5,15]. When neutrophils finish their mission, they enter apoptosis and they are phagocytosed [5]. Shortly after neutrophils, circulating monocytes arrive at the wound site attracted by a diversity of chemoattractants [6,15,21]. When activated in the wound site, monocytes differentiate into macrophages. These differentiated cells reside in the provisional fibrin-based ECM to phagocyte debris in the wound site [5,15,21]. These immune cells can acquire two types of inflammatory phenotype: M1 (pro-inflammatory) or M2 (anti-inflammatory) [28,29]. In the early inflammatory phase, when resident macrophages are activated, they mainly acquire a pro-inflammatory M1 phenotype, which will produce pro-inflammatory

mediators such as IL-1, IL-6 and tumour necrosis factor (TNF)-α [28,29]. With the progression of the healing process, these cells acquire a reparative M2 phenotype. These macrophages M2 expressed anti-inflammatory mediators and GFs, such as IL-1 receptor (IL-1R) antagonist, IL-10, TGF-β, vascular endothelial growth factor (VEGF), insulin-like growth factor (IGF)-1, EGF and fibroblast growth factor (FGF). This M1–M2 transition is crucial for the resolution of inflammation and progression to the proliferative phase [5,27,28].

- **Proliferation**

The proliferative phase of normal wound healing begins usually on the third day after the injury and lasts about three weeks [5,15]. This phase is characterized by a few processes, such as formation of granulation tissue, re-epithelialization and neovascularization. During proliferative phase, dermal fibroblasts migrate to the wound site and proliferate [5,6,21,30]. In this journey, fibroblasts navigate the provisional matrix along the fibronectin fibres [27,31,32]. They may encounter a diversity of cellular and matrix compounds that can pose a problem for their migration. Thus, the expression of numerous matrix metalloproteinases (MMPs) becomes crucial [33]. MMPs have an important role in such a wide variety of biologic processes, given that these molecules have the ability, among other, to recognize and degrade ECM, promoting fibroblast migration [27,33,34].

In the proliferative phase of wound healing, besides the enrolment of fibroblasts in migration or proliferation processes, these cells also participate on the production of ECM [15,35,36]. Thus, in the case of injury, wound fibroblasts substitute the provisional fibrin-fibronectin matrix by depositing collagen, GAGs and proteoglycans [5,6,35]. Collagen have two purposes in wound healing: provide strength to the wound, and facilitate the movement of the other cells, such as endothelial cells and macrophages. Additionally to producing collagen, fibroblasts are also responsible for the synthesis of proteoglycans, fibrin, fibronectin, tenascin and HA [5,35]. The structure of ECM has an important influence on angiogenesis [36]. Fibronectin, collagen and vitronectin, components of ECM, serve as a repository of important GFs, such as FGF and TGF-β and also provide structural support for the invading capillaries [5,36].

In order to re-establish the normal supply of nutrients and oxygen to wound cells, endothelial cells begin to migrate into the wound along the provisional ECM. This event marks the beginning of angiogenesis, or neovascularization, which is a process dependent of endothelial migration [6,15]. Angiogenesis is regulated and stimulated by several GFs and cytokines, produced during the inflammatory phase of wound healing, such as VEGF, FGF and PDGF [5,27,36,37]. The

migration of endothelial cells along the ECM is a process dependent of the expression of integrins and MMPs.

Proliferating fibroblasts and endothelial cells form a granulation tissue that serve as the foundation for scar tissue development [5,21]. This tissue has a pink granular appearance due to numerous capillaries that invade the wound stroma [6,15]. Granulation tissue is made up of proliferating fibroblasts, capillaries and macrophages structurally supported by a matrix of collagen, GAGs and glycoproteins, such as fibronectin and tenascin. The granulation tissue favours the re-epithelialization process [5]. This important process is dependent on the keratinocytes migration across the granulation tissue and their proliferation [36]. As the migration of fibroblasts and endothelial cells, keratinocytes migration is MMPs secretion dependent [25,33]. These cells are coming from the proximity of the wound, aiming to form a new barrier between the wound and external conditions.

- **Remodelling**

The remodelling phase is the last phase of the wound healing and begins 2 to 3 weeks after injury [5,6]. This last phase of wound healing process has as main objective the formation of a mature scar, which over time tends to be more like undamaged skin. This phase involves wound contraction and reorganization of the granulation tissue, increasing tissue strength and reducing redness, in order to form a mature scar [5,6,15].

Wound contraction is correlated in time with differentiation of fibroblasts into myofibroblasts [15,39]. Myofibroblast is a contractile phenotype of dermal fibroblasts that helps to connect wound edges, mainly in the remodelling phase [6,15,31]. The contractile properties of myofibroblasts are attributed to increased levels of actin filaments, mainly α-smooth muscle actin (SMA) [39]. Dermal fibroblast and myofibroblasts work in harmony, contributing to the synthesis and alignment of collagen and, thus, help the closure of the wound [6,15,31].

Besides wound contraction, remodelling phase implies the reorganization of granulation tissue. This process is related with remodelling of ECM, produced in proliferative phase, and involves a visible decrease of redness. ECM synthesis and remodelling are initiated concurrently with the development of granulation tissue and continue over a prolonged period [6]. The scar will probably never have the same physical properties as those of the uninjured tissue [5]. But the remodelling tissue will manifest increasing tensile strength and decreasing thickness [15]. As the matrix matures, fibronectin and HA are broken down and collagen bundles increase in diameter, corresponding to increasing wound tensile strength [5,15]. The amount of type I collagen increases while there is a decrease of type III collagen [15,16,40]. This decrease of type III collagen is

accompanied by a decrease of proteoglycans and water. In early stages, the deposition of collagen bundles is highly disorganized. However, over the time, the new collagen matrix becomes more oriented and crosslinked. The removal of accumulated connective tissue is attributed to production and activity of MMPs and TIMPs [5,33,38]. Thus, a proper wound maturation seems to require a coordinated expression of MMPs and TIMPs [33,41,42]. The balance between the production of ECM components, the destruction of immature matrix and the inhibition of such destruction results in the formation over time of a mature ECM. This maturation of dermis structure is accompanied by a decrease of redness of the scar [6,15]. This transformation comes from the reduction of the density of capillaries in the wound, resulting from the release of several antiangiogenic mediators. In addition, over time, fibroblasts and myofibroblasts undergo apoptosis and their numbers are reduced [5,15,43]. Ultimately, these facts result in a relatively acellular mature scar.

In conclusion, it seems clear that this process is highly regulated and strongly dependent on all interveners, be they cellular or molecular components. As mentioned above, the mode of action of Exo-Wound may be related to the induction of the proliferative phase. This phase involves many cellular and molecular processes, including formation of granulation tissue, re-epithelialization and neovascularization. However, the proliferative phase is clearly dependent of ECM production and assembly as well as GFs secretion, which ensure the progress of the wound healing process.

1.3 Synthesis and Role of Extracellular Matrix and Growth Factors on Wound Healing

As highlighted before, wound healing is a complex and prolonged process. To be successfully complete, each element involved in healing must act in the correct time and manner. Two key elements indispensable for wound closure are ECM and GFs [16,44]. The ECM is the component that provides physical scaffolding for the cellular constituents and their activities [16,45]. GFs are responsible for transmitting cellular messages to stimulate migration, adhesion, differentiation or proliferation of wound cells [44]. In chronic wounds, the production of these molecules is inappropriate [27,46]. The prolongation of the inflammatory phase, typical of this type of wounds, results in the deregulation of the ECM production and remodelling, since chronic wounds are characterized by a predominance of proteins characteristic of an early proliferative phase. Additionally, there are also evidences of the decreased production of GFs by macrophages, fibroblasts or keratinocytes, that are essential to the progression of wound repair [27,47–50].

There is a significant percentage of patients with skin lesions that, despite receiving standard treatments, do not achieve complete healing of the wounds within months. Currently, there are numerous developed and emerging biological therapies which have shown efficacy for the treatment of otherwise difficult-to-heal wounds [51]. In this area, the investigational interest in ECM components and GFs based therapies is evident. Actually, there are advanced therapies for chronic wounds treatment based in application of ECM products or GFs administration [12,51,52]. Studies performed with these products and other promising molecules have demonstrated the importance of GFs and ECM role in the progression of wound healing process [53–55].

More recently, exosomes-based technologies have been shown to influence the modulation of matrix production and growth factors by skin cells. *In vitro* studies reported that when dermal fibroblasts are treated with exosomes derived from stem cells, at early stages of wound healing, these cells have an increase in expression of structural ECM components like collagen I and III and elastin [56,57]. However, a work published in 2017, shows that a similar product derived from human amniotic epithelial cells can down-regulate the expression of ECM components such as collagen I and III [58]. At the same time, the authors reported an up-regulation of the expression of MMP-1 relatively to TIMP-1. This suggests that in this case there may be a stimulation of the remodelling phase of wound healing. In parallel, some studies show that this type of products can activate pathways which also promote the production of growth factors. An investigation performed in 2016 describes the increased expression of FGF-2 and VEGF by endothelial cells after the treatment with extracellular vesicles derived from endothelial progenitors UCB cells [59]. Another

study performed with a similar product derived from platelet rich-plasma, refers to an increase in the production of FGF-2 and TGF-β1 [60]. The production and assembly of ECM and the production of GFs is closely linked and sometimes there is a need to investigate these two processes simultaneously. Proof of this is the study conducted in 2017, where the effects on the regulation of ECM remodelling promoted by exosomes secreted by adipose mesenchymal stem cells are evaluated by assessing production of Col1, Col3 and TGF-β1, among other molecules [61]. Taken together, these studies indicate that the modulation of ECM production and GFs secretion can be a possible mode of action of exosomes-based technologies to accelerate the wound healing.

All these evidences suggest that a possible mode of action of Exo-101 can be exerted via the modelling of ECM or GFs production by patient skin cells, without exogenous application of ECM or GFs or even cells. Thus, this section has as main goal to introduce some key features about the molecules that will be evaluated in the practical section of this master thesis.

1.3.1 Expression and Production of ECM Components

The ECM is the non-cellular component present within all tissues and organs [6,16,62]. This matrix provides essential physical scaffolding for the cellular constituents and initiates crucial biochemical and biomechanical cues that are required for numerous biological processes [62]. The ECM consists of a large variety of matrix macromolecules whose precise composition and specific structures vary from tissue to tissue [45]. In dermal skin layer, the ECM is the largest component and its synthesis is the responsibility of dermal fibroblasts [6,16,45]. The major constituents of dermal ECM are fibrous-forming proteins, PGs, and GAGs [16,45,62]. These molecules are associated in multi-molecular structures, which also associate with each other, building the complex three-dimensional matrix network.

The biological importance of ECM is due not only to its scaffold function, but also related to regulation of many cellular processes including growth, migration, differentiation, proliferation and adhesion [16,45]. Thus, the influence of ECM on diverse cellular processes demonstrate that this macromolecules network is a vital participant in tissue activity and wound healing. In case of skin lesion, particularly when tissue has been substantially damaged, ECM synthesis is a key for successful wound healing [16]. During the proliferative phase of wound healing, the secretion of extracellular matrix components, such as fibronectin and collagen, by dermal fibroblasts is critical [63–65]. The successful wound repair is dependent on their production and assembly since they re-establish the mechanical strength of the wound. Due to their beneficial properties in wound healing, ECM components are already used in advanced treatments to chronic wounds and there is a continuous investigation for emerging medicines based on ECM as scaffolds [12,51,66]. In this

work, we particularly focus on three main dermal ECM fibrous proteins: fibronectin (Fn), collagen I (Col1) and collagen III (Col3). These molecules are not only common constituents of normal dermal skin layer but also have a significant role in wound healing process [65]. Thus, in next topics will be presented some introductory concepts about these fibrous proteins.

- **Fibronectin**

Fibronectin is dimeric glycoprotein ubiquitously expressed, which can be found in blood or in connective tissue [62,67]. This fibrous protein acts not only as an important scaffold to maintain and direct ECM organization, but also has a crucial role in mediating cell attachment and function [62,68,69]. Continuous Fn matrix production allows dynamic tissue remodelling, formation or repair [16]. Fn can be presented by two distinct forms: soluble plasma Fn and cellular Fn molecules [67,68]. Both forms of Fn participate in wound healing process [68–70]. However, each one of these Fn forms has differential functions during tissue repair, both in terms of timing and final goal. Soluble plasma Fn is synthetized by hepatocytes and secreted in blood plasma in a compact and inactive form [23,68]. This form of Fn participates in hemostasis phase of wound healing to form a fibrin-fibronectin clot. The cellular Fn is synthetized by many cell types including fibroblasts, endothelial cell, chondrocytes, synovial cells and myocytes [16,65,68]. However, at beginning of granulation tissue formation, cellular Fn is mainly deposited by fibroblasts that repopulate the wound. In addition, this dimeric protein seems to influence the assembly of other molecules of ECM, such as collagen [69,71,72]. Thus, cellular Fn represents an important and abundant component of granulation tissue, and this Fn form is the one of the most interest in this work.

Although Fn molecules are the product of a single gene, the resulting protein can exist in multiple forms [45,67]. As many as 20 variants of human Fn arise from alternative splicing of a single pre-mRNA. The monomer of Fn has an approximate size of 250kDa [45,68,70]. Each Fn monomer is composed of three different types of modules: twelve Fn type I repeats (FNI), two Fn type II repeats (FNII), and eighteen Fn type III repeats (FNIII) (Figure 3). Fifteen of the FNIII repeats are constitutively expressed and three are alternatively spliced. Indeed, the third FNIII of human fibronectin mediates cell adhesion and migration [69]. In addition, the fourth and fiftieth FNIII involved in the Fn matrix assembly of 3D matrices [73]. The modules that composed Fn monomer are organized into three functional domains: N-terminal domain (FNI1-9), the central binding domain (FNIII1-12) and the heparin-binding domain HepII (FNIII12-14). In its structure, Fn has several binding sites to other Fn dimers, to collagen, to heparin and to cell-surface integrin receptors. When secreted, Fn is presented as a dimer joined by two C-terminal disulphide bonds and it must be assembled into super molecular fibres, since its functional form *in vivo* is a fibrillar

state [45,62]. Even *in vitro*, fibroblasts rapidly assemble Fn, that is adsorbed on surfaces and used to help adhesion and migration of dermal fibroblasts [67,74,75,69].

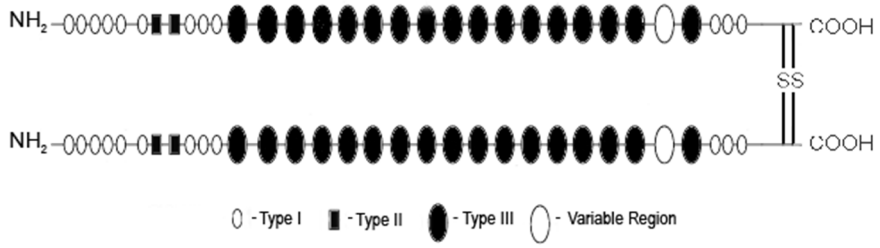

Figure 3 - Schematic of the fibronectin homodimer.
The three types of repeating homology units (FNI, FNII and FNIII) and the variable regions are shown. *Adapted from Fubao Lin, et al,2014 [70].*

- **Collagen I and III**

Collagens form a large family of proteins that serve as scaffolds for the attachment of cells and other matrix proteins in many tissues in human body [62,76]. As main structural element of the ECM, collagen provides tensile strength, regulates cell adhesion, supports migration and tissue development [16,62,77]. In dermal layer of skin, residents or recruited fibroblasts are responsible by synthesis and secretion of collagen that compose dermal ECM [16,62]. Besides secretion, dermal fibroblasts are able to remodel and organize collagen fibrils by exerting tension on the matrix. This process has a great impact on alignment of collagen fibres and thereafter influence in wound healing process. In human body, collagen molecules are associated in fibres which are generally a heterogeneous mix of different types of collagen [77]. Depending on tissue, there are one type of collagen that usually predominates. In dermal ECM, Col1 and Col3 are the most representative collagens and they have an important role in wound healing process [78].

Structurally, collagen molecules are trimer. Thus, collagens can be homotrimers, if the three polypeptide chains are either identical, or heterotrimers, if at least one of the chains is distinct [76,77]. Col1 is a heterotrimer composed by two collagen I α-chains 1 (Col1α1) and one collagen I α-chain 2 (Col1α2). While Col3 is a homotrimer of three identical two collagen III α-chains 1 (Col3α1). Thus, each different chain is encoded by a different gene, but they have arisen from a common progenitor [76]. The COL1A1 and COL1A2 genes encode the 2 types of chains that compose Col1 and COL3A1 gene encode the single chain type that constitutes Col3 molecule. As represented in Figure 4, inside the cell, collagen chains are first synthesized in precursor form, pro-α chains [77–79]. Individual pro-α chains are submitted to numerous post-translational modifications: hydroxylation of proline and lysine residues, glycosylation of lysine and hydroxylysine residues [79]. These modifications allow the formation of the triple stranded helix of procollagen [77,79]. Procollagen molecules consists of a rod-like central triple-helical region

(∼300kDa) with globular pro-peptide extensions at both the N- (∼50kDa) and C- (∼90kDa) termini [77]. Within the endoplasmic reticulum, the C-propeptides play key roles in determining correct chain association during trimerization, notably in cells producing different collagen types. After secretion of procollagen in extracellular space, proteolytic cleavage of the N- and C- termini by allows the formation of tropocollagen that it is able to form collagen fibrils [77–79]. In dermal skin, Col1 and Col3 fibres are assembly in a complex ECM, where other matrix macromolecules are also found to associate and decorate collagen fibrils providing them with specific structural and functional properties. In addition, there are evidences that indicate the interdependence of Fn and Col network secretion and assembly [72,80].

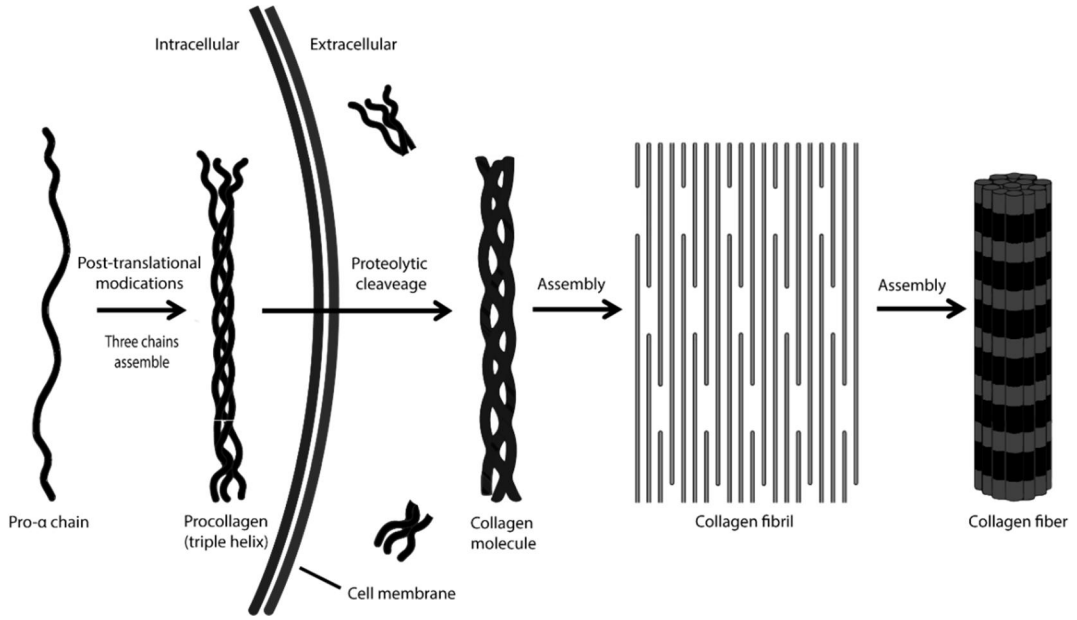

Figure 4 - Schematic representation of production of collagen molecule and the assembly of collagen fibres. Inside the cell, collagen chains are synthesized in the precursor form, pro-α chains [77-79]. These chains are submitted to numerous post-translational modifications, which allows the formation of the triple stranded helix of procollagen. Procollagen molecules consist of a rod-like central triple-helical region with globular pro-peptide extensions at both the N- and C-termini. After secretion of procollagen to extracellular space, proteolytic cleavage of the N- and C- termini allows the formation of tropocollagen. This collagen is able to form fibrils, which can then be associated in heterofibres composed of different types of collagen.

As mentioned above, in the dermis, the dominating types of collagens are types I and III [76,78]. However, Col3 is generally less abundant than Col1. At complex ECM, these two types of collagen commonly form heterofibrils, which contribute to mechanical strength. During the transition of inflammatory to proliferative phase of healing, however, there is an increase of collagen type III expression and assembly [16,76,78]. Although disorganized, the ECM formed in this phase of wound healing give to the tissue the feature of tensile strength [65,76]. With the progress of the healing process, in remodelling phase, Col3 is often replaced by Col1, forming an organized and definitive ECM [81]. In proliferative phase of wound healing, with increase of production of Col3, the collagen I/III ratio will be lower in wound site as compared to "normal" skin [16,78]. Thus, the

collagen I/III ratio is a reference that is commonly used in order to receive information on the progress of ECM remodelling and consequently information about wound healing stage [78].

Therefore, it is clear the crucial role of ECM, namely of Fn and collagens, in both skin structure and wound healing process. In Figure 5, it is represented the normal wound healing process referencing the timing of Fn, Col1 and Col3 production by dermal fibroblasts.

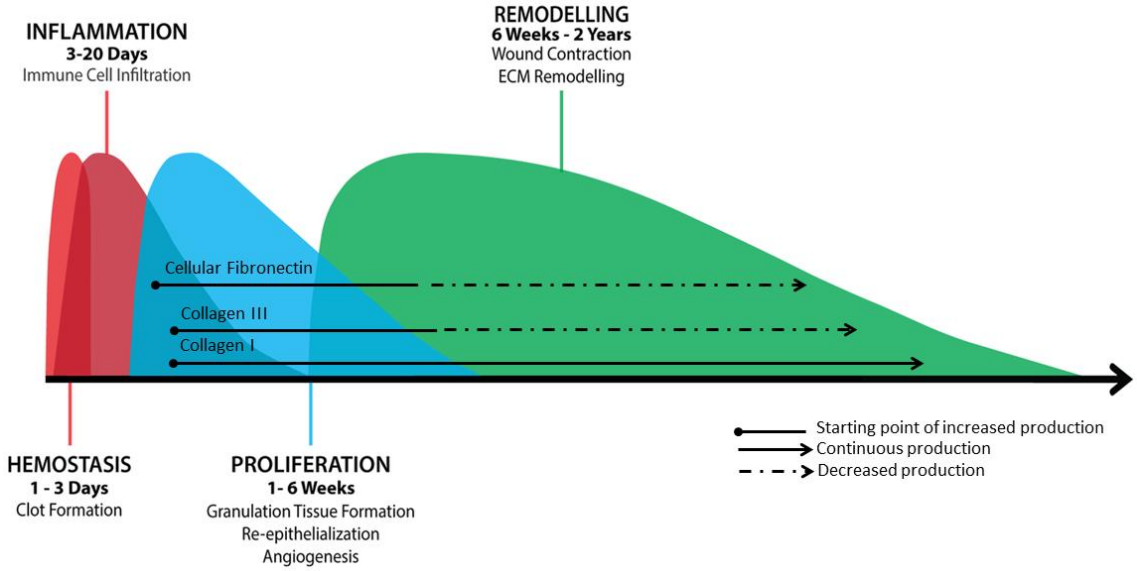

Figure 5 - Graphic representation of normal wound healing process referencing the timing of fibronectin, collagen I and collagen III production by dermal fibroblasts.
At beginning of granulation tissue formation, dermal fibroblasts, which repopulate de wound site, deposit cellular Fn to create a new and immature ECM. During the transition of inflammatory to proliferative phase of healing, Col1 and Col3 are produced and assembled by dermal fibroblasts. Although disorganized, the ECM formed in this phase of wound healing provides tensile strength to the tissue. With the progress of the healing process, in remodelling phase, Col3 is often replaced by Col1, forming an organized and definitive ECM. *Adapted from: Enluxtra Wound Care [22]*

1.3.2 Expression and Production of Growth Factors

Growth factors are diffusible signalling proteins that controls some cells activities, such as cell growth, differentiation, survival or migration [44]. After its production and secretion, a growth factor can exert their stimulation though endocrine, paracrine or autocrine mechanisms. Typically, the signal transduction of growth factors is initiated by binding to their receptors on the surface of target cells. These molecules are essential for cellular proliferation and viability of normal cells [27,44]. Thus, the study of GFs expression and production has extreme relevance to understand the biological cellular state, physiologically and in pathologic conditions.

During wound healing process, the need of production of GFs is increased, since this extremely coordinated process is executed and regulated by a signalling network involving, among other signalling molecules, numerous growth factors [27,44]. In case of injury, GFs are not only necessary to regulate normal biological processes of dermal fibroblasts and keratinocytes. These molecules are responsible to coordinate other cells such as endothelial cells or inflammatory cells

and specific biological process of wound healing. During wound healing, all wound cell types involved produce and secrete GFs, which can act autocrine or paracrine manner. This thesis work will focus on GFs that are expressed, produced and secreted by dermal fibroblasts and keratinocytes, to achieve complete and successful wound heal. Of particular interest is the TGF-β family, FGF family and VEGF. Thus, in next topics, some introductory notions about GFs that will be studied in practical work will be presented.

- **Transforming Growth Factor-β**

TGF-β superfamily is a group of growth and differentiation factors, which are encoded by 33 genes [82]. These 33 known human TGF-β family polypeptides includes, among other molecules, the three TGF-β isoforms, TGF-β1, TGF-β2 and TGF-β3 [27,82]. Of all the molecules that constitute the TGF-β family, the three TGF-β isoforms are the best-studied factors and their key role in wound healing process is known [27]. All three proteins are encoded by three different genes: TGFB1, TGFB2 and TGFB3 [83]. In the cell, these isoforms are produced in a homodimer form [44,82–84]. When secreted and properly activated, TGF-β can interact with its receptors (TGFβR) and exert its function on target cells.

The TGF-β isoforms are multifunctional growth factors that are secreted by macrophages, fibroblasts, keratinocytes, and platelets [27]. This GF exerts pleiotropic effects on wound healing by regulating cell proliferation and migration, differentiation and ECM components production, such as collagen and fibronectin [82,85]. Each TGF-β isoform shows a unique expression pattern spatially and temporally *in vivo*, also pointing at distinct functions during cutaneous wound repair [82]. However, particularly, TGF-β1 and TGF-β3 seem to play a most important role than TGF-β2 in tissue repair [82,83,86].

Although isoforms 1 and 3 are largely homologous, they may exert different effects interacting with the same receptors [82,83,86]. In early phases of wound healing, TGF-β3 is more prevalent than TGF-β1 [82,87]. While TGF-β1 is present at high levels in wound healing only after the initiation of epithelialization, between proliferative and remodelling phases, TGF-β3 appears up-regulated in the migrating epidermis. TGF-β1 is initially release by platelets, which plays a critical part in macrophage and fibroblast chemotaxis to the wound [83]. Besides that, TGF-β1 released by macrophages, fibroblasts and keratinocytes during other phases promotes angiogenesis, collagen synthesis and contraction, and keratinocytes migration. However, TGF-β3 may slow keratinocyte proliferation without affecting reepithelialisation and it promotes scar-free healing [27,82,87]. In conclusion, the isoforms of TGF-β1 and 3 have different roles in wound healing. TGF-β1 seems to promote the main processes of wound healing, but it may promote

fibrosis when unchecked [84]. In contrast, TGF-β3 may balance the effects of TGF-β1, having an anti-fibrotic role in tissue repair [87].

- **Fibroblast Growth Factor**

The FGF family is composed of 23 homologues members [27]. The FGFs are single chain polypeptides, which have one conserved domain flanked by non-conserved extensions [88,89]. During wound healing, some elements of this GF family are produced by wound cells, such as keratinocytes, fibroblasts and endothelial cells and they generally stimulate proliferation of major cell types involved in wound healing, both *in vitro* and *in vivo* [27,88]. In basis of their key in wound healing, this work will focus on two of them: FGF-2 and FGF-7.

FGF-2, or basic FGF, is increased in the acute wound and plays a role in proliferative and remodelling phases [27,88,90]. It is described that at wound, fibroblasts, keratinocytes and endothelial cells are responsible by FGF-2 production. *In vitro* studies have demonstrated that FGF-2 influences fibroblasts action, promoting their migration [91–93]. In addition, this FGF regulate synthesis and deposition of various ECM components to granulation tissue formation and stimulates them to produce MMPs [92]. This GF also increases keratinocyte motility, promoting reepithelialisation process [27,94]. In wound healing, FGF-7 or keratinocyte growth factor (KGF)-1 is produced mainly by dermal fibroblasts [27,88]. FGF-7 act in a paracrine fashion through the FGFR2IIIb receptor found only on keratinocytes [88]. Thus, its direct effects are in keratinocytes behaviour, namely stimulating reepithelialisation [27,88,95]. Indeed, FGF-7 causes significant changes to the organization of the wound keratinocytes, inducing migration, proliferation and an increase adhesion of its target cells [95].

- **Vascular Endothelial Growth Factor**

VEGF-A belong to VEGF family, which includes: VEGF-A, VEGF-B, VEGF-C, VEGF-D, VEGF-E, and placenta growth factor [96,97]. The VEGF-A is considered the main proangiogenic factor in wound healing. This GF is encoded by VEGFA gene that contains nine exons [97]. This gene undergoes an extensive alternative splicing following transcription, thereby leading to the production of several isoforms. Three exons code for C-terminal domains which, through their occurrence and arrangement, determine the biological function and tissue localization of the peptides. The final product is a glycosylated, disulfide-linked homodimeric protein. When secreted, VEGF-A interacts with VEGF receptor (VEGFR) 1 and 2, which are found primary in endothelial cells.

In case of skin injury, VEGF-A is produced by endothelial cells, keratinocytes, fibroblasts, among other wound cells [27,96,97]. Its transcription and secretion are stimulated when blood flow is reduced, decreasing delivery of oxygen and nutrients to tissues, a common condition in skin lesions [98]. In this case, VEGF-A will interact with its receptors in surface of endothelial cells. Consequently, this GF will promote the early events of angiogenesis and neovascularization [90,99,100]. The main effects of VEGF-A are the stimulation of migration and proliferation of endothelial cells. In addition to increase oxygen and nutrients in wound, these events influence the optimal of granulation tissue formation [98]. The repression of VEGF-A expression delays the wound healing process [99].

Concluding, GFs have many important functions during wound healing process and they are crucial to maintenance of skin homeostasis. In Figure 6, it is represented the normal wound healing process referencing the timing of TGF-β1, TGF-β3, FGF-2, FGF-7 and VEGF production at wound site.

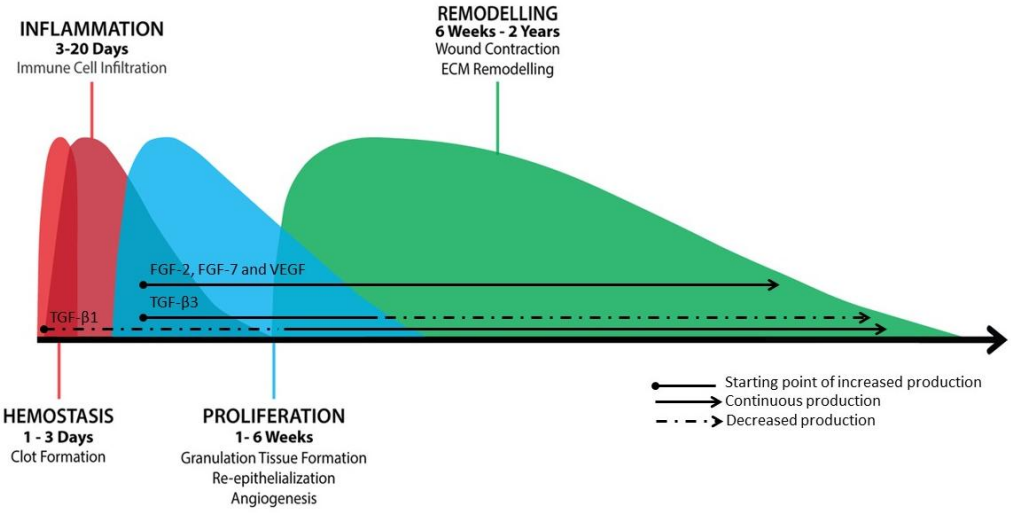

Figure 6 - Graphic representation of normal wound healing process referencing the timing of TGF-β1, TGF-β3, FGF-2, FGF-7 and VEGF production at wound site.
TGF-β1 is initially release by platelets, which plays a critical part in macrophage and fibroblast chemotaxis to the wound. Besides that, TGF-β1 released by macrophages, fibroblasts and keratinocytes, during other phases, promotes angiogenesis, collagen synthesis and contraction, and keratinocytes migration. However, in early phases of wound healing, TGF-β3 is more prevalent than TGF-β1, and may slow keratinocyte proliferation without affecting reepithelialisation and promote a scar-free healing. FGF-2 is increased in the acute wound and plays a role in proliferative and remodelling phases of wound healing. FGF-7 is produced mainly by dermal fibroblasts and it has direct effects on keratinocytes behaviour, namely stimulating reepithelialisation. VEGF is produced mainly by endothelial cells, keratinocytes and fibroblasts and stimulate the angiogenic process. *Adapted from: Enluxtra Wound Care [22].*

1.4 Biomolecular methods to evaluate expression and production of ECM components and GFs by skin cells *in vitro*

As evidenced above, it is important to Exogenus Therapeutics the identification and understanding of the effects and the mode of action *in vitro* of Exo-101. These effects can include the modulation of ECM components and GFs production, as with other similar technologies. Thus, the evaluation of modulation of these molecules implies the implementation of analytical methods, which is one of the main objectives of this work.

After reviewing the literature and weighing the benefits for Exogenus Therapeutics, it was concluded that it would be more beneficial to focus on Fn, Col1 and Col3 expression and production. These three proteins normally found in the dermis ECM of and they are actively involved in the wound healing process. Expression and production of these proteins are usually evaluated in order to infer the production of ECM by dermal fibroblasts, both *in vivo* and *in vitro*. In studies of expression and production of specific molecules, there are relatively common laboratory techniques that are currently used. For the evaluation of gene expression, the Reverse Transcription Real-Time Chain Reaction (RT-qPCR) is normally used [58,61,67,75,101]. However, this technique only give information about gene expression It is known that not all genes which are expressed give rise to proteins due to the entire highly regulated process of protein synthesis. Thus, it is also necessary to implement techniques that evaluate the synthesis of these proteins. In this sense, there are many options of methodologies. In order to assess the production of ECM proteins *in vitro*, the most used techniques appear to be Western Blot (WB) and Immunocytochemistry (ICC) [58,61,67,74,75,101,102].

In addition to the implementation of methods to enhance the secretion of ECM by fibroblasts, other objective of this work is the implementation of techniques to evaluate the expression of GFs by skin cells *in vitro*. After reviewing the literature, it is noticeable that there are numerous growth factors produced by skin cells during the healing process [27,44,59,60]. Thus, it was decided by Exogenus Therapeutics' team to first evaluate only the modulation of GFs expression in two skin cell lines: fibroblasts and keratinocytes. The selected GFs were TGF-β1, FGF-2, FGF-7 and VEGF-A. To evaluate the expression of these GFs, will be implemented the RT-qPCR. This approach allows to evaluate the expression of these several different types of GFs in both fibroblasts and keratinocytes lineages. An analysis of the synthesis of GFs that have a positive model for healing after treatment with Exo-101 will be further evaluated.

In summary, to assess the expression of Fn, Col1 and Col3 by fibroblasts *in vitro* after exposure of Exo-101, laboratory work will involve the implementation of RT-qPCR, WB and ICC in

Exogenus Therapeutics' laboratory. The RT-qPCR will be implemented and optimized in order to assessing also the expression of growth factors. The present section has the goal to introduce some concept about these techniques to support the following laboratorial work.

RT-qPCR has been developed in the final of 20th century [103]. To performance a RT-qPCR, the RNA is used as starting material and this technique implies the reverse transcription of RNA, the amplification of the resulting cDNA using the PCR and finally the detection and quantification of products in real time (Figure 7) [103,104]. In this method, RNA is first transcribed into cDNA by reverse transcriptase from total RNA or messenger RNA. The cDNA is then used as the template for the qPCR reactions. These reactions depend on four essential components: cDNA template, DNA polymerase, primers and nucleotides (dNTPs). There are three major steps that make up each cycle in a qPCR which occurs at different temperatures: denaturation (usually 95ºC), annealing (temperature defined by primers, but typically ≈ 60ºC) and extension (dependent on the enzyme used in the reaction). Reactions are generally run for 40 cycles. The detection of amplified products is done in real time through detection methods such as Taq-Man or SYBR Green-based detection.

In RT-qPCR, the amplification step is combined with fluorescent reporter dyes which allows the detection in real time [104,105]. The DNA produced in each cycle is proportional to the fluorescent signal which is detected and allows the analysis of gene expression. Thus, each qPCR reaction is characterized by a parameter known as the threshold cycle or quantification cycle (C^T or Cq) [105]. This value is described as "the PCR cycle at which fluorescence first rises above a defined or threshold background fluorescence", thus, the C^T value is inversely proportional to the quantity of target there is in the starting material. The correlation between fluorescent signal and the amount of target in sample allows the relative or the absolute quantification of expressed RNA [104,105]. However, to analyse the data from RT-qPCR there are several methods described in literature. The most used method of presenting quantitative real-time PCR data is the comparative C^T method, also known as the $2^{-\Delta\Delta C_T}$ method. To use this method, the investigator must assume that the PCR efficiency is approximately 1 and that the efficiency of the target gene amplification reaction is similar to the efficiency of amplification of the reference gene.

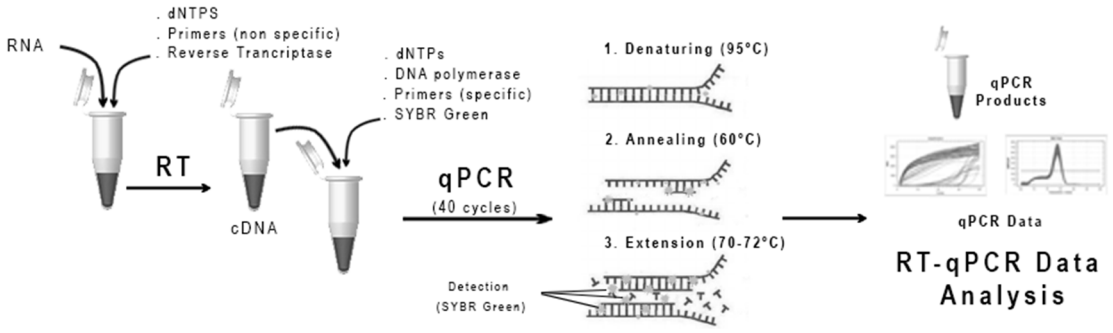

Figure 7 - Schematic representation of the RT-qPCR technique steps and most relevant molecular events. RNA is first transcribed into cDNA by reverse transcriptase. The cDNA is then used as the template for the qPCR. There are three major steps that make up each cycle in a qPCR which occurs at different temperatures: denaturation (usually 95ºC), annealing (temperature defined by primers, but usually ≈ 60ºC) and extension (dependent on the polymerase used in the reaction). The detection of amplified products is done in real-time through detection methods such as the one depicted, SYBR Green-based detection. *Adapted from: Chang C-M, et al, 2013.[106]*

Regarding all these aspects, the implementation of RT-qPCR method has many advantages when it is intended to evaluate several genes in different conditions. In this way, this technique is perfectly applied to the objectives of this work, since it will be necessary to evaluate the expression of ECM components and growth factors by two different cell lines when treated with Exo-101.

WB or immunoblotting, has been a commonly used technique for the determination and semi-quantitation of protein expression in cells or tissues. WB was first described by H. Towbin et al in 1979 [107]. In WB, protein samples are usually the soluble components of cell or tissue lysates [108]. After this samples are reduced by addition of reducing components, such as β-mercaptoethanol, and denatured by boiling, they are load in a polyacrylamide gel and fractioned using electrophoresis with sodium dodecyl sulfate, sodium salt (SDS) [109]. This technique is commonly referred as SDS-PAGE. The SDS binds the proteins in the sample, providing a negative charge to protein and uniformizing the density of the charges. In other words, the SDS gives negative charge to a particular protein proportionally to its molecular weight (MW). Thus, the separation of the proteins in the samples by SDS-PAGE is caused by their attraction to anode, but based on the MW of each protein. The polyacrylamide gel allows the physic support to protein migration and separation by their MW. After SDS-PAGE, the protein in gel are then transferred onto a polyvinylidene difluoride (PVDF) or nitrocellulose membrane. The protein of interest is recognized by the specific primary antibody after a blocking step. This step is important because it blocks the possible non-specific binding of the primary antibody. The primary antibody is recognized by a secondary antibody, which is commonly tagged with the enzyme horseradish peroxidase (HRP) [110]. This enzyme catalyses the oxidation of luminol (substrate), leading to the emission of light at

428nm which is detected by digital imagers. The principal WB steps are represented in Figure 8.

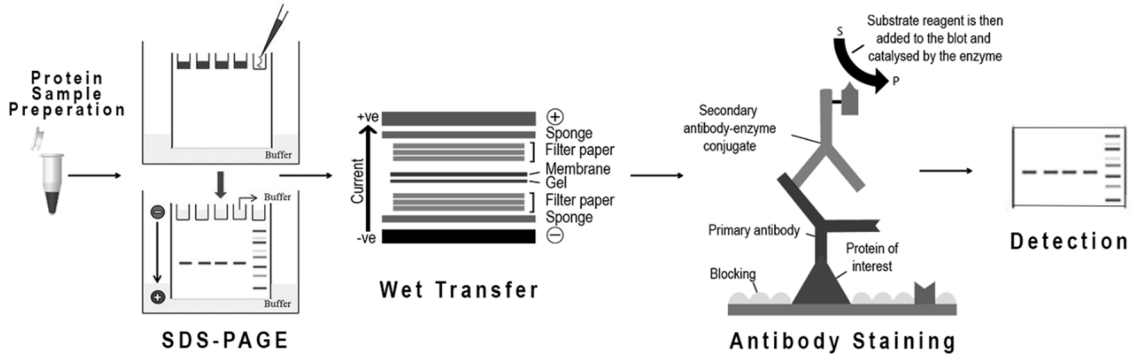

Figure 8 - Scheme representing the Western Blot technique steps and important molecular events.
Samples are previously prepared and then loaded into a polyacrylamide gel, followed by SDS-PAGE. After the SDS-PAGE, the proteins in the gel are then transferred onto a membrane, which is then submitted to a blocking step. The protein of interest is recognized by the specific primary antibody, which is in its turn recognized by a secondary antibody, commonly tagged with HRP. The peroxidase catalyses the oxidation of a substrate, leading to the emission of light that can be detected with digital imagers. *Adapted from: Protein Blotting Guide, Bio-Rad [111]*

The association of SDS-PAGE, to separate proteins by MW, and the specificity of antibody-antigen interaction make WB a sensitive and specific technique [108]. Thus. this technique has been an essential analytical tool to identify a specific protein in a complex mixture [109]. The data providing by WB is most commonly used to a semi-quantitative quantification of specific proteins production. However, WB can also be used as an absolute quantification method.

Applying these concepts to proteins of interest for this work, it is noticeable that there are two characteristics inherent in them that might influence the results of WB: their MW and the way they are secreted and assembled. The theoretical MW calculated by ExPASy for the proteins or interest are: Fn =260kDa; Col1a1=95kDa; Col1a2=94kDa; Col3a1=95kDa. Proteins with MW greater than 140kDa may not being transferred to the membrane [112]. In wet transfer, when the proteins of interest have a MW greater than 80kDa, in order to increase the efficiency of transfer it is advisable to use a small percentage of SDS in the constitution of the transfer buffer. *In vivo*, these proteins are produced, secreted and naturally assembled in a complex network of biomolecules in the extracellular space [16]. However, this process *in vitro* isn't so well described, and in a mono cell culture we did not find the cellular and molecular complexity that we observed *in vivo*. Nevertheless, there are evidences that dermal fibroblasts construct an ECM composed of Fn and Col even *in vitro,* depending on the culture time of these cells [58,75]. Thus, the implementation of the WB technique can be an asset to the company, not only to evaluate the modelling of the production of ECM components, with the necessary optimizations due to the particularities of these proteins, but also to other activities of the company itself.

Immunocytochemical staining is also commonly used for the analysis of protein expression in isolated cells or cell cultures. In ICC, the cells are seeded in appropriated material and

subsequentially fixed [113]. There are various fixation methods described and the most commonly used are the fixation with paraformaldehyde (PFA), cold methanol or acetone [113,114]. As in the WB, after a blocking step, the protein of interest will be identified using a primary antibody, and a secondary antibody is used to recognize the first one. In ICC, secondary antibody is tagged with a fluorophore which allows the detection through a fluorescence microscope. To obtain more comprehensible results it is common to label some cellular structures, such as the nuclei or cytoskeleton, in order to have a better perception about the cellular location of the protein of interest.

In contrast to WB, using ICC can provide relevant information about the cellular or extracellular location of interest protein [108,113,114]. However, only using this technique, the investigator can't distinguish nonspecific recognition from the true one predicted by the molecular mass of the interest protein. Thus, WB and ICC are commonly used together, complementing each other and allowing more robust conclusions. Besides that, as evidenced above, the manner in which ECM proteins are secreted and assembled may influence the results of ICC. Although the process of secretion and assembly of ECM *in vitro* by dermal fibroblasts isn't so well described, there are studies evaluating the production of ECM protein by ICC [58,75]. Even so, the implementation of the ICC together with WB technique is expected to generate interesting results on the modelling of ECM production and assembly.

Altogether, in this master thesis we implemented and used the above mentioned biomolecular methods to evaluate the mechanism of action of Exo-Wound, *in vitro*. In this work, we focus on the modulation of growth factors expression by keratinocytes and dermal fibroblasts, and on the effects on ECM components expression and production by dermal fibroblasts.

Chapter 2:
Material and Methods

2. Materials and Methods

This chapter provides a detailed description of all the protocols used in this work. The procedures described include 2.1. Cell Culture and Treatment, 2.2. Sample Collection, 2.3. Reverse Transcription Real-Time Chain Reaction, 2.4. Immunocytochemistry, and 2.5 Western Blot. The description of the mentioned procedures refers to typical conditions used for its accomplishment. These protocols, namely, RT-qPCR, ICC and WB may have undergone several changes after implementation and optimization steps described in chapter 3 – Results and Discussion – 3.1 - Implementation and optimization of biomolecular methods. In Figure 9 is exposed the experimental workflow intended to experimental work performed since the implementation of biomolecular methods to the validation of the use of these techniques to evaluate the expression and production *in vitro* of molecules of interest to this study, realizing preliminary tests.

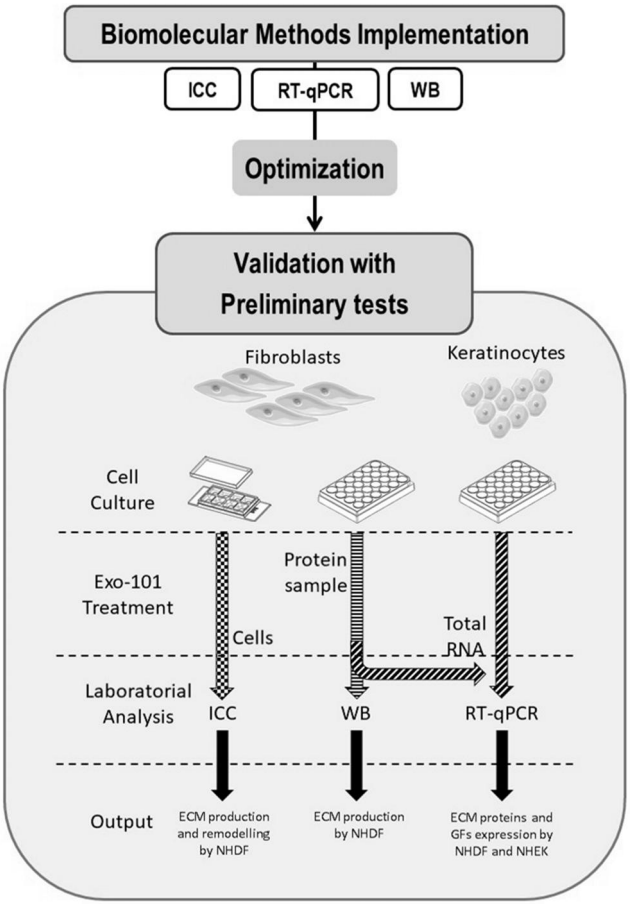

Figure 9 - Schematic overview of the experimental workflow intended for experimental work.
After implementation and optimization of the biomolecular methods RT-qPCR, ICC and WB, we performed some preliminary tests to validate their use in further evaluation of the expression of GFs and secretion of ECM components by fibroblasts and keratinocytes *in vitro*. Fibroblasts are cultured in the appropriate culture plates and treated with Exo-101. Then fibroblasts are analysed by ICC to evaluate production and remodelling of ECM. In addition, the secretion of ECM components is analysed by WB and the expression of these components and GFs are evaluated by RT-qPCR. Keratinocytes are treated with Exo-101 and the expression of GFs is studied by RT-qPCR.

2.1 Cell Culture and Treatment

- **Keratinocytes Culture**

Normal Human Epidermal Keratinocytes (NHEK; Lonza, Switzerland) were cultured in T75 culture flasks, maintained in an incubator with controlled temperature (37 ºC), CO_2 level (5%). NHEK cells were cultured in complete culture medium that is Dermal Basal Medium (LGC; ATCC-PCS-200-030; USA), supplemented with Keratinocytes Growth Kit - Low Serum (LGC; ATCC-PCS-200-040; USA), and 0.5% (v/v) PenStrep (GE Healthcare Life Sciences; SV30010). The cellular density advised by supplier to seed is 1000 cells/cm^2. Cells were subcultured when reaching ≈80% confluence. Briefly, cells were washed with pre-warmed phosphate-buffered saline (PBS) without Ca^{2+} and Mg^{2+} (Biochrom-Merck), detached with 0.05% (v/v) trypsin (GIBCO; 15400054) solution in PBS (Biochrom-Merck) at 37 ºC and then the reaction was stopped with culture medium. After that, cells were centrifuged for 5 minutes at 300x*g* and suspended in complete culture medium. The new cell culture has an initial density of approximately 1000 cells/cm^2.

- **Fibroblasts Culture**

Normal Human Dermal Fibroblasts (NHDF; Lonza, Switzerland) were cultured in T75 culture flasks, maintained in an incubator with controlled temperature (37 ºC), CO_2 level (5%). NHDF cells were cultured in complete culture medium composed of Fibroblasts Basal Medium (LGC; ATCC-PCS-201-030; USA) supplemented with Fibroblasts Growth Kit - Low Serum (LGC; ATCC-PCS-201-041; USA), which contains 2% (v/v) Fetal Bovine Serum (FBS), and with 0.5% (v/v) PenStrep (GE Healthcare Life Sciences; SV30010). The cellular density advised by supplier to seed is 1000 cells/cm^2. Cells were subcultured when reaching ≈80% confluence. Briefly, cells were washed with pre-warmed PBS (Biochrom-Merck) without Ca^{2+} and Mg^{2+}, detached with 0.05% (v/v) trypsin (GIBCO; 15400054) solution in PBS (Biochrom-Merck) at 37 ºC and then the reaction was stopped with culture medium. After that, cells were centrifuged for 5 minutes at 300x*g* and suspended in complete culture medium. The new cell culture has an initial density of approximately 1000 cells/cm^2.

- **Treatment with Exo-101**

To analyse the expression of GFs by human keratinocytes, when they are treated by Exo-101, were performed RT-qPCR. NHEK were counted using a Neubauer chamber (Sigma-Aldrich) and 0.4% (v/v) Trypan Blue (GE Healthcare Life Sciences; SV30084.01) solution in PBS (Biochrom-Merck). Then NHEK were cultured in a 24-well plate at a cellular density of 15000 cells/cm^2. NHEK were first cultured in respective complete culture medium and they were incubated in a humidified atmosphere at 37 °C with 5% CO_2 for 24 hours. After this, the medium was removed

and replaced by complete culture medium (composition described above – Fibroblasts Culture), exosome-depleted. To obtain the NHEK complete culture medium exosome-depleted, the complete culture medium is previously centrifuged for 14h at 100000x*g,* in order to remove the extracellular vesicles which may be present in the culture medium due to the FBS supplement. Then, Exo-101 was added to the medium using PBS (Biochrom-Merck) as a vehicle.

The secretion of GFs and ECM components by human fibroblasts, when they are treated by Exo-101, was assessed by WB, RT-qPCR and ICC. For all techniques, NDHF were counted using a Neubauer chamber (Sigma-Aldrich) and 0.4% (v/v) Trypan Blue (GE Healthcare Life Sciences; SV30084.01) solution in PBS (Biochrom-Merck). Then the cells were seeded at an appropriated density. To WB and RT-qPCR methods NHDF were cultured in a 24-well plate (VWR; 734-1306) in a cellular density of 12000 cells/cm^2. To perform ICC procedure NHDF were cultured in glass Culture Slides (VWR; 734-0089) in a cellular density of 15000 cells/cm^2. NHDF were first cultured in respective complete culture medium and they were incubated in a humidified atmosphere at 37 °C with 5% CO_2 for 24 hours. After this, the medium was removed and replaced by in Dulbecco's Modified Eagle Medium (DMEM) exosome-depleted, supplemented with 0.5% (v/v) FBS and 0.5% (v/v) PenStrep. Exo-101 was added to the medium using PBS (Biochrom-Merck) as a vehicle.

The treatment with Exo-101 was administrated at final concentration of 2.5 x 10^9 part/ml. Cells in treatment group with Exo-101 were treated in a repeated dose schedule of twice daily for 2 days (according to the scheme in Figure 10). The control group were treated with filtered PBS (Biochrom-Merck). Treatment was administered without medium replacement. The cells conditions were follow by microscopic observation with Inverted Microscope Zeiss Primo Vert during treatment period and before cells are detached. All cultures that acquired a strange morphological appearance or in which the culture medium had an abnormal colour were excluded.

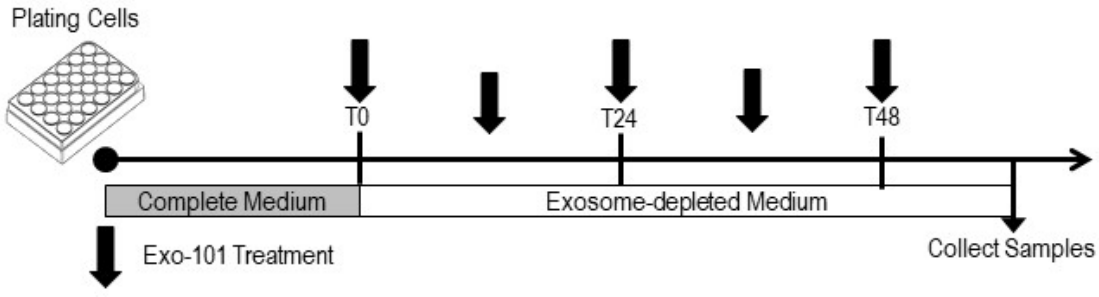

Figure 10 - Schematic overview of the Exo-101 treatment workflow used this study.
NHEK and NHDF are plated in 24-well plates or in culture slides with respective complete medium. After 24 hours, the culture medium is replaced by the appropriate exosome-depleted medium and the time of treatment begins (T0). The Exo-101 is applied in a repeated dose schedule of twice daily for 2 days. 24 after the last treatment, the CM and cells are collected.

2.2 Samples Collection

To perform the WB and RT-qPCR analysis were collected protein samples (conditioned medium and cell lysates) and total RNA samples. The procedures applied to collect these samples are described in present section.

- **Conditioned Medium (CM) Collection**

The CM from NHDF culture was collected and centrifuged at 300x*g* for 10 minutes at 4ºC and the pellet was discarded. The resulting samples were preserved at -20ºC. The total protein of each sample was quantified with a Pierce™ BCA protein assay (Thermo Fisher Scientific).

- **Cell Lysates Collection**

NHEK and NHDF were cultured in complete medium and cultured as previously described. Cultured cells were washed with pre-warmed PBS (without Ca^{2+} and Mg^{2+}), detached with trypsin 0.05% at 37 ºC and then the reaction was stopped with culture medium. After that, cells were centrifuged for 5 minutes at 300x*g* and then suspended in 200µl of radioimmunoprecipitation assay (RIPA) lysis buffer supplemented with proteases inhibitor. The resulting samples were collected and incubated for 30 minutes on ice. After ice incubation, the samples were centrifuged at 14000x*g* for 10 minutes at 4ºC and supernatant were preserved at -20ºC. The total protein of each sample was measured using Pierce™ BCA protein assay (Thermo Fisher Scientific).

- **Total RNA Extraction**

The total RNA of NHEK and NHDF cultures was isolated using an organic method with Trizol reagent (NZYol; NZYTech). After CM collection, each well was washed two times with PBS and then Trizol was added. After all the cells were detached and the solution was collected. At this stage, samples could be stored for at least one month at -80°C. Before initiate the RNA extraction, samples were incubated at room temperature for 5 minutes. Chloroform (DNase, RNase and protease free; Fisher Bioreagents) was added. The solution was shacked vigorously for 15 seconds, incubated for 5 minutes at room temperature and then centrifuged at 12000x*g* for 15 minutes at 4ºC. After this step, 3 phases were formed: Aqueous colorless (containing RNA); Interphase white (containing DNA); and Organic green (containing protein). The aqueous phase was collected and then the RNA was precipitated with addiction of isopropanol for molecular biology (Fisher Bioreagents). The solution was incubated at room temperature for 10 minutes and then centrifuged at 12000x*g* for 10 minutes at 4ºC. The resulting pellet was washed with 75% ethanol absolute for molecular biology (Fisher Bioreagents) solution and centrifuged at 7500x*g* for 5

minutes at 4ºC. The supernatant was discarded. When dry, the resulting pellet was resuspended in 20µl of ddH_2O (NZYTech) and the RNA concentration was measured in NanoDrop (Thermo Scientific). All RNA samples were stored at -80ºC.

2.3 Reverse Transcription Real-Time Polymerase Chain Reaction

To detect GFs and ECM components expression in response to Exo-101 treatment, the NHEK and NHDF total RNA was isolated using an organic extraction method with Trizol described above. Then mRNA samples were analysed by RT-qPCR to detect the expression of Fn, Col1, Col3, TGF-β1, FGF-2, FGF-7 and VEGF-A. The protocol of RT-qPCR described in this section refers to a typical protocol of this technique (Figure 11). Changes and optimizations to this protocol are described in chapter 3 – Results – 3.1 - Implementation and optimization of laboratory techniques.

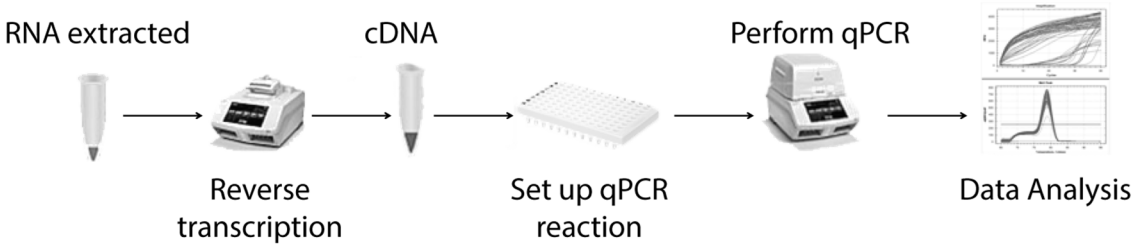

Figure 11 - Schematic workflow summarizing a RT-qPCR protocol commonly used in laboratories of cellular and molecular biology.
After RNA extraction and the reverse transcription, the resulting cDNA is then used as the template for the qPCR. All components involved in qPCR are prepared and mixed, and then the reaction is performed. The detection of amplified products is done in real-time and the analysis of the resulting data is posteriorly executed.

- **cDNA Synthesis**

RNA was reverse-transcribed according to manufacturer's instructions of SuperScript IV VILO Master Mix (Invitrogen). This master mix contains the necessary components for reverse transcription, including reverse transcriptase, random hexamer primers, $MgCl_2$ and dNTPs. 500ng of RNA were mixed with 4µl of the referred mix master mix. DEPC H_2O were add to 20µl of a final volume. All mixtures were incubated in a thermocycler first at 25ºC for 10 minutes, then at 50ºC for 10 minutes and finally at 85ºC for 5 minutes. After reverse transcription, the cDNA was immediately used for RT-qPCR or were preserved at -20ºC.

- **qPCR**

To performer RT-qPCR, each cDNA sample was amplified using DyNAmo HS SYBR Green qPCR Kit (Thermo Fisher Scientific) on the 7500 Fast Real-time PCR System (Applied Biosystems). Briefly, the reaction conditions consisted of 1µl of cDNA (1:5 dilution), and a solution composed of 0.5µM of each primer pair, 5µl of DyNAmo HS master mix and 3.5 µl of DEPC H_2O. The master mix used contains the necessary components for real time polymerase chain reaction, such as DNA polymerase, SYBR Green I, $MgCl_2$ and dNTPs. The qPCR cycling parameters were 95°C for 15 minutes (initial denaturation); 40 cycles of 1 minute at 95°C, 1 minute at 60°C (annealing) and extension at 72°C. The primers were listed in Table 1. GAPDH was used as an

endogenous control to normalize each sample. This experiment was performed with technical triplicates.

Table 1 - List of primer pairs used in RT-qPCR procedures.
In this list is discriminated the name, reference and amplicon length of each primers pair used.

Name	Sequence (5' to 3')	Amplicon	Reference
GAPDH	F: ACAGTTGCCATGTAGACC	76 bp	Sigma
	R: TTGAGCACAGGGTACTTTA		
FN1	F: CCATAGCTGAGAAGTGTTTTG	103bp	Sigma
	R: CAAGTACAATCTACCATCATCC		
COL1A1	F: GCTATGATGAGAAATCAACCG	199 bp	Sigma
	R: TCATCTCCATTCTTTCCAGG		
COL3A1	F: ATTCACCTACACAGTTCTGG	83 bp	Sigma
	R: TGCGTGTTCGATATTCAAAG		
TGFB1	F: AACCCACAACGAAATCTATG	146 bp	Sigma
	R: CTTTTAACTTGAGCCTCAGC		
FGF2	F: TGGCTTCTAAATGTGTTACG	129 bp	Sigma
	R: GTTTATACTGCCCAGTTCG		
FGF7	F: CTTCTGCCTGTTGATTTATGG	180 bp	Sigma
	R: TAGTAAGTTCAGTTGCTGTG		
VEGFA	F: AATGTGAATGCAGACCAAAG	106 bp	Sigma
	R: GACTTATACCGGGATTTCTTG		

- **Data Analysis**

The resulting data from RT-qPCR was analysed using Thermo Fisher Cloud Design and Analysis app. Each triplicate gives a mean number of amplification cycles for each reaction. If there is an outsider in the triplicate group, analysing the standard deviation of the mean, the furthest is excluded. Each melting curve was analysed in terms of melting temperature and peak numbers. The relative expression of the genes of interested was analysed according to the $2^{-\Delta Ct}$ method and the comparison between experimental groups was performed using this data.

2.4 Immunocytochemistry

To visualize the possible modulation of the production and remodelling of ECM proteins by NHDF in response to Exo-101 treatment, these cells were subjected to ICC with immunofluorescence staining to Fn, Col1 and Col3. The protocol of ICC described in this section refers to a typical protocol of this technique (Figure 12). Changes and optimizations to this protocol are described in chapter 3 – Results – 3.1 - Implementation and optimization of laboratory techniques.

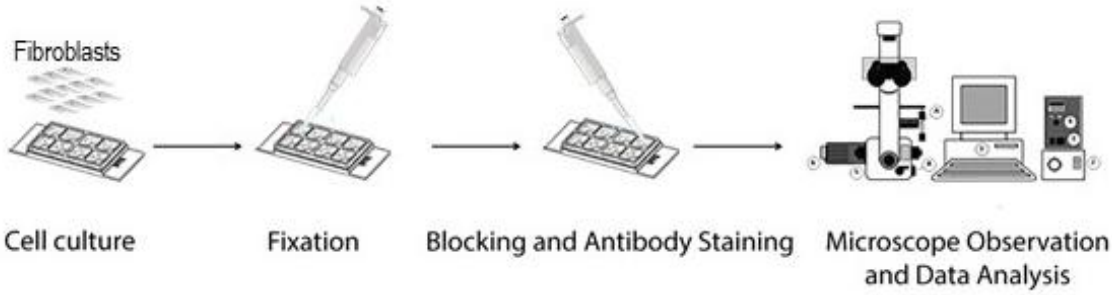

Figure 12 - Schematic workflow summarizing the Immunocytochemistry protocol commonly used in laboratories of cellular and molecular biology.
Cells are cultured in glass slides, and then exposed to the fixation protocol. Specific primary antibodies are used according to the proteins of interest, as well as secondary antibodies and/or fluorescent dyes. Finally, cells are inspected under microscope.

- **Cell preparation and Fixation**

NHDF were cultured for 24 hours cultured in glass Culture Slides using complete medium. Theoretically, the proteins of interest in this test, Fn, Col1 and Col3, should be in extracellular space, therefore a step of permeabilization seems to be unnecessary. Culture medium were removed and cells were washed 2 times with PBS. Then, cells were fixed using a typical fixation method to ICC, the PFA (VWR) fixation. NHDF were fixed using 4% solution of PFA in PBS for 15 minutes at room temperature and preserved at 4ºC. Fixed cells were preserved in unfiltered PBS at 4ºC.

- **Blocking and Staining**

Before staining cells with appropriated solutions, each well was blocked using a 5% bovine serum albumin (BSA; Sigma-Aldrich) solution in PBS for 1 hour at room temperature and washed 3 times with PBS for 5 minutes. To immune staining each well was incubated with appropriated primary antibodies in a solution of 1% BSA solution in PBS overnight at 4ºC. Cells were washed 3 times with PBS for 5 minutes. The appropriated secondary antibody conjugated to an Alexa Fluor dye was added in a solution of 1% BSA solution in PBS. Information about the used antibodies are shown in the Table 2. In addition, to nuclei staining was used 4',6-diamidino-2-phenylindole (DAPI; VWR) which was added at a concentration of 1µg/mL in PBS for 15 minutes at 37ºC.

Table 2 - List of antibodies used in Immunocytochemistry procedure.
In this list is discriminated the name, reference and dilution of each antibody used.

Antibody	Reference	Dilution
Anti-Human Fibronectin	11324553, Invitrogen	1:200
Anti-Human Collagen I	ab34710, Abcam	1:100
Anti-Human Collagen III	ab7778, Abcam	1:100
Alexa Fluor 488 Anti-Mouse	10544773, Invitrogen	1:500
Alexa Fluor 568 Anti-Rabbit	15656405, Invitrogen	1:500

- **Microscope Observation and Image Analysis**

After staining, the cells were observed with a fluorescence microscope, Carl Zeiss Axio Imager Z2, with ApoTome2 and Stereo-Investigator. The cells were observed with several levels of magnification (10x, 20x, 40x). The obtained images were analyzed and mean fluorescence intensity (MFI) was quantified using ImageJ (NIH) software for each protein of interest analysed. In detail, the MFI was obtained using Measure tool and normalized to nucleus counting, analysing at least three fields for each well/condition.

2.5 Western Blot

To detect ECM components production or secretion in response to Exo-101 treatment, the WB technique. The protocol of WB described in this section refers to a typical protocol of this analytical technique (Figure 13). Changes and optimizations to this protocol are described in chapter 3 – Results – 3.1 - Implementation and optimization of laboratory techniques.

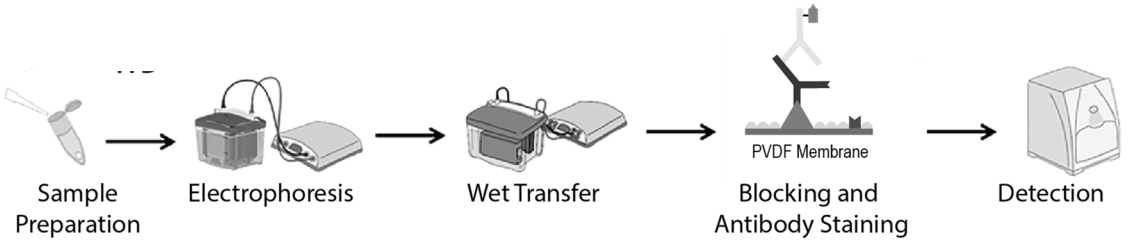

Figure 13 - Schematic workflow summarizing the Western Blot protocol commonly used in laboratories of cellular and molecular biology.
Samples are previously prepared and then it is performed an electrophoresis, namely SDS-PAGE. After this step, the proteins in the gel are transferred onto a membrane, which is then submitted to a blocking and antibody staining steps. The secondary antibody is conjugated with a detection method that allows its detection.

- **Samples preparation**

After total protein quantification with a Pierce™ BCA protein assay (Thermo Fisher Scientific), each sample was aliquoted with the same protein quantity (µg). To reach a reasonable volume to load in acrylamide gel, some samples were subjected to an evaporation step using an Eppendorf Vacuum Concentrator (Eppendorf) system. To denature and reduce the proteins in samples, a 4x Laemmli Sample Buffer (Bio-Rad) with β-mercaptoethanol (Fisher Bioreagents) was added at proportion of 1:4. The mixture was heated at 95°C for 5 minutes. Then, an electrophoresis was performed.

- **SDS-PAGE**

The gels used in the SDS-PAGE technique are characterized by the percentage of polyacrylamide in its constitution that may vary depending on the type of proteins under study. An SDS-PAGE gel is normally composed by two parts: i) the running gel allows migration and separation of protein in samples by their MW; and ii) the stacking gel is where the samples are loaded and its function is to pack all the sample, assuring that they will start the migration at the same time. A 10% polyacrylamide gel was used as a standard gel for this technique. Each gel used was composed by one 4% stacking gel (ddH2O, acrylamide, tris-HCl 0.5 M, pH 6.8, SDS 10%, Adenosine 5'-Phosphosulfate (APS; Fisher Bioreagents) 10%, Tetramethylethylenediamine (TEMED; Fisher Bioreagents) that have wells where the samples are loaded, and one 10%

resolving gel (ddH2O, acrylamide, tris-HCl 1.5 M, pH 8.8, SDS 10%, APS 10%, TEMED), where the proteins are separated. The gels components and their quantity are listed in Table 3.

To run the sample in electrophoresis the gels were submerged in 1x running buffer (0.25M Tris, 1.92M Glycine, 1% SDS pH 8.6). Running buffer provides not only the proper ions to transmit the necessary charge to electrophoresis separation, but also a reservoir of weak acid and base, which keeps the pH within a narrow range. The components of the running buffer and their quantity are listed in Table 4. Then the samples and 5µl of molecular weight ECL Rainbow Marker - Full range (Amersham Life Science) were load in wells of stacking gel. The electrophoresis run at a voltage between 90V and 120V. When the dye molecule or the "migration front" reached the bottom of the gel, the power is turned off and proceeded immediately to transfer.

Table 3 - Reagents used in preparation of 10% Acrylamide gels and their corresponding and correspondent quantities.

	Resolving Gel (10%)	Stacking Gel (4%)	Reference
ddH2O	3.8 mL	3.1 mL	---
Acrylamide (40%)	2 mL	500 µL	Fisher Bioreagents
1.5M Tris pH 8.8	2 mL	…	Bio-Rad
0.5M Tris pH 6.8	---	1.25 mL	Bio-Rad
10% SDS	80 µL	50 µL	Fisher Bioreagents
10% APS	80 µL	50 µL	Fisher Bioreagents
TEMED	8 µL	5 µL	Fisher Bioreagents

Table 4 - Reagents used in preparation of Running buffer and their corresponding quantities.

	Running Buffer (1L)	Reference
ddH2O	890 mL	---
0.25M Tris, 1.92M Glycine	100 mL	Bio-Rad
SDS 10%	10 mL	Fisher Bioreagents

- **Wet Transfer**

In wet transfer, the proteins in electrophoresis gel were transferred to PVDF membranes (Amersham Life Science) using an electrical potential, only after the PVDF membranes have been activated in methanol for 10 seconds. This activation is necessary because PVDF is very hydrophobic, and without the previous methanol treatment the aqueous buffers, such as transfer buffer, will not penetrate the membrane, resulting in poor transfer efficiency. The gel and membrane are stacked between sponge and paper filter and all are clamped tightly together after ensuring no air bubbles have formed between the gel and membrane. The transfers occurred submerged in transfer buffer (0.25M Tris, 1.92M Glycine, methanol, pH 8.3) on ice at 100V for 90 minutes. This buffer, such as running buffer, transfer buffer is used not only to humidify the system but also to maintain conductivity and pH. In addition, methanol is normally included in the transfer

buffer to promote binding of proteins. The components of the transfer buffer and their quantity are listed in Table 5.

Table 5- Reagents used in preparation of Transfer Buffer and their corresponding quantities.

	Transfer Buffer (1L)	Reference
ddH2O	690 mL	---
0.25M Tris, 1.92M Glycine	100 mL	Bio-Rad
Methanol	200 mL	Fisher Bioreagents
SDS 10%	10 mL	Fisher Bioreagents

- **Blocking, antibody incubations, signal development and detection**

After transfer, the membrane was washed in ddH2O and it can be stained with Ponceau Red (Alfa Aesar) to guarantee that the SDS-PAGE and transfer steps were successful. The membrane stained with Ponceau Red must be washed with ddH2O until the staining is completely removed. Then, the membrane immunostaining step is followed. The membranes were blocked with a solution of non-fat milk 5% in Tris Buffered Saline (TBS) with Tween-20 (TBS-Tween) for at least 30 minutes at room temperature. TBS-T solution was prepared diluting TBS 10x solution, with the reagents that are listed in Table 6, to 1x and adding 0.1% of Tween-20 (Fisher Bioreagents). After blocking the membrane were washed 2 times in TBS-Tween for 5 minutes. Then, the blots were incubated with the appropriate primary antibodies, diluted in TBS-Tween with 0.5% of non-fat milk, overnight at 4ºC. After incubation with primary antibodies, each membrane was washed 3 times in TBS-T for 5 minutes. The membranes were then incubated with appropriated peroxidase-conjugated secondary antibodies for 90 minutes to 2 hours at room temperature. Information about the used antibodies are shown in the Table 7. To signal development and detection, each membrane was washed 3 times in TBS-T for 5 minutes and incubated with ECL chemiluminescence detection reagents (GE Healthcare Life Sciences) for 5 minutes. The signal was detected and visualized using a chemiluminescent detection system of VWR imager Chemi 5QE Image Capture Software. Images were analysed by ImageJ software (NIH).

Table 6 - Reagents used in preparation of TBS and their corresponding quantities.
After all reagents were mixed, ddH2O was added to volume of 1L.

	TBS 10x (1L)	Reference
ddH2O	900 mL	---
Tris base	24g	Fisher Bioreagents
NaCl	88g	VWR
HCl	Until pH=7.6	Fisher Bioreagents

Table 7 - List of antibodies used. In this list is discriminated the name, reference and dilution of each antibody used.

Antibody	Reference	Dilution
Anti-Human Actin C4	MAB1501, Merck Millipore	1:2500
Anti-Human Fibronectin	11324553, Invitrogen	1:1000
Anti-Human Collagen I	ab34710, Abcam	1:1000
Anti-Human Collagen III	ab7778, Abcam	1:5000
ECL Rabbit IgG	NA934-1ML, GE Healthcare	1:1000
ECL Mouse IgG	NA931-1ML, GE Healthcare	1:1000

2.6 Statistical Analysis

Statistical analysis of the data was performed with GraphPad Prism 6 software. The analyses were performed using an unpaired and non-parametric test, namely Mann-Whitney test. The statistical significant level chosen for all statistical tests was p-value (p)<0.05. Results were shown as mean ± standard error of the mean (SEM) and, when appropriated, they are marked with one asterisk (*) if p<0.05 and non-significant (ns) if p>0.05.

Chapter 3:
Results and Discussion

3. Results and Discussion

3.1 Implementation and Optimization of Biomolecular Methods

This section describes the main steps required for the implementation and optimization of laboratorial techniques. The techniques implemented following this work were RT-qPCR, Immunocytochemistry and Western Blot. These techniques are typical procedures used in a biochemistry laboratory and were not available in Exogenus Therapeutics' laboratory. Thus, the implementation of these techniques was an important step for the company, enabling the partial assessment of the product mode of action *in vitro*.

3.1.1 Reverse Transcription Real-Time Polymerase Chain Reaction

RT-qPCR is a technique currently used in biochemistry laboratories that aims to assess mRNA expression in different samples. Using this technique, it is possible to achieve a relative or an absolute quantification of expression of molecules of interest using specific primers. RT-qPCR allows the analysis of gene expression of several molecules in multiple samples in the same experiment.

a. Implementation

The implementation of RT-qPCR technique for evaluation of ECM components and GFs expression in Exogenus' laboratory involved the order of needed material, the assembly of work area and the optimization of some conditions. In a first phase of RT-qPCR implementation, the protocol performed were described in 2. Material and Methods – 2.3 Reverse Transcription Real-Time Chain Reaction. All primers were tested with RNA samples extracted from NHDF or NHEK cultured with typical conditions using the RNA extraction method described in 2. Material and Methods – 2.2 Samples Collection. The quantification and the values used to analyse the quality of samples are shown in Table 8. All primers, ECM components and GFs genes, were tested with NHDF samples, and only primers to GFs genes were tested with NHEK. In this first experiment, it was analysed the C^T mean values (Table 9) and melt curves of each reaction (Figure 14).

Table 8 – Example of the data that is obtained in RNA total quantification using NanoDrop (Thermo Scientific).

Sample	Total RNA Quantification (ng/µl)	A260/280	A260/230
NHDF	4163,4	1,81	1,32
NHEK	4505,4	1,76	1,77

The data resulting of total RNA analysis in NanoDrop shows a great concentration of RNA in both samples. However, the values corresponding to A260/280 and A230/260 aren't the optimal. These two ratios of absorbance provide indications on contamination of RNA samples. The value of A260/280 ratio should be between 1.8 and 2.1 and provides indications mainly of protein contamination. The ratio value A260/230 should be between 1.6 and 2.0 and provides indications of contamination with organic solvents. Although the values of the analysed samples are not optimal, they are close to the recommended limits. thus, it was decided to proceed with the RT-qPCR procedure.

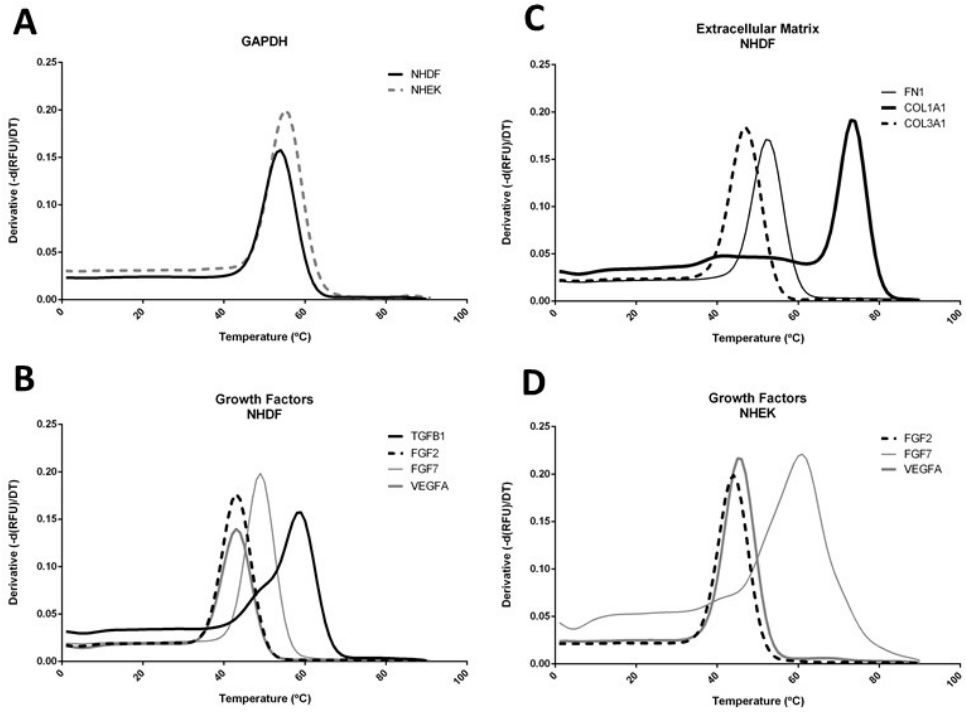

Figure 14 - Melting Curves of the amplification products of the genes tested with NHDF and NHEK RNA samples.
A) GAPDH melting curve resulting of RT-qPCR performed with NHDF and NHEK RNA samples. **B)** TGFB1, FGF2, FGF7 and VEGFA melting curves resulting of RT-qPCR performed with NHDF RNA sample. **C)** FN1, COL1A1 and COL3A1 melting curves resulting of RT-qPCR performed with NHDF RNA sample. **D)** FGF2, FGF7 and VEGF-A melting curves resulting of RT-qPCR performed with NHEK RNA sample.

Table 9 - C^T mean values of the amplification reactions for each primer pair tested with NHDF or NHEK RNA samples.
(*) – TGFB1 wasn't tested with NHEK RNA sample.

Gene Name	C^T mean value with	
	NHDF RNA sample	NHEK RNA sample
GAPDH	20.4	19.4
FN1	17.8	----------
COL1A1	19.9	----------
COL3A1	18.8	----------
TGFB1	24.7	*
FGF2	24.3	25.1
FGF7	26	32
VEGFA	29.3	24.2

The resulting data from the implementation experiment of RT-qPCR show that GAPDH, FN1, COL1A1, COL3A1, FGF2 and VEGFA seems to have a correct amplification, since these genes have C^T mean values lower than 30, to both RNA samples tested. These genes have presented normal melting curves and melting temperatures near to the expected. To NHDF RNA sample, the TGFB1 gene have a good C^T mean (C^T=24.7), however the melting curve present a sight elevation before the peak. Due to that this gene wasn't tested with NHEK RNA sample. When the FGF7 gene is tested to NHDF seems to have a correct amplification and melting curve. However, when this gene is tested to NHEK RNA sample, it shows an abnormal melting profile and a high C^T mean (C^T=32). Concluding, the RT-qPCR procedure to GAPDH, FN1, COL1A1, COL1A3, FGF2, FGF7 and VEGFA genes in RNA sample from NHDF can be further used, since these genes shown good amplification and melting outputs. To RNA samples from NHEK, the RT-qPCR procedure to the GAPDH, FGF2 and VEGFA can advance too. The TGFB1 and FGF-7 genes will be tested with a higher annealing temperature in a step for optimization of annealing temperature.

b. Optimization

Along with the previously experiment, were also tested some variables that influence the obtained results, such as number of cells for RNA extraction, RNA quantity to cDNA synthesis, cDNA quantity to qPCR and primers concentration. The exact procedures of these optimizations are described on the basis of primer test in first experiment. Most optimizations were performed with GAPDH, but some were performed for optimization of specific primers.

- **RNA Extraction**

A concern in RNA extraction is the initial number of cells and correspondent starting amount of RNA. In this perspective, we tested the RNA quantity extracted from cellular cultures with different cell numbers and from different well plates (Figure 15A). The cells were seeded in different numbers and in different well plates, and 24h later the cells were removed with Trizol reagent (NZYol; NZYTech). After culture. each well was washed two times with PBS and then Trizol was added. After all the cells were detached, the solution was collected and chloroform was added. The remainder protocol was followed as described earlier in 2. Material and Methods – 2.3 Reverse Transcription Real-Time Chain Reaction section. With this experience, we want to understand if it is possible to obtain enough quantity of RNA from a cell culture in 24 well plate extracted with Trizol method. This will help to decide what number of cells and which plate is better to perform the experiment with Exo-101 treatment.

A

24 well plate	12 well plate
20 000 cells/well	30 000 cells/well
30 000 cells/well	40 000 cells/well
40 000 cells/well	50 000 cells/well

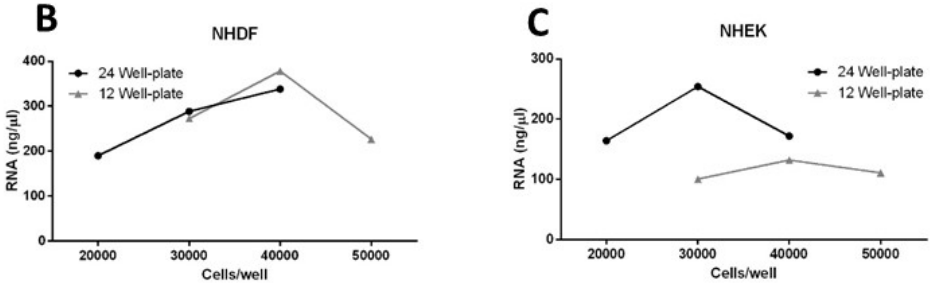

Figure 15 - Information relative to different cell culture conditions to RNA extraction procedure.
A) Table with types of well plate used and correspondent number of cells seeded to posterior RNA extraction. **B and C)** Amount of RNA extracted from NHDF **(B)** and NHEK **(C)** cultured in different types of plates and with different numbers of cells seeded.

Relatively to NHDF, these results showed that the quantity of RNA extracted is optimized for 40000 cells/well in both 24 well plate or 12 well plate (Figure 15B). However, this quantity of RNA was extracted 24 hours after they were seeded. In an experiment with treatment, the cells were maintained in culture for three days. It is expected that in this time the cell increases their number. Then, 30000 cells/well can be a better option for RNA extraction and subsequent RT-qPCR, since from these cultures we can extract a reasonable amount of RNA. Relatively to the well plate to use, these results showed that with 30000 the quantity of RNA extracted is approximately the same in both 24 well plate or 12 well plate. Then, in this case we will chose the 24 well plate because they have a less consumption of culture media and test substance, and this allows to increase the experimental replicates.

In the experiment using NHEK, the results do not follow the same pattern as for NHDF extraction (Figure 15C). This can be due to variability induced by RNA extraction method or may be related with the differences between these two cell types. However, with these conditions it was obtained enough quantity of RNA from 24 well plate of any cell density to perform a RT-qPCR. Then, we will choose the 24 well plate because they have a less consumption of cells, culture media and test substance, and this allows to increase the experimental replicates.

- **RNA/cDNA quantity**

To verify which is the best RNA quantity to optimize the RT-qPCR reactions, we tested different quantities of RNA of NHDF sample, which was later reverse transcribed to cDNA before the qPCR experiment. cDNA synthesis was performed as described in 2. Material and Methods – 2.3 Reverse Transcription Real-Time Chain Reaction. In addition to different quantities of RNA used to cDNA synthesis, also different concentrations of cDNA were used in qPCR. qPCR

procedure was performed as described in 2. Material and Methods – 2.3 Reverse Transcription Real-Time Chain Reaction section. All tested conditions and results are represented in Figure 16. The primer pair used in this experiment was the one for amplification of GAPDH gene, which was the normalization gene used in RT-qPCR experiments.

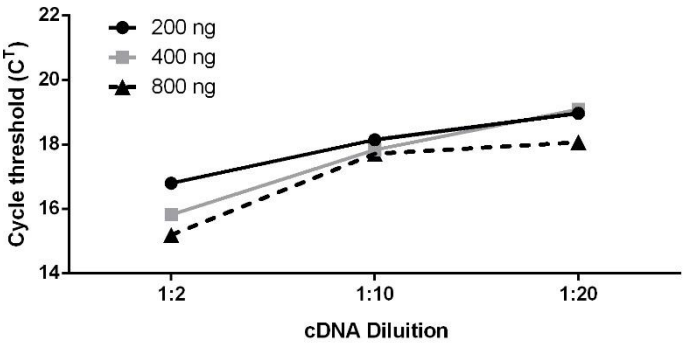

Figure 16 - The influence of starting RNA amount and cDNA dilution on the performance of RT-qPCR.
The RNA starting quantities (200ng, 400ng, 800ng) and the correspondent cDNA dilutions (1:2, 1:10; 1:20) used in RT-qPCR procedure are presented and related to the resulting amplification C^Ts of GAPDH.

These results showed that when more quantity of cDNA is used in qPCR a smaller number of amplification cycles is needed to reach the amplification threshold (Figure 16). With a quantity of 800ng of RNA and a cDNA dilution of 1:2 we could obtain a lower C^T in the amplification reaction of GAPDH (~15 cycles). However, with a quantity of 400ng of RNA and a cDNA dilution of 1:10 GAPDH amplification threshold increased to approximately to 17 cycles, which is an acceptable C^T number for a typical qPCR experiment, and further represents a significant saving in the quantity of RNA/cDNA to be used. In order to assure an optimized experimental workflow in the laboratory work, the following RT-qPCR experiments were performed with 500ng of starting total RNA, to reverse transcription reaction, and a 1:5 dilution of cDNA.

- **Primer concentration**

To attest if the primer concentration needed to be optimized, four different concentrations (0.3 µM, 0.5 µM, 0.7µM and 1µM) of GAPDH primer pair were tested in qPCR with NHDF RNA standard sample.

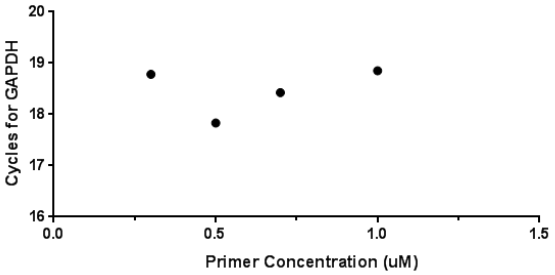

Figure 17 - Graphic representation of amplification cycle obtained with different primer concentrations used in RT-qPCR to amplify GAPDH gene.

The obtained results showed that with a concentration of 0.5µM we reached a smaller number of qPCR cycle threshold to amplify GAPDH (Figure 17). Thus, 0.5µM will be used as our standard primer concentration. However, it can be changed according to the particular results of each of the primer pairs.

- **qPCR Master Mix**

In Exogenus Therapeutics' laboratory, there are two master mixes available that can be used in qPCR reaction: the NZYSpeedy qPCR Green Master Mix (2x; with ROX) and the DyNAmo™ HS SYBR™ Green qPCR Kit. The DyNAmo master mix was the first ordered master mix and it was used in the in most of the experiences described above. Due to irrelevant reasons for this work, this master mix were replaced by NZYSpeedy master mix. Thus, to understand if the differences between these master mixes can significantly affect the performance of the qPCR reaction, we tested different samples of RNA with both master mixes in a qPCR procedure using GAPDH primers. This experiment was performed in a different equipment, CFX96 Touch™ Real-Time PCR Detection System (Bio-Rad). The qPCR cycling parameters were 95°C for 2 minutes (initial denaturation); 40 cycles of 5 seconds at 95°C, 30 seconds at 60°C (annealing) and extension at 72°C. All the other procedure was kept. The resulting melting curves are shown in the Figure 18.

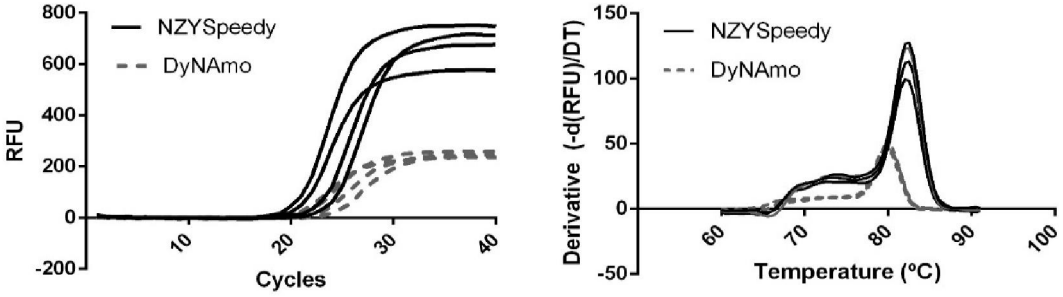

Figure 18 - Amplification curves (A) and melting curves (B) from the qPCR runs.
This experiment was planned to compare the NZYSpeedy qPCR Green Master Mix and the DyNAmo™ HS SYBR™ Green qPCR Kit. We tested four different samples and amplified the GAPDH gene.

The data resulting of this experiment (Figure 18) show that the NZYSpeedy master mix have better amplification performance, wherein the relative fluorescence units (RFU) are significantly higher, amplifying some samples earlier than the DyNAmo master mix. Relatively to melting curves, with NZYSpeedy master mix there is a deviation of the melting peak higher values (≈3ºC). This difference in melting peak can be due to the different composition of the two master mixes tested and not to the amplification of different products. Thus, the following experiences were performed with NZYSpeedy master mix, in the machine CFX96 Touch™ Real-Time PCR Detection System (Bio-Rad) and under the described conditions of denaturing, annealing and extension.

- **Annealing temperature**

In RT-qPCR implementation experiment, evaluating the resulting melting curves, some pairs of primers, namely TGFB1 and FGF7, showed a need of optimization of the annealing step (annealing temperature) in the qPCR run. This experiment was performed with an annealing temperature of 60ºC. In the present experiment, we tested an annealing temperature of 62ºC. The increase of annealing temperature increases the specificity of primers preventing the unspecific reaction and possible dimers formation. Thus, we tested RNA sample from both NHDF and NHEK lineages to the three pairs of primers, TGFB1 and FGF7 at an annealing temperature of 62ºC. The resulting amplification and melting curves are shown in the Figure 19.

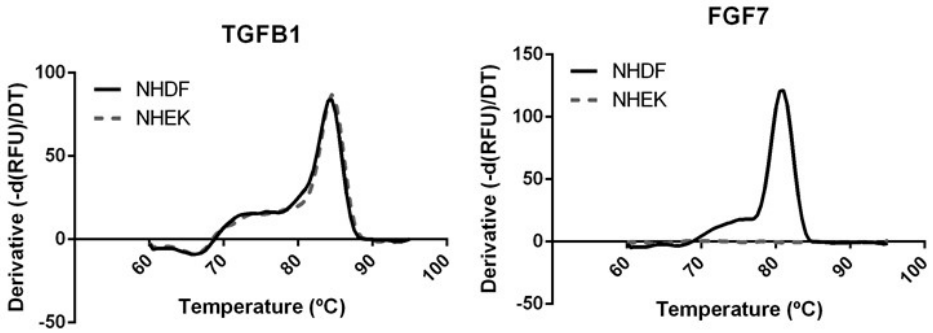

Figure 19 - Melting curves of the amplification products of TGFB1 and FGF7 genes.
We performed a qPCR experiment where the annealing temperature tested for these 2 primer pairs was 62ºC. This annealing temperature was tested for RNA samples of both NHDF (black regular) and NHEK (grey dashed) cellular lineages. C^t values: TGFB1, NHDF=27.5, NHEK=24.2; FGF7, NHDF=27.4.

The data resulting of this experiment, Figure 19, shows some differences relatively to the RT-qPCR implementation experiment. In the first experiment of RT-qPCR, in which the annealing temperature was 60ºC, this gene showed a melting curve present a sight elevation before the peak. Thus, a second experiment was carried out, in which the annealing temperature was increased by about 2°C. The annealing temperature is the temperature which allows the annealing of the primers to complementary regions of the template. If the annealing temperature is too low, primers may bind non-specifically to the template, which may lead to the appearance of other peaks or elevations that do not represent the true annealing peak because they reflect amplification products that are unspecific. Increasing the annealing temperature allows a more specific annealing of the primers to the template, and thus prevents the appearance of such nonspecific peaks. Thus, making this optimization of annealing temperature it was possible to eliminate the elevation that appeared before the true annealing curve. The melting curves of TGFB1 gene in both samples appear to be improved, losing the slight elevation before the peak observed in the experiment with the annealing temperature of 62ºC.

This type of optimization was also tried with FGF7 to improve their amplification with NHEK RNA samples. With this primer pair and sample, the optimization didn't work. These results may suggest that the lineages in question do not express this gene or the primers used are not suitable. FGF-7 or KGF is normally produced by dermal fibroblasts. Its expression by fibroblasts is commonly verified by RT-qPCR experiments performed with NHDF RNA [115]. However, its expression by keratinocytes is less referenced in the literature. And, when its expression and production in NHEK was evaluated, it was noted that it is a much lower expression level in relation to NHDF [116]. Thus, it seems natural that the NHEK cultured *in vitro* did not express this gene. Thus, the RT-qPCR procedure to GAPDH, FN1, COL1A1, COL1A3, FGF2, FGF7 and VEGFA genes can proceed with annealing temperature of 60ºC, while TGFB1 gene will be tested with an annealing temperature of 62ºC for both lineages (Table 10).

Table 10 - Summary of annealing temperature to apply in RT-qPCR procedure to each gene.
In addition, this table allows the easy perception of which genes will be evaluated in each of the cell lines under study.

Gene Name	Annealing temperature	NHDF	NHEK
GAPDH	60ºC	✓	✓
FN1	60ºC	✓	---
COL1A1	60ºC	✓	---
COL3A1	60ºC	✓	---
TGFB1	62ºC	✓	✓
FGF2	60ºC	✓	✓
FGF7	60ºC	✓	X
VEGFA	60ºC	✓	✓

3.1.2 Immunocytochemistry

ICC is a procedure used to evaluate the presence of molecules of interest in cultured cells. This technique uses the specificity of antibodies which bind to a protein or antigen thereby allowing visualization and examination under a microscope. ICC is an indicated tool for the determination of a cellular content from individual cells or of their extracellular space. Then, the implementation and optimization of immunocytochemistry technique in Exogenus Therapeutics' laboratory may be an advantage in the evaluation of production and remodeling of ECM.

a. Implementation

The implementation of ICC technique for evaluation of ECM secretion and remodeling in Exogenus Therapeutics' laboratory involved the order of necessary material, the assembly of work area and the optimization of some conditions. In a first phase of ICC implementation, the protocol performed were described in 2. Material and Methods – 2.4 Immunocytochemistry. In the same section, the antibodies and the dilutions used in this experimentare listed in Table 2. The cells were observed and the obtained images were in Figure 20.

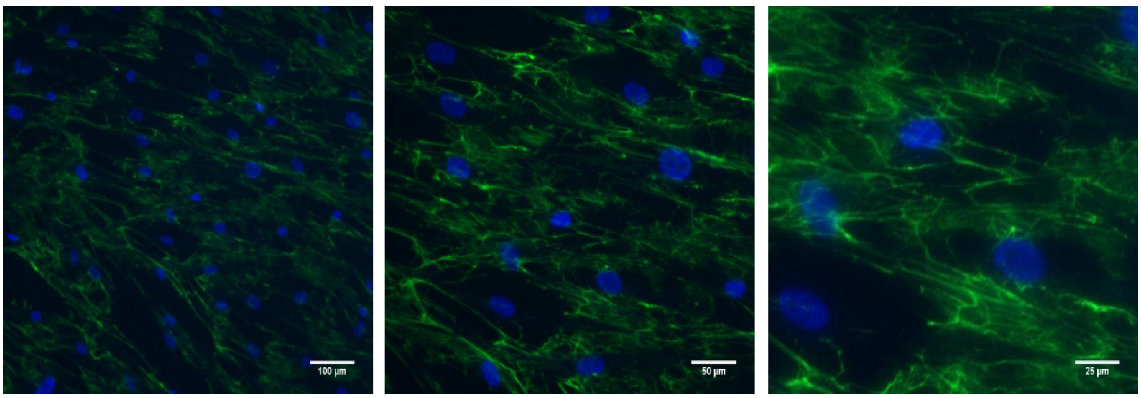

Figure 20 – Representative images of Immunoctochemistry protocol implementation.
NHDF were cultured for 24 hours in complete medium. Cells were fixed with PFA 4% and immunostained to fibronectin with appropriate antibodies (Table 2). Nuclei were counterstained with Hoechst. Images were acquired in a fluorescence microscope Carl Zeiss Axio Imager Z2, with ApoTome2 and Stereo-Investigator using different magnifications (10x, 20x and 40x) and analysed using ImageJ software.

In Figure 20, nuclei and fibronectin staining seem good and suitable for following experimental plans. Unfortunately, the labelling of collagens did not result in these conditions, thus the results from staining of collagens were not represented. Next steps comprise mainly the optimization of the conditions for a better Col1 and Col3 staining.

b. Optimization

- **Fixation Method**

To optimize the previous results of ICC, we thought of changing the fixation method. There are some different methods to fix cells to ICC staining and their application depends specifically on

the antigen of interest. Some references describe the fixation with methanol in ICC to collagen I and III. Thus, NHDF were 24 hours cultured in complete medium in in culture slides. Cells were fixed using methanol, previously precooled at -20ºC, for 10 minutes on ice (4ºC). To ensure a better signal in the staining of collagens, the dilution used in the preparation of anti-collagen I and anti-collagen III antibodies solutions was decreased. Information about the used antibodies are shown in Table 11. All the other conditions described above were maintained. After staining, the cells were observed with a fluorescence microscope, Carl Zeiss Axio Imager Z2, with ApoTome2 and Stereo-Investigator. The obtained images were represented in Figure 21.

Table 11 - List of antibodies used in Immunocytochemistry optimization.
In this list is discriminated the name, reference and dilution of each antibody used.

Antibody	Reference	Dilution
Anti-Human Actin C4	MAB1501, Merck Millipore	1:500
Anti-Human Fibronectin	11324553, Invitrogen	1:200
Anti-Human Collagen I	ab34710, Abcam	1:50
Anti-Human Collagen III	ab7778, Abcam	1:50
Alexa Fluor 488 Anti-Mouse	10544773, Invitrogen	1:500
Alexa Fluor 568 Anti-Mouse	LTI A11004, Invitrogen	1:500
Alexa Fluor 568 Anti-Rabbit	15656405, Invitrogen	1:500

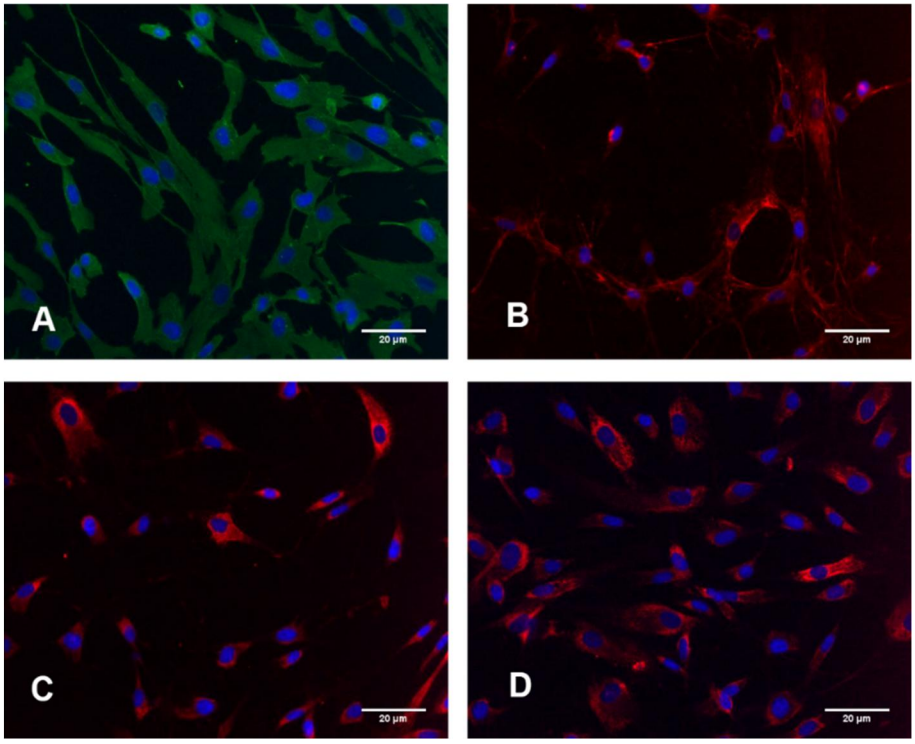

Figure 21 - Representative images of Immunocytochemistry protocol optimization.
NHDF were cultured for 24 hours in complete medium in culture glass slides. Cells were fixed with methanol and immunostained to β-Actin **(A)**, Fn **(B)**, Col1 **(C)** and Col3 **(D)** with appropriate antibodies (Table 13). Nuclei were counterstained with DAPI. Images were acquired in a fluorescence microscope Carl Zeiss Axio Imager Z2, with ApoTome2 and Stereo-Investigator using 20x magnification and analysed using ImageJ software.

All stainings seem to result with these fixation (Figure 21). Col1 and Col3 staining appears to be cytoplasmic, which is described in literature, and therefore actin staining will be used simultaneously as a control.

At first, we used PFA fixation which resulted for Fn labelling, but not for the collagens. Accordingly, we also tested methanol fixation. This fixation method is compatible with stainings for Fn, Col1 and Col3. While Col1 and Col3 present a cytoplasmic pattern of expression, Fn has a more fibrillar pattern, suggesting that is might be at the membrane of at the extracellular space. The PFA fixation cause a covalent cross-linking between molecules, such as proteins and nucleic acids, attaching them into an insoluble meshwork [117]. Methanol preserve cells through a process of dehydration and precipitation of proteins. In addition, the fixation with organic solvents, such as methanol, also permeabilizes the cells, removing lipids from the cell membrane and allowing the antibodies to recognize intracellular antigens. It seems that the permeabilization caused by the methanol fixation allowed the recognition of the two types of collagens under study. Believing that the antibodies used specifically recognize Col1 and Col3 it is possible to affirm that these proteins are still present in the NHDF cytoplasm.

3.1.3 Western Blot

Western Blot is a technique currently used to find out if a specific protein is expressed or not, and, in some cases, to assess their relative expression in different conditions. This technique can be used for various proteins types and have many applications in a usual biochemistry laboratory. These facts allied to the need of assess the expression of ECM proteins, such as Fn, Col1 and Col3, by dermal fibroblasts in different conditions of treatment, favored the implementation of WB in Exogenus Therapeutics' laboratory, that can be an advantage in the evaluation of the expression of ECM proteins.

a. Implementation

The implementation of WB technique in Exogenus' laboratory involved the purchase of WB material/equipment such as the electrophoresis and blotting systems, buffers, antibodies, and other necessary reagents and the assembly of western blot area. In a first phase of WB implementation, typical conditions were tested first. The samples used were total cell lysates from NHDF and NHEK. In this experiment, different quantities of protein of each sample (15µg, 20µg and 30µg) were tested. Thus, samples were aliquoted by protein quantity and prepared as described in Material and Methods. The SDS-PAGE and transfer were performed as described in 2. Material and Methods – 2.5 Western Blot. The resulting membrane was stained with Ponceau Red (Figure 22). Then, the blot was incubated with mouse antibody Anti-Human β-Actin (Table 7) in TBS-T solution. The staining with secondary antibody and signal detection were performed as foreseen in 2. Material and Methods – 2.5 Western Blot. The resulting image was posteriorly analysed with ImageJ software (Figure 23).

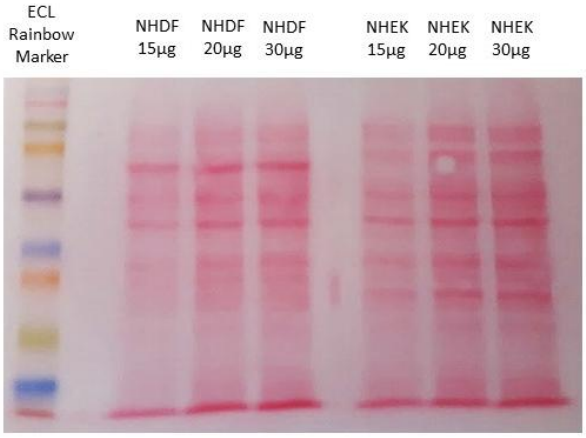

Figure 22 - Exemplificative image of a PVDF membrane stained with Ponceau Red solution.

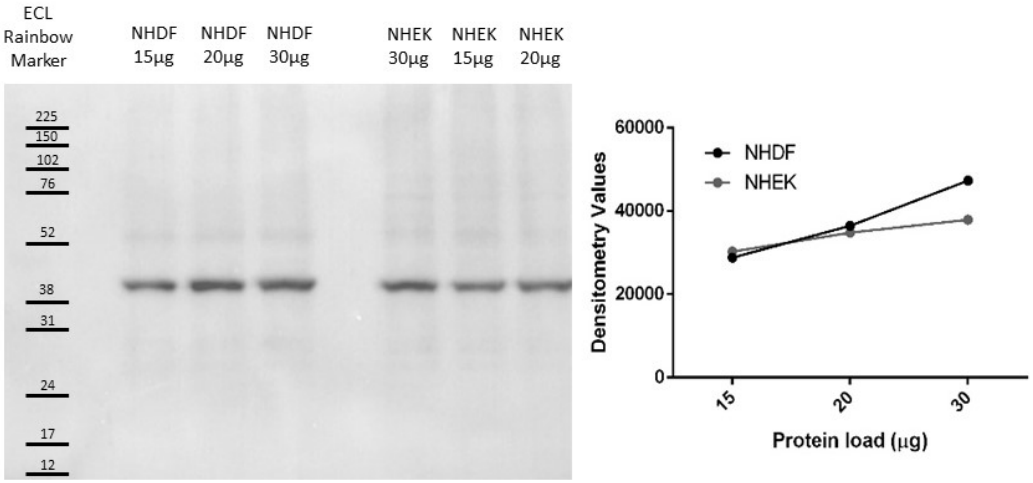

Figure 23 - WB analysis of β-Actin (42kDa) presence in cellular lysates: effect of total protein amount.
A) PVDF membrane with detected signal of β-Actin in NHDF and NHEK. **B)** Graphic representation of densitometric values after analysis of the bands observed in A. Densitometric analysis was performed using ImageJ software.

The results presented in Figure 23 were achieved with this experiment and show that the Western Blot was implemented successfully. Next steps describe the optimization of some conditions of WB procedure to identify Fn, Col1 and Col3 secreted by NHDF.

b. Optimization of ECM components identification by WB

One of the objectives of WB implementation is the identification and evaluation of ECM components secretion by NDHF. Relatively to previously test of WB implementation, there were some conditions that needed to be optimized to identify Fn, Col1 and Col3. These proteins have some characteristics which make them particular, such as their molecular weight and their assembly in ECM, and these properties have impact in conditions of WB technique. Thus, in first experiment to find this ECM components, different types of samples were analysed, which are described in next topic and some conditions of electrophoresis and blotting steps were altered.

- **Samples collection**

ECM proteins, such as Fn, Col1 and Col3, are usually assembled in a complex ECM. This can be a problem in identification by western blot, because the usual sample used are cellular lysates or CM. Thus, one of the steps of optimization is to choose the best source to evaluate the production of these ECM proteins. To understand which source of sample would be the best option to evaluate, by western blot, the production of extracellular matrix proteins by NHDF, samples from different sources were collected. In this western blot experiment, different types of samples were tested: sample resulting of two different methods of ECM extraction, samples of cellular lysates from NHDF and NHEK culture and three different samples CM from fibroblasts culture.

Cellular lysates

NHDF and NHEK were cultured in complete medium. Cultured cells were washed with pre-warmed pre-warmed PBS (Biochrom-Merck) without Ca^{2+} and Mg^{2+}, detached with 0.05% (v/v) trypsin (LGC) solution in PBS (Biochrom-Merck) at 37 ºC and then the reaction was stopped with culture medium. After that, cells were centrifuged for 5 minutes at 300x*g* and then suspended in 200µl of RIPA buffer supplemented with proteases inhibitor. The resulting samples were collected and incubated for 30 minutes on ice. After ice incubation, the samples were centrifuged at 14000x*g* for 10 minutes at 4ºC and supernatant were preserved at -20ºC. The total protein of each sample was measured using Pierce™ BCA protein assay (Thermo Fisher Scientific).

CM Collection

NHDF were cultured in three different culture media: i) complete medium, ii) DMEM 0.5% FBS, and iii) basal medium. The CM was collected and centrifuged at 300x*g* for 10 minutes at 4ºC and the pellet was discarded. The resulting samples were: A – CM complete, B – CM DMEM 0.5% FBS, and C – CM basal medium. The samples were preserved at -20ºC. The total protein of each sample was quantified with a Pierce™ BCA protein assay (Thermo Fisher Scientific).

ECM extraction

ECM components are naturally assembled in a complex matrix. Thus, one hypothesis is that fibronectin and the collagens can be assembled and so their identification by assessing cellular lysates or CM can be compromised. Some investigators use specific methods to extract the biomolecules that compose ECM [118]. Thus, we tested two methods to extract ECM proteins from NHDF cultures: i) Acetic Acid method and ii) Triton x-100 method. Cells were cultured in 6-well plate for 72 hours or 7 days, and then they were removed from the surface of the culture plate with 2 mM EDTA in PBS for 7 minutes at 37°C, two times. Detached cells were discarded, and remaining ECM proteins attached to the surface of culture plates were washed with the same solution. Cell removal was controlled under the microscope.

Using the Acid Acetic method, after cells were completely removed, matrix proteins were covered with 5% acetic acid and incubated at 4°C overnight. Then, acetic acid was removed and exchanged with a buffer containing 125mM Tris-HCl, pH 6.8, 0.1% SDS, 10% glycerol, mercaptoethanol, phosphatases inhibitor and proteases inhibitor cocktail, and incubated at 37°C for 1 hour. Proteins were removed with a scraper. All protein extracts were combined and ECM proteins were precipitated by adding five volumes of acetone. After incubation at –20°C overnight and centrifugation at 7000x*g* for 15 minutes, the protein pellets were dissolved in RIPA supplemented with proteases inhibitor.

Using the Triton X-100, Dishes were filled with 1% Triton X-100 and incubated at 37°C for 30 minutes. The extraction was repeated three times. Then, Triton X-100 was removed and exchanged with a buffer containing 125mM Tris-HCl, pH 6.8, 0.1% SDS, 10% glycerol, mercaptoethanol, phosphatase inhibitor and protease inhibitor cocktail, and incubated at 37°C for 1 hour. Proteins were removed with a scraper. The procedure was repeated three times. After incubation at –20°C overnight and centrifugation at 7000x*g* for 15 minutes, the protein pellets were dissolved in RIPA supplemented with proteases inhibitor.

Total protein of each sample was measured using Pierce™ BCA protein assay (Thermo Fisher Scientific), and using BSA as a standard. Samples to load in SDS-PAGE gel were prepared as described in 2. Material and Methods – 2.5 Western Blot.

- **SDS-PAGE**

The size of proteins of interest has impact in choice of SDS-PAGE gel percentage. To identify large proteins the best option is to opt for acrylamide gel with less percentage of acrylamide, such as 7-8%. In this perspective, and knowing that fibronectin is the biggest protein we want to identify and has a molecular weight of 245kDa, it was used a 7% SDS-PAGE gel. The components of the 7% acrylamide gel and their quantity are listed in Table 12. All the other conditions were maintained.

Table 12 - Reagents used in preparation of Resolving and Stacking gels and their corresponding quantities.

	Resolving Gel (7%)	Stacking Gel (4%)
ddH2O	4.4 mL	3.1 mL
Acrylamide (40%)	1.4 mL	500 µL
1.5M Tris pH 8.8	2 mL	---
0.5M Tris pH 6.8	---	1.25 mL
10% SDS	80 µL	50 µL
10% APS	80 µL	50 µL
TEMED	8 µL	5 µL

- **Blotting – Wet transfer**

In WB with large proteins it's advisable add SDS to transfer buffer, to a final concentration of 0.1%. This discourage the tendency of these proteins to precipitate in gel. Thus, we used a transfer buffer with 0.1% SDS and the reagents of the transfer buffer with 0.1% SDS and their quantity are listed in Table 13. All the other conditions were maintained.

Table 13 -Reagents used in preparation of Transfer Buffer and their corresponding quantities.

	Transfer Buffer (1mL)	Reference
ddH2O	690 mL	---
0.25M Tris, 1.92M Glycine	100 mL	BioRad
Methanol	200 mL	Fisher Bioreagents
SDS 10%	10 mL	Fisher Bioreagents

- **Blocking, antibody incubations, signal development and detection**

All the conditions described in "WB Implementation – Blocking and Antibody incubation" and "WB Implementation – Signal development and detection" were maintained. Information about the used antibodies are shown in the Table 14. The results obtained are shown in Figure 24.

Table 14 - List of antibodies used in Western Blot optimization.
In this list is discriminated the name, reference and dilution of each antibody used.

Antibody	Reference	Dilution
Anti-Human Fibronectin	11324553, Invitrogen	1:1000
Anti-Human Collagen I	ab34710, Abcam	1:1000
Anti-Human Collagen III	ab7778, Abcam	1:1000
ECL Rabbit IgG	NA934-1ML, GE Healthcare	1:1000
ECL mouse IgG	NA931-1ML, GE Healthcare	1:1000

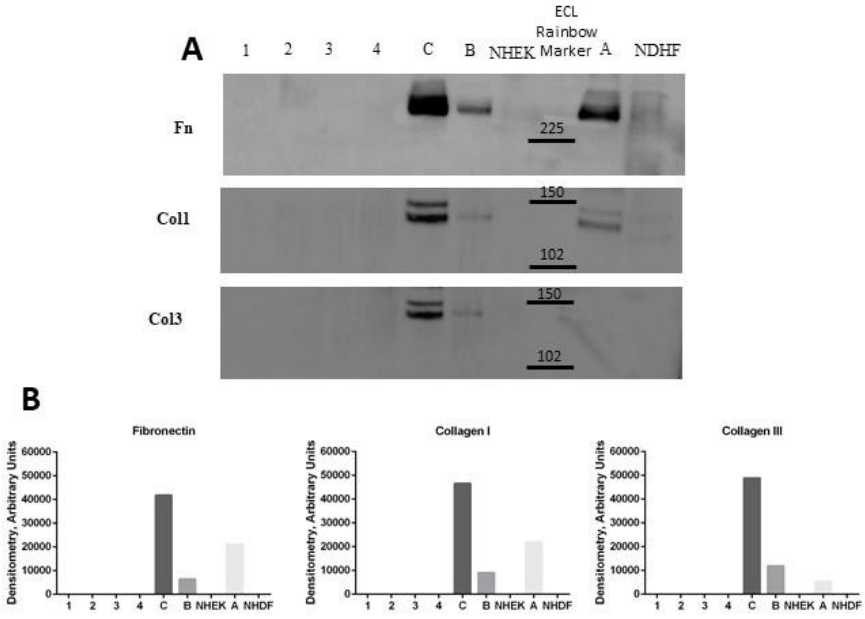

Figure 24 - WB analysis of fibronectin (245kDa), collagen I (130kDa) and collagen III (138kDa) proteins.
A) Images of western blot analysis to Fn, Col1 and Col3. The samples analysed were: 1 – Acid Acetic 7 days; 2 – Triton X-100 7 days; 3 – Acid Acetic 72 hour; 4 Triton X-100; A – CM complete (2% FBS); B – CM basal; C – CM DMEM 0.5% FBS; NDHF – cellular lysate of NDHF culture; and NHEK - cellular lysate of NHEK culture. B) Graphic representation of densitometric values after the analysis of the observed bands. Densitometric analysis was performed with Image J software

Summarizing, it was tested nine samples: 1 – Acid Acetic 7 days; 2 – Triton X-100 7 days; 3 – Acid Acetic 72 hour; 4 Triton X-100; A – CM complete; B – CM basal; C – CM DMEM 0.5% FBS; NDHF – cellular lysate of NDHF culture; and NDEK - cellular lysate of NDEK culture. All these samples were tested in a western blotting to fibronectin, collagen I and collagen III, where 50µg were load of each sample. In this experiment, the visible bands appear only in CM samples (Figure 24). The absence of signal in samples resulting of ECM extraction by Acid Acetic and Triton X-100 demonstrates that this extraction was not efficient or the culture conditions of NHDF do not allow the assembly of ECM. Only by visualization of WB membrane, the signal in CM samples seem to

be more intense in CM 0.5% FBS than in CM Basal or in CM Complete. When their intensity is analysed by densitometry we observe that difference is real. This can be due to percentage of FBS in each medium, that in CM Complete is 2% while CM Basal doesn't have any. Thus, in this perspective, cells can react differentially depending on the percentage of FBS, in terms of expression of ECM components. Another hypothesis is that in WB the relative abundance of FBS proteins in CM Complete can mask the proteins of interest, such as fibronectin or collagen. In conclusion, these results demonstrated that the samples of CM are the best option to assess the Fn, Col1 and Col3 secretion. In addition, the culture of NHDF with DMEM supplemented with 0.5% FBS seems to improve the results of WB bands.

In the literature, there is no consensus about the best source to evaluate the production of these ECM components. Some works refer to fibroblast lysates grown *in vitro* as the best source, others refer to the conditioned medium of these cells [119,120]. On the other hand, some researchers use matrix extraction methods to collect the ECM produced by these cells *in vitro* [118]. The results from WB in this experiment show that the three matrix proteins under study were found only in the CM of NHDF cultured *in vitro*, and not in cell lysates or in samples from described matrix extraction protocols. Thus, it can be seen that there is production and secretion of matrix proteins but it appears that these proteins are not being assembled in an extracellular network but are in their soluble state.

In WB experience, the fact of using CM to evaluate the secretion of ECM components brought an important limitation, the absence of a secreted normalizing proteins. When cellular extracts are used to WB procedures, it is common use a housekeeping protein, such β-actin, β-tubulin or GAPDH, to normalize the results of interest proteins [121–123]. In alternative, some researchers use total protein normalization, which is based on the intensity of all proteins in a lane on WB membrane, to normalize the results from WB. These methods include, for example, Coomassie Blue or Ponceau Red staining and its use has been increasing mainly since this normalization does not depend on expression of a single protein.

In an attempt to use total protein normalization, was performed a Ponceau Red staining in the procedures for the identification of ECM proteins. However, this attempt to normalize the WB results was not successful, since no sample showed staining when labelled with the Ponceau Red solution. In Results section of this work, was shown a membrane stained with Ponceau Red solution (Figure 22). This membrane resulted from a wet transfer using a transfer buffer without SDS in its composition. The membranes used to identification of ECM proteins were resulted from wet transfers using a transfer buffer with 0.1% SDS in its composition. The use of SDS in composition of transfer buffer has the objective of giving a negative charge to the proteins in the gel and

improving the transfer of the higher molecular weight proteins to the membrane. However, the SDS can compete with Ponceau Red solution for protein binding. The description available of how the Ponceau Red solution binds to proteins includes the fact of this agent be a negative stain. Thus, Ponceau Red binds to the positively charged amino groups and possibly non-covalently to non-polar regions in the proteins. As already mentioned, the SDS is an anionic detergent that coat protein R-groups with negative charges and denature proteins into its primary structure, disrupting hydrophobic areas. After the transfer performed with transfer buffer containing SDS, it is expected that the proteins are negatively charged and without non-polar regions, impairing the binding of the ponceau agent to proteins in the membrane. Together, these facts can influence the recognition of proteins by Ponceau Red staining. Thus, without a source of normalization, we attempted to normalize the amount of protein loaded, relying on the quantification of the total protein. Then, the results of treated conditions were normalized against to the respective control [119]. The samples from the treatments and the respective controls were always analysed in the same WB procedure, trying to minimize the variability of the technique.

- **Collagen I and collagen III detection**

Relatively to detection of Col1 and Col3, there are some particularities which we must consider. The WB performed for these proteins resulted in the appearance of two bands instead of one, as is expected in a typical WB procedure. Studies that refer to the use of the same or other antibodies to Col1 and Col3 verify the presence of more than one band in WB to Col1 and Col3 [119,120]. The authors and the antibodies supplier, Abcam, consider the presence of two bands normal, associating with the two predominant splice variants. Thus, in the following results it was considered as Col1 or Col3 the two bands presented.

Another characteristic is that the detection of Col1 and Col3 can be affected by their reduction and denaturation, that are two normal steps of sample preparation for western blot. To analyse samples by WB typically is necessary denature and reduce the protein order to allow the migration of proteins in SDS-PAGE. The reducing conditions are related to the addition of reducing substances, like β-mercaptoethanol, to western blot samples. The denaturing conditions are associated to the boiling of the sample before loading the sample. These two steps can modify some characteristics of proteins and, in some cases, these modifications can prevent the recognition of the protein. According to the information provided by the supplier of antibodies anti-Collagen I and anti-Collagen III, these two steps, denature and reduce, can diminish the signal of western blot, because the development of this type specific antibodies is dependent on non-denatured three-dimensional epitopes. Thus, the reduction and denaturation of ECM samples were

tested in order to understand the impact of this conditions in western blot signal of Col1 and Col3. So, three different samples of conditioned medium (1, 2 and 3) were tested. Each sample was subjected to two different conditions: A- reducing and denaturing conditions; and B - non-reducing and non-denaturing conditions.

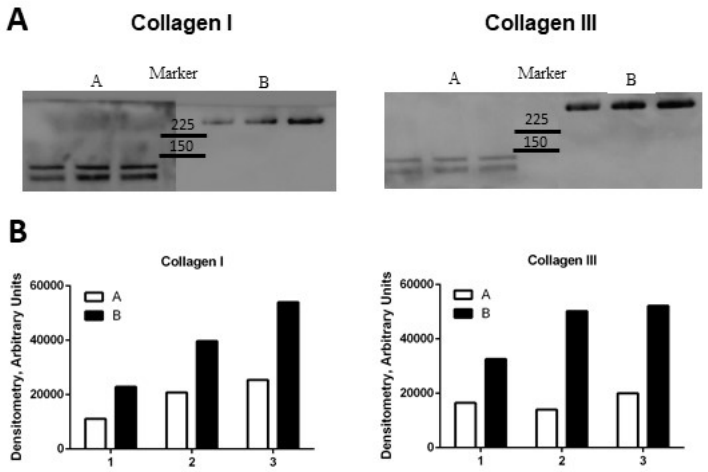

Figure 25 - Detection of collagen I (130kDa) and collagen III (138kDa) in conditioned medium by Western Blot. A) Images resulting from WB procedure. Three different samples (1, 2, 3) were exposed to two different conditions: A - Reducing and Denaturing conditions; B - Non-reducing and denaturing conditions. All these samples were tested in two different WB membranes, one used for analysis of collagen I and another for analysis of collagen III. **B)** Graphic representation of densitometric values after analysis of bands observed in Figure 25A**.** Densitometric analysis was performed using Image J software

These results showed that the reducing and denaturing conditions diminish the signal in western blot relatively to samples in non-reducing and denaturing conditions (Figure 25). This signal weakening seems to be more notable in Col3 identification. Besides that, in denatured and reduced samples there are two visible bands that are visible at 130-140kDa, which is in accordance with alliteration and indications of the antibody supplier. However, in non-reduced and non-denatured samples there is only one band with a MW higher than 225kDa.

These observations are due to effect of non-reducing and non-denaturing conditions. For the identification of Col1, the denaturing and reducing conditions affect the signal leaving it weaker, however the signal is still reasonable and can be easily identified. For the identification of Col3 the denaturing and reducing conditions greatly affect the signal leaving it much weaker and may be a problem in later experiments. The difference between MW in the two conditions is probably related to the fact o proteins in non-denaturing and non-reducing conditions are in their native conformation, preserving their native charge-to-mass ratio and protein-protein interactions. Thus, the migration is no longer based on their mass as in SDS-PAGE and, due to the preserved native charge, proteins can migrate towards either electrode. This causes an unpredictable migration in

SDS-PAGE. Thus, some proteins are retained at the top of the running gel and appear to have a higher molecular weight than expected.

Therefore, for subsequent experiments to evaluate Col1 the samples will normally be denatured and reduced. For experiments with Col3, the samples do not go through the denaturation and reduction steps, considering that the bands obtained with those conditions are above the expected molecular weight for this protein.

- **Protein Load**

To verify the intensity of WB signal of ECM proteins relatively to total protein loaded in acrylamide gel, we tested different quantities of protein of the same CM sample. With this experiment, we also aim, if possible, to determine the appropriate protein quantity to load in WB experimentto recognize ECM proteins of interest. Thus, were tested four different quantities of total protein: 15µg, 25µg, 35µg and 50µg. This samples were loaded in a 7% acrylamide gel and the resulting membrane of WB procedure were incubated with anti-fibronectin and anti-collagen antibodies. The resulting images and the corresponding graphs of densitometry analysis are shown in Figure 26.

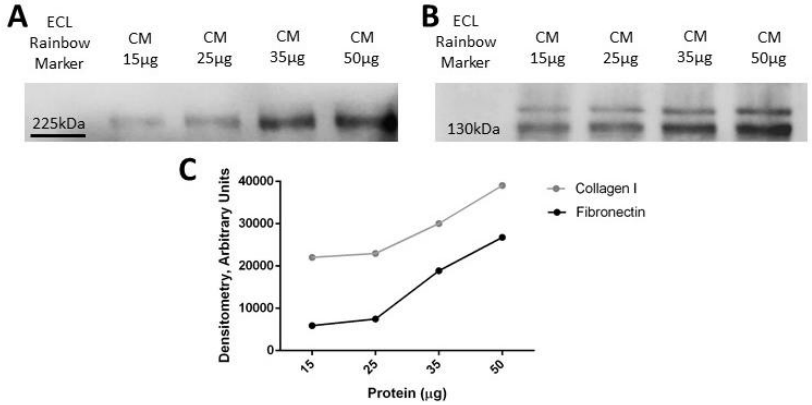

Figure 26 - WB analysis of fibronectin (245kDa) and collagen I (130kDa): studying total protein load.
A) and B) show images of a WB procedure to detect fibronectin **(A)** and collagen I **(B)**. Four different quantities of total protein of the same CM sample were tested: 15µg, 25µg, 35µg and 50µg. **C)** Graphic representation of densitometric values after analysis of the protein bands observed in A and B. Densitometric analysis was performed with Image J software.

With the results of this experiment (Figure 26), it was demonstrated that the signal of WB performed to Fn and Col1 seems to be dependent and correlated with the total protein load. Assessing the densitometry analysis, it is noticeable that loading 35µg to 50µg of total protein it is possible to reasonably detect the signals of both fibronectin and collagen I. In further experiments, it will be used 35µg of total protein to Fn and Col1 detection by WB. This amount of protein corresponds to signals detected in the linear range, allowing a better evaluation of putative alterations in Fn and Col1 secretion upon different treatment conditions.

3.2 Preliminary Results

a. Total Protein Quantification of Conditioned Medium

The CM was used to analyse the production of ECM components in the different condition by WB. After collection, CM was centrifuged at 300x*g* for 10 minutes at 4ºC and the pellet was discarded. The resulting samples were preserved at -20ºC. The total protein of each sample was quantified with a Pierce™ BCA protein assay. In Figure 27 is shown a graphic representation of the protein quantification in different samples of CM, where the amount of protein is compared between the CM of cells treated with Exo-101, cells treated with PBS and cells that have not received any type of treatment.

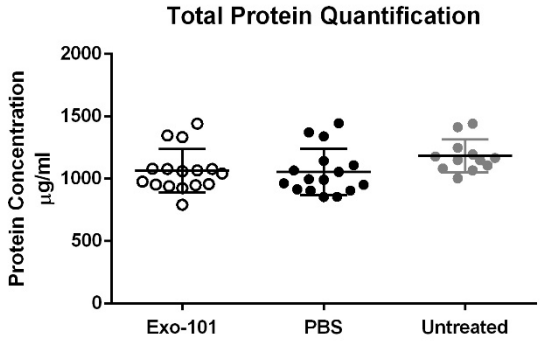

Figure 27 - Protein quantification in different samples of CM.
The total amount of protein is compared between the CM of cells treated with Exo-101, cells treated with PBS (as experimental control; n=16) and cells that have not received any type of treatment (untreated; n=12). The total protein of each sample was quantified with a Pierce™ BCA protein assay.

The results from quantification of several different CM samples shows that that the amount of total protein in each sample does not appear to vary significantly between samples and between groups.

b. Analysing fibronectin and collagen I secretion by WB applying Different Exo-101 Treatment Schemes

To understand if different treatment schemes elicit different results in modulation of ECM components production by NHDF, these cells were cultured and treated with different dose scheme and different Exo-101 concentration in particles/ml. NHDF were treated with four different dose schemes of treatment with Exo-101: one condition single dose (SD), and three different repeated doses. The dose schemes of repeated dose are characterized by application of Exo-101 treatment twice daily for 1 (RD1), 2 (RD2) or 3 (RD3) days, without medium replacement. Besides that, all dose schemes were treated with the therapeutic concentration of Exo-101, $2.5x10^9$ particles/ml (C1). Additionally, the dose schemes of RD2 and RD3 were also used Exo-101 in concentration of

5x10^9 particles/ml (C2). 24h after the last application of Exo-101 the CM of each condition was collected.

The CM samples were prepared as previously described in 2. Material and Methods chapter. The WB was perfomed with the optimizations described in 3.1 Implementation and optimization of biomolecular methods section. The signal was visualized using a chemiluminescent detection system of VWR imager Chemi 5QE Image Capture Software. The obtained images were analysed by densitometric measurement in ImageJ software.

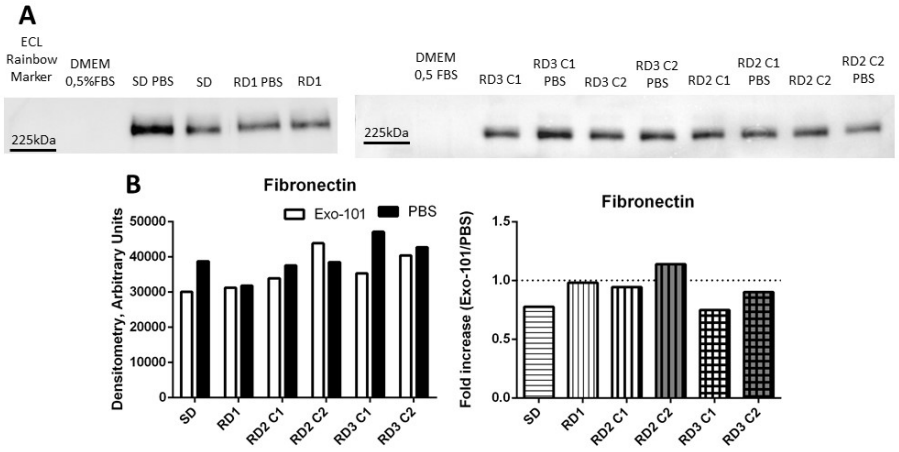

Figure 28 - WB analysis of fibronectin (≈245kDa) secretion in NDHF after Exo-101 treatment.
A) Fibronectin detection by WB using six different treatments/samples (SD, RD1, RD2C1, RD2C2, RD3C1, RD2C2) and their respective controls (PBS). Additionally, it is shown in first lane a sample of culture medium alone (DMEM 0.5% FBS), which proves that there isn't Fn in the culture medium used in the experiments. **B)** Densitometric analysis of the WB observed bands. Graph on left represent the resulting values from densitometric analysis of treatment conditions (Exo-101) and controls (PBS). Graph on right represent the ratio Exo-101/PBS.

The results from WB procedure to fibronectin (≈245kDa), where six different conditions (SD, RD1, RD2C1, RD2C2, RD3C1, RD2C2) and their respective controls (PBS) were analysed are presented in Figure 28A. This shows that it is possible detect this protein by WB in any of the conditions tested, and there are no perceptible differences only by visualizing the signals of the WB bands. It is also possible to ascertain that the culture medium used for the NHDF culture during the treatment period (DMEM 0.5% FBS) does not contain detectable Fn in its composition. The resulting densitometric analysis and the corresponding fold increase (Exo-101/PBS) reveal that only the RD2 C2 treatment condition seems to have more detectable Fn relatively to control (Figure 28B). The cells treated in SD and RD3C1 conditions with Exo-101 seems to secrete less Fn than cells in control treatment. Despite this, all the conditions seem to be similar to the control, not being an achievement to stand out for the production of Fn.

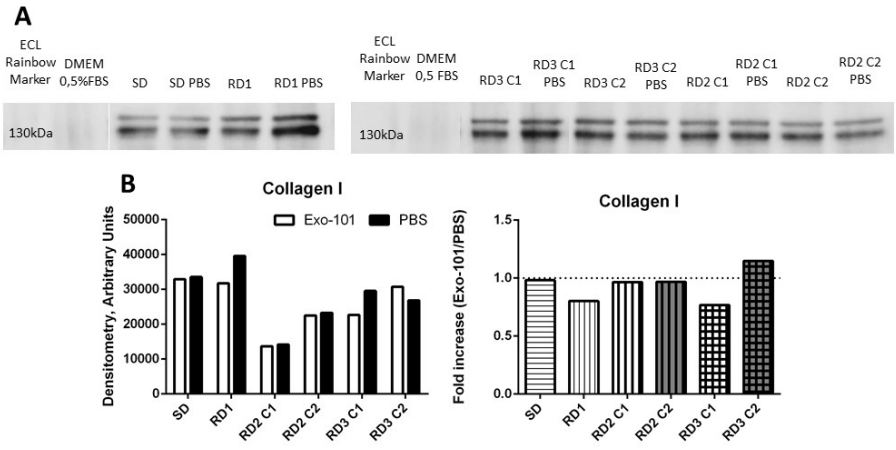

Figure 29 - WB analysis of collagen I (≈130kDa) secretion in NDHF after Exo-101 treatment.
A) Collagen I detection by WB using six different treatments/samples (SD, RD1, RD2C1, RD2C2, RD3C1, RD2C2) and their respective controls (PBS). Additionally, it is shown in first lane a sample of culture medium alone (DMEM 0.5% FBS), which proves that there isn't Col1 in the culture medium used in the experiments. B) Densitometric analysis of the WB observed bands. Graph on left represent the resulting values from densitometric analysis of treatment conditions (Exo-101) and controls (PBS). Graph on right represent the ratio Exo-101/PBS.

The results from WB procedure to Col1 (≈130kDa), where six different conditions (SD, RD1, RD2C1, RD2C2, RD3C1, RD2C2) and their respective controls (PBS) were analysed, are presented in Figure 29A. These results are similar to fibronectin analysis. The resulting densitometric analysis and the corresponding fold increase (Exo-101/PBS) reveal that only the RD3 C2 treatment condition seems to have more detectable Col1 relatively to control (Figure 29B). The cells treated in RD1 and RD3C1 conditions with Exo-101 seems to secrete less Col1 than cells in control treatment. Despite this, and also to the case of Fn levels, all the conditions seem to be similar to the control, without significant alterations in Col1 levels. In conclusion, the results of this experiment show that the differences between control and Exo-101 in terms of Fn and Col1 secretion do not seem to be attributable to or influenced by the treatment conditions. It is important to note that in this experiment only one experimental replica was evaluated for each test condition. Thus, the subsequent experiments will follow a standard treatment schedule (RD2 C1), which is described and detail in Material and Methods chapter.

3.3 Analysing the expression of Growth Factors by Keratinocytes

The total RNA from NHEK cultured and treated with Exo-101 and respective control was isolated and used to RT-qPCR procedure, as referred in 2. Material and Methods chapter. This experiment aims to understand if the expression of GFs, such as TGF-β1, FGF-2 and VEGF-A is modulated by Exo-101 treatment. The RT-qPCR was perfomed with the optimizations described in 3.1 Implementation and optimization of biomolecular methods section. This experiment comprised three different experimental replicates in the treatment group with Exo-101, and only one in the control group (PBS). Prior to performing the RT-qPCR, the total RNA in the samples must be quantified and their quality checked. Thus, the quantification and the values used to analyse the quality of samples are shown in Table 15.

Table 15 – Keratinocytes RNA analysis in NanoDrop (Thermo Scientific).

Sample	Total RNA Quantification (ng/µl)	A260/280	A260/230
NHEK N1	223,5	1,77	0,4
NHEK N2	98,4	1,6	0,2
NHEK N3	90,1	1,59	0,19
NHEK PBS	45,3	1,57	0,13

The data resulting of total RNA analysis in NanoDrop shows a lower concentration of RNA in these samples relative to the samples previously tested (section 3.1.1). Besides that, the values corresponding to A260/280 and A230/260 are not optimal. Relatively to A260/280 ratio values, they are below recommended (1.8-2.1), but not significantly lower. Nonetheless, the values of A260/230 ratio are well below the recommended level (1.6-2.0), suggesting contamination with organic solvents. Even though this contamination may reduce the efficiency of this technique, we decided to proceed with the RT-qPCR protocol, but envisage to optimize the RNA extraction method.

The resulting data from RT-qPCR was analysed using Bio-Rad CFX Manager software. The reference gene used in this experiment was GAPDH. This gene served as a normalizer for the genes under study. To obtain the relative expression of the genes of interest it was used the mathematical formula of $2^{-\Delta Ct}$. The fold increase was obtained using the mathematical formula of $2^{-\Delta\Delta Ct}$. Data is presented as the mean ± SEM of independent experiments.

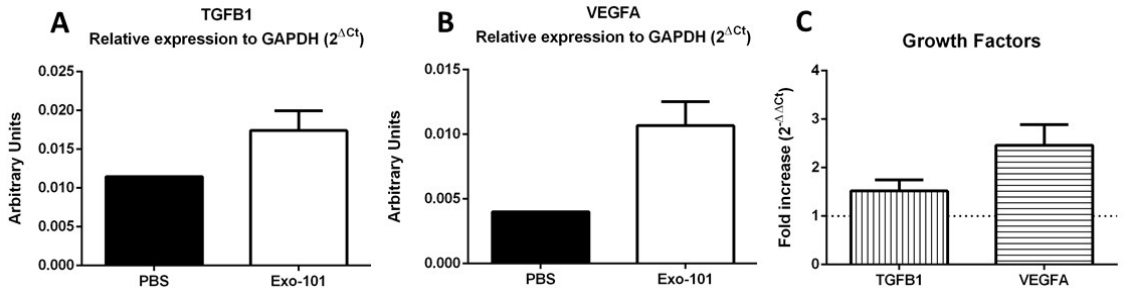

Figure 30 - Gene expression analysis of TGFB1 and VEGFA in NHEK.
Graphs A and B represent the mean of relative expression of TGFB1 **(A)** and VEGFA **(B)** to reference gene (GAPDH). Data is presented as the mean ± SEM of independent experiments. Graph **C** represents the fold increase of the expression of TGFB1 and VEGFA genes in NHEK treated with Exo-101 relatively to control (PBS). Total RNA samples from NHEK treated with Exo-101 or PBS were used (n=3 for Exo-101; n=1 for PBS).

The analysis of data resulting from RT-qPCR of TGFB1 and VEGFA genes expressed by NHEK during Exo-101 treatment, where three different experimental replicates of treatment group with Exo-101 and only one to control group (PBS) were tested, are showed in Figure 30. The expression of FGF2 gene was shown to be very low in this experiment, and therefore the results for this gene are not represented in Figure 30. The TGFB1 gene was tested with a different annealing temperature (T_a=62ºC) relatively to VEGFA (T_a=60ºC). From analysis of both genes, it is possible to verify that cells treated with Exo-101 shows an increased expression of TGFB1 and VEGFA relatively to control group. The evaluation only included one control against three treatment replicates, so it was only possible to analyse the fold increase for each treatment replicate. Due to the lack of experimental replicates in control group it is not possible to effectively conclude about the effect of Exo-101 on the expression of these growth factors. The trend of positive response of these GFs in response to Exo-101 treatment should be further explored in later studies. These two GFs are closely linked to the progression of the healing process [124]. Besides that, there are evidences which show that TGF-β1 has an up regulative effect on the expression of VEGFA by keratinocytes [125]. The TGF-β1 is involved in promoting epithelialization, collagen synthesis and contraction, and angiogenesis, being typically higher at the end of the proliferative phase of wound healing. Thus, it is positive that there is a moderate increase of it expression during healing process [124]. The angiogenesis is characterized by migration and proliferation of endothelial cells, is promoted by several mechanisms, that include the VEGF-A production by cells within the wound. This growth factor accelerate efficiently the proliferation and migration of endothelial cells, stimulating angiogenesis [126]. In addition, VEGF produced by keratinocytes promote wound repair through paracrine process, stimulating endothelial cells, and autocrine pathway [127]. Thus, these results suggest that, in keratinocytes, Exo-101 may act by stimulating expression of TGFB1 and VEGFA which will promote healing, namely by modulating angiogenesis.

3.4 Analysing the expression and secretion of Growth Factors and Extracellular Matrix components by Fibroblasts

3.4.1 Modulation of Growth Factors by Exo-101

The total RNA from NHDF cultured and treated with Exo-101 and respective control was isolated and used to RT-qPCR procedure, as referred in 2. Material and Methods chapter. This experiment aims to understand if the expression of GFs, such as TGF-β1, FGF-2, FGF-7 and VEGF-A is modulated by Exo-101 treatment. The total RNA was isolated from NDHF, as described in 2. Material and Methods chapter. This experiment comprised three different experimental replicates in the treatment group with Exo-101 (NHDF N1, NHDF N2 and NHDF N3), and only two in the control group (NHDF PBS1 and NHDF PBS2). Prior to performing the RT-qPCR, the total RNA in the samples must be quantified and their quality checked. Thus, the quantification and the values used to analyse the quality of samples are shown in Table 16.

Table 16 - Fibroblasts RNA analysis in NanoDrop (Thermo Scientific).

Sample	Total RNA Quantification (ng/µl)	A260/280	A260/230
NHDF N1	112,7	1,68	0,2
NHDFN2	74,6	1,7	0,15
NHDF N3	125,8	1,7	0,22
NHDF PBS1	183,9	1,68	0,19
NHDF PBS2	161,5	1,81	0,61

Such as the keratinocytes RNA samples, the data resulting of total RNA analysis in NanoDrop shows a lower concentration of RNA and it confirms mainly contamination with organic solvents. Even though this contamination may reduce the efficiency of this technique, we decide to proceed with the RT-qPCR protocol.

The RT-qPCR was perfomed with the optimizations described in 3.1 Implementation and optimization of biomolecular methods section. In this experiment were performed three different experimental replicates to Exo-101 treatment. The resulting data from RT-qPCR was analysed using Bio-Rad CFX Manager software. The reference gene used in this experiment was GAPDH. This gene served as a normalizer for the genes under study. To obtain the relative expression was used the mathematical formulation of $2^{-\Delta Ct}$. The fold increase was obtained using the mathematical formulation of $2^{-\Delta\Delta Ct}$. Data is presented as the mean ± SEM of independent experiments.

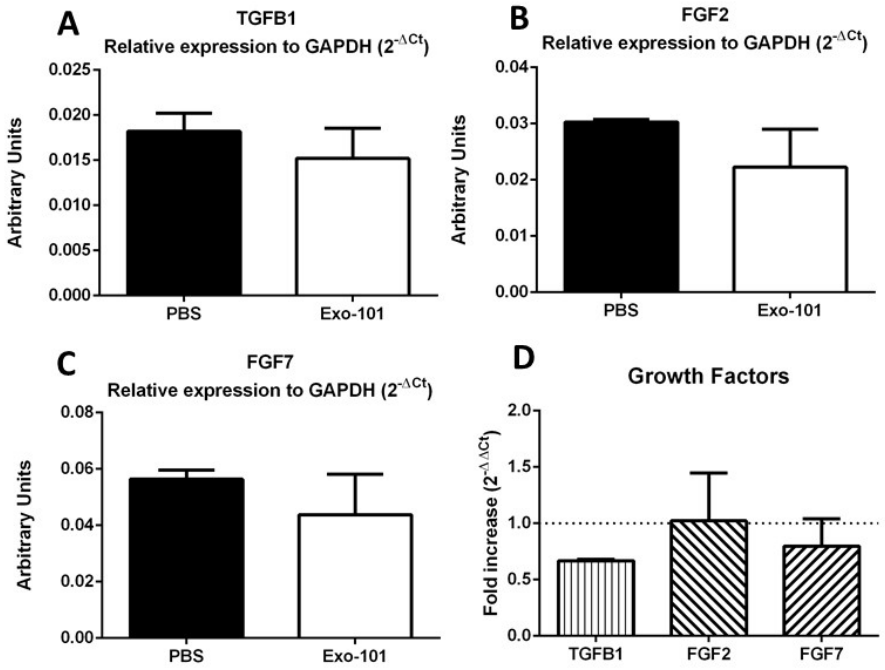

Figure 31 - Gene expression analysis of TGFB1, FGF2 and FGF7 in NHDF.
Graphs A, B and C represent the mean of relative expression of TGFB1 **(A)**, FGF2 **(B)** and FGF7 **(C)** to reference gene GAPDH. Data is presented as the mean ± SEM of independent experiments. Graph **D** represent the fold increase of the mean expression of TGFB1, FGF2 and FGF7 genes in fibroblasts treated with Exo-101 relatively to control (n=3 for Exo-101; n=2 for PBS).

The analysis of data resulting from RT-qPCR procedures to TGFB1, FGF2 and FGF7 genes expressed by NHDF during Exo-101 treatment, where three different experimental replicates were tested, are showed in Figure 31. The expression of VEGFA gene was shown to be very low in this experiment, and therefore the results for this gene are not represented in Figure 31. The TGFB1 gene was tested with a different annealing temperature (T_a=62ºC) relatively to FGF2 and FGF7 (T_a=60ºC). Comparing the mean of relative expression of both groups under study for the four genes of interest, TGFB1, FGF2 and FGF7, it is perceptible that the differences are not noticeable (Figures 31A, B and C). Analysing the mean of fold of each gene, it is noticeable that TGFB1, FGF2 and FGF7 have mean values of fold increase approximated to 1 (Figure 31D).

The NHDF lineage was treated with Exo-101 and the TGFB1, FGF-2 and FGF-7 expression was analysed by RT-qPCR. This analysis showed that the differences between the expression of these genes by treated group and by control group aren't clear. Analysing the increase-fold means, it is possible to that the TGFB1 gene appears to be less expressed in the treated group compared to the control (fold increase <1), showing a little tendency of less expression of these gene by NHDF treated with Exo-101. The same happens when FGF7 expression is assessed, but to a lesser extent and showing a larger standard deviation. However, there may be a slight tendency to down regulate the expression of the TGFB1 gene, which can be explored in later studies. Thus, the possible conclusion to be drawn from this evaluation is that the active substance under study

seems to not affect the expression of TGFB1, FGF2 and FGF7 genes by NHDF in the tested conditions.

3.4.2 Modulation of Extracellular Matrix Components by Exo-101

To detect ECM components expression and secretion by NHDF in response to Exo-101 treatment, these cells were cultured and treated as described in 2. Material and Methods chapter. After cells treatment with Exo-101 and respective control (PBS), the conditioned medium was collected to WB analysis and the resulting total RNA of NHDF cells was isolated to RT-qPCR analysis. Alongside this, NDHF were cultured in culture glass slides and were subjected to the same treatment scheme shown in Figure 10. After cells treatment with Exo-101 and respective control (PBS), the cells were fixed to ICC analysis of ECM components.

a. Analysing Fibronectin, Collagen I and Collagen III expression by RT-qPCR

The total RNA from NHDF cultured and treated with Exo-101 and respective control was isolated and used to RT-qPCR procedure, as referred in 2. Material and Methods chapter. This experiment aims to understand if the expression of ECM components, such as Fn, Col1 and Col3, is modulated by Exo-101 treatment. The total RNA was isolated from NDHF, as described in Material and Methods chapter. The RT-qPCR was perfomed with the optimizations described in 3.1 Implementation and optimization of biomolecular methods section. In this experiment were performed three different experimental replicates to treatment group with Exo-101 and only two to control group (PBS). The RNA samples used to perform this analysis were that same analysed in 3.4.1 Modulation of Growth Factors by Exo-101 section. The resulting data from RT-qPCR was analysed using Bio-Rad CFX Manager software. The reference gene used in this experiment was GAPDH. This gene served as a normalizer for the genes under study. To obtain the relative expression was used the mathematical formulation of $2^{-\Delta Ct}$. The fold increase was obtained using the mathematical formulation of $2^{-\Delta\Delta Ct}$. Data is presented as the mean ± SEM of independent experiments.

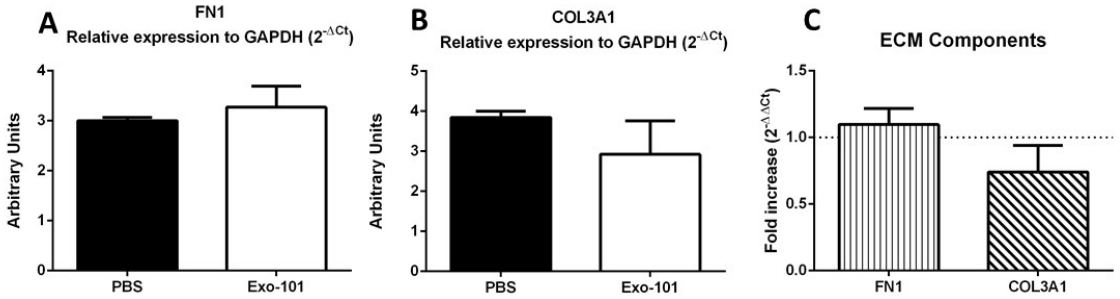

Figure 32 - Gene expression analysis of FN1 and COL3A1 in NHDF.
Graphs A and B represent the mean of relative expression of FN1 (A) and COL3A1 (B) to reference gene GAPDH. Data is presented as the mean ± SEM of independent experiments. Graph C represent the fold increase of the mean expression of FN1 and COL3A1 genes in fibroblasts treated with Exo-101 relatively to control (n=3 for Exo-101; n=2 for PBS).

The analysis of resulting data from RT-qPCR procedures to FN1 and COL3A1 genes, where three different experimental replicates were tested, are showed in Figure 32. The expression of COL1A1 gene was shown to be very low in this experiment, and therefore the results for this gene are not represented in Figure 32. Comparing the mean of relative expression of both groups under study for the three gene of interest, FN1 and COL3A1, it is perceptible that the differences are not perceptible (Figure 32A and B). Analysing the mean of fold increase, it is noticeable that FN1 have mean values of fold increase approximated to 1 (Figure 32C). Only the COL3A1 gene shows a mean of fold increase of less than 1, reinforcing that this gene appears to be less expressed in the treated group compared to the control.

As in the analysis of FGF2 expression by NHEK and analysis of VEGFA expression by NHDF, the COL1A1 expression also was shown to be very low. When the RT-qPCR technique was implemented, these genes showed good expression levels in the respective cell lines (C^T<30). The lower expression of these genes can be due to cell conditions during experience, the RNA samples quality or even an effect of Exo-101. In this experiment, the conditions of the cellular culture under study were regularly observed under an optical microscope, ensuring that the cells remained normal. The possible influence of Exo-101 on these results seems to be unlikely since the samples used as controls also show very low expressions of these genes. In addition, it is important to note that in general all genes seem to have lower expressions compared to the results obtained in the implementation of this technique. Thus, the analysis of RNA samples quality, ascertained in Tables 15 and 16, revealed that these samples could not be in the best conditions for the realization of RT-qPCR. This fact may have influenced the obtained results to expression of FGF-2, by NHEK, VEGF-A and Col1, by NHDF. The quality of RNA sample is a critical issue to RT-qPCR performance and can be influenced by some technical conditions, such as RNA extraction method. In this experiment, the RNA extraction was performance using an organic method with Trizol reagent. There are several indications that the use of this type of methods can lead to contamination with

organic solvents or protein. These contaminations may impair the efficiency of reverse transcription (cDNA synthesis) and PCR steps. Thus, the achievement of these results shows that for a more consistent evaluation of gene expression an optimization of total RNA extraction is required.

b. Analysing Fibronectin, Collagen I and Collagen III secretion by ICC

In order to verify if the results from the procedure were not influenced by non-specific binding of the secondary antibodies, ICC tests were performed without the use of the primary antibodies. Figure 33 shows the resulting images of this negative control test.

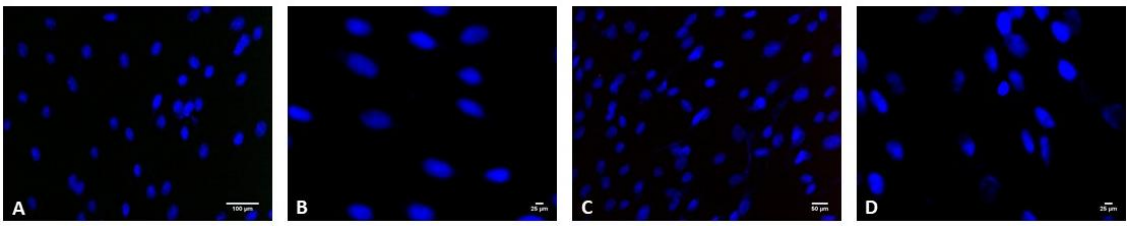

Figure 33 – Negative controls in Immunochemistry experimental protocol.
NHDF were cultured for 3 days in DMEM 0.5% FBS. Cells were fixed with methanol and incubated with Alexa Fluor 488 Anti-Mouse (green, **A** and **B**) or with Alexa Fluor 568 Anti-Rabbit (red, **C** and **D**) antibodies. Cells were also counterstained with nuclei staining (blue). Images were acquired by Carl Zeiss Axio Imager Z2, with ApoTome2 and Stereo-Investigator at different magnifications (20x, A and C; 40x B and D).

The results show that there seems to be no recognition of non-specific proteins by the secondary antibodies used in the ICC experiments.

After culture and Exo-101 treatment of NHDF, these cells were fixed with methanol and the following protocol was accomplished according the optimizations in 3.1 Implementation and optimization of biomolecular methods section. This experiment aims to understand if the production and remodelling of ECM is modulated by Exo-101. In this experiment were performed one replica to each group (Exo-101 and PBS). The ECM proteins visualized by this tchenique at this work were Fn, Col1 and Col3. Cells were also stained with nuclei staining with DAPI. Three images of each condition were acquired randomly in 20x and 40x magnifcation. The tree images acquired in 20x magnification were used to MFI analysis performed in ImageJ software. The obtained MFI to each image was normalized to nucleus counting and data was presented as the mean ± SEM of the tree images analysed.

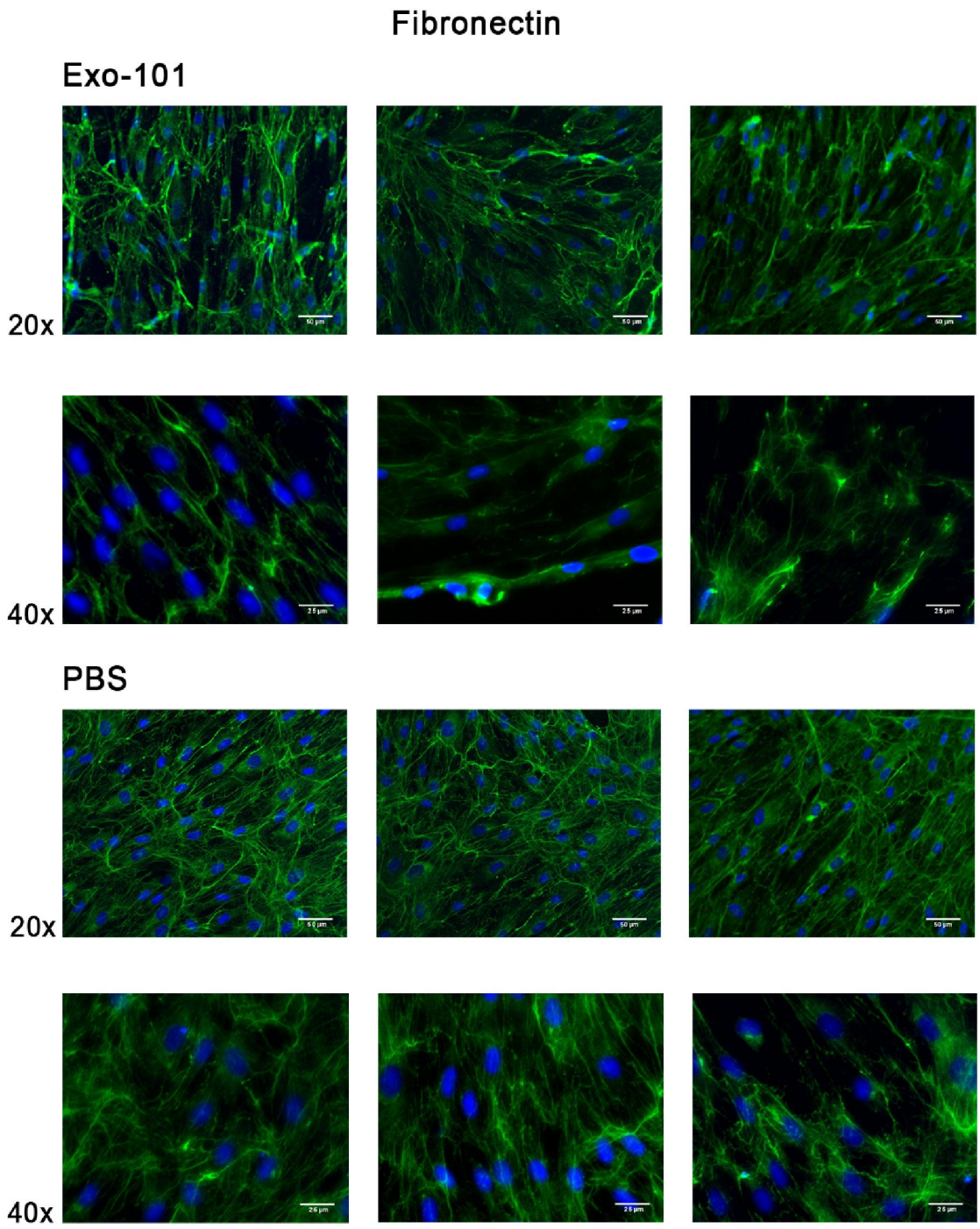

Figure 34 - Fibronectin production in NHDF.
NHDF were treated with Exo-101 or PBS (control) and then ICC was performed. Fibrnectin was detected using a specific antibody and a fluorescent secondary antibody (green) and images were acquired at different magnifications (20x and 40x) using a fluorescence microscope. Cells were also stained with DAPI (blue) for nuclei counterstaining. The three images presented in each line correspond to the same experimental condition.

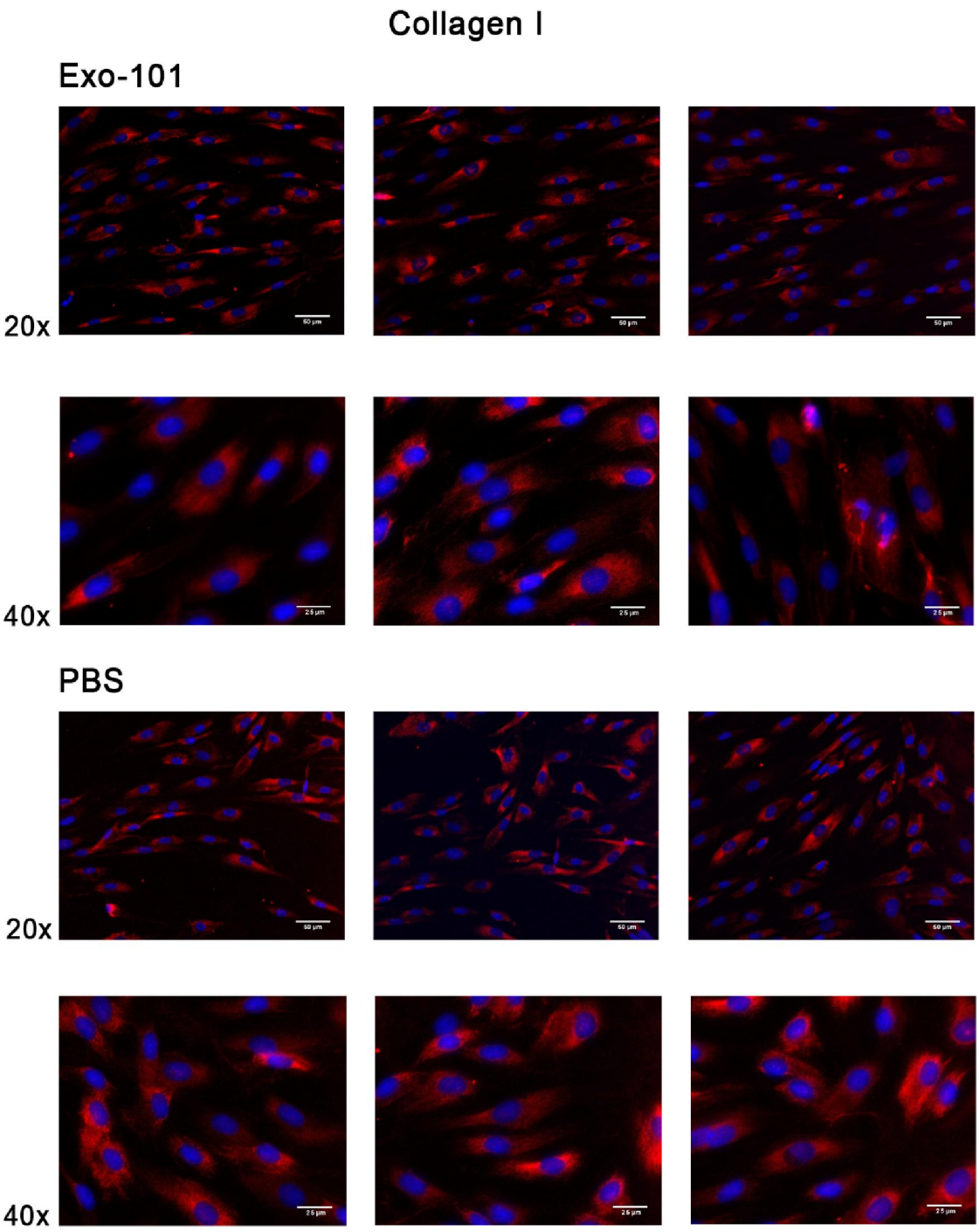

Figure 35 – Collagen I production in NHDF.
NHDF were treated with Exo-101 or PBS (control) and then ICC was performed. Collagen I was detected using a specific antibody and a fluorescent secondary antibody (red) and images were acquired at different magnifications (20x and 40x) using a fluorescence microscope. Cells were also stained with DAPI (blue) for nuclei counterstaining. The three images presented in each line correspond to the same experimental condition.

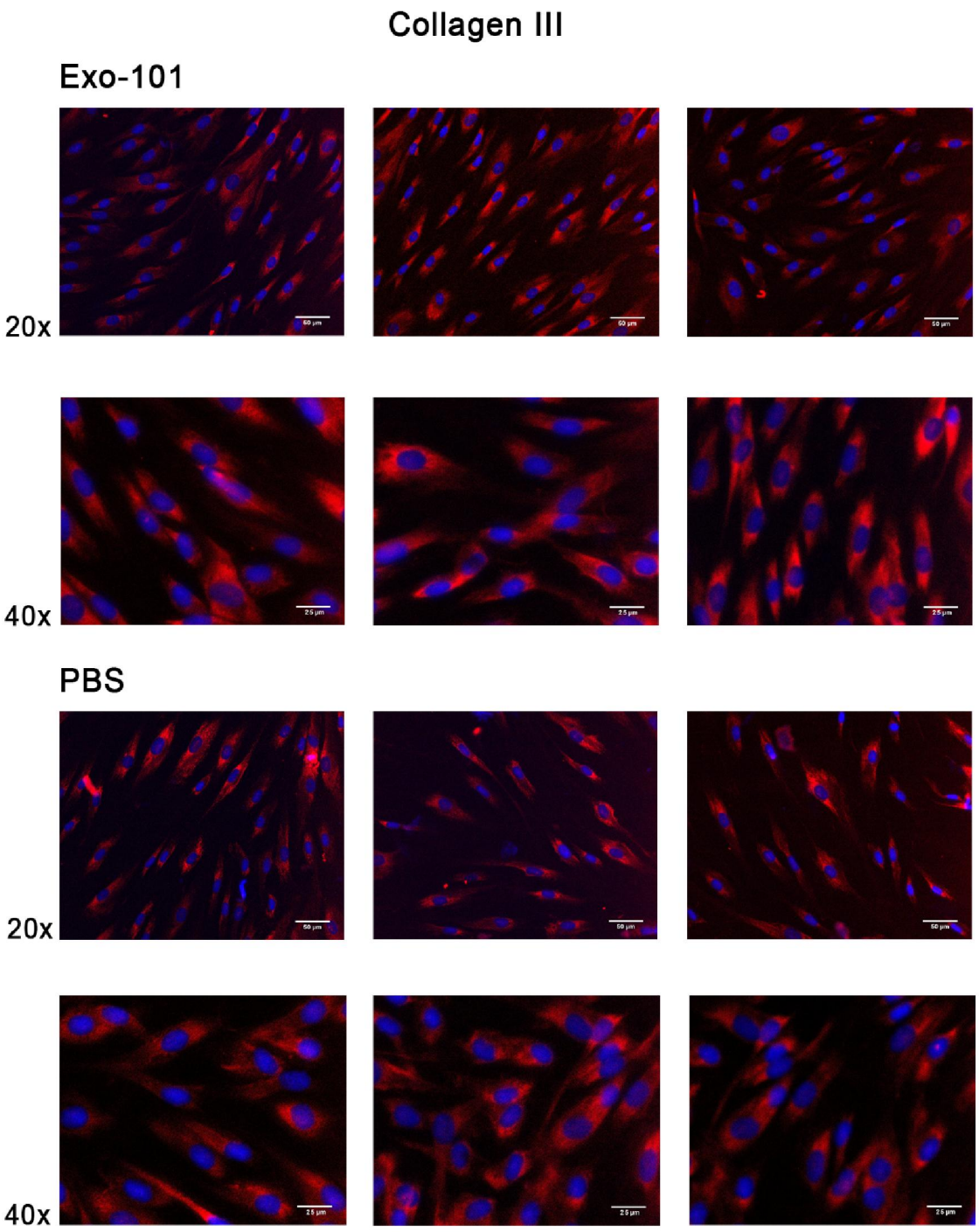

Figure 36 - Collagen III production in NHDF.
NHDF were treated with Exo-101 or PBS (control) and then ICC was performed. Collagen III was detected using a specific antibody and a fluorescent secondary antibody (red) and images were acquired at different magnifications (20x and 40x) using a fluorescence microscope. Cells were also stained with DAPI (blue) for nuclei counterstaining. The three images presented in each line correspond to the same experimental condition.

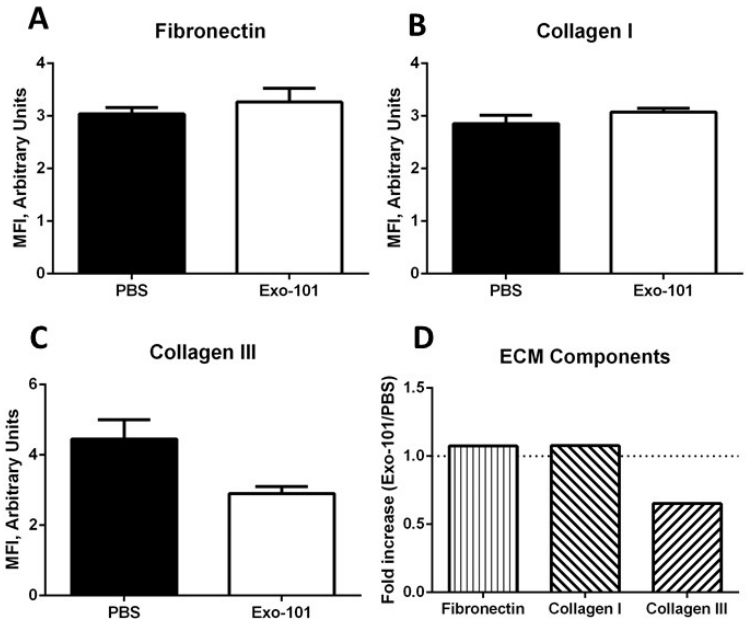

Figure 37 – Production of ECM components in fibroblasts: effect of Exo-101.
The fluorescence intensity of the ICC images obtained was quantified and presented here as Mean Fluorescence Ratio (MFI) for each ECM component: Fn **(A)**, Col1 **(B)** and Col3 **(C)**. The images acquired with 20x magnification were analysed in ImageJ software and the obtained MFI values were normalized to nucleus counting. At least three independent frames analysed and the data is presented as mean ± SEM. The graph in **D** represents the fold increase of MFI values of Fn, Col1 and Col3 in NHDF treated with Exo-101 relatively to PBS control (Exo-101/PBS).

Observing the ICC images for the three proteins under study, we observe no substantial differences between the cells treated with Exo-101 and those treated with PBS (Figures 34, 35 and 36). After MIF analysis (Figure 37), it is possible to note that fluorescence intensity for both Fn and Col1 appear to be identical in the two groups under analysis (Figure 37A and B), while Col3 labelling appears to be more intense in the control group than in the Exo-101 treated group (Figure 37C). It is important to emphasize that this experiment only included one experimental replica (n=1). Accordingly, although ICC is not a quantitative technique, the results suggest that Exo-101 does not have a strong effect on the intercellular expression of Fn, Col1 and Col3. Future work should address secreted ECM, namely by staining, imaging and quantification of deposited ECM after decellularizing the samples.

c. Analysing Fibronectin and Collagen I secretion by WB

The conditioned medium from NHDF treated with Exo-101 or respective control was collected and used in WB analysis. This experiment also aimed to further understand if the production of ECM components, such as Fn and Col1, is modulated by Exo-101. The samples were prepared as previously described in 2. Material and Methods chapter. The WB was perfomed with the optimizations described in 3.1 Implementation and optimization of biomolecular methods section. In this experiment, we used three different experimental replicates in the treatment group (N1, N2, N3). The light signal was visualized using a detection system of VWR and Chemi 5QE

Image Capture Software. The images were analysed by densitometric measurement with ImageJ software. Statistical analysis was performed using GraphPad Prism 6 software, applying Mann-Whitney test (p=0.05; ns if p>0.05).

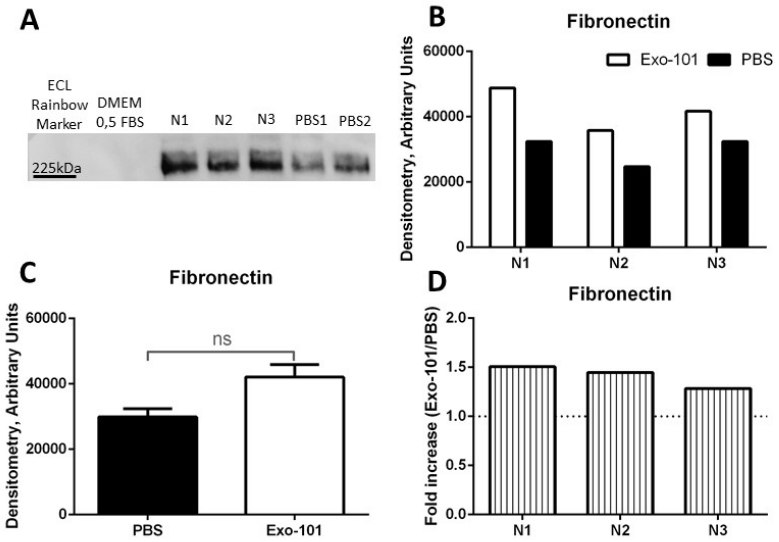

Figure 38 - WB analysis of fibronectin (≈245kDa) secretion in NDHF after Exo-101 treatment.
A) Total protein (35µg) of CM collected from Exo-101-treated cells (n=3) and control cells (n=2) was loaded in a polyacrylamide gel and analysed by WB to detect fibronectin. Additionally, a sample of culture medium (DMEM 0.5% FBS) was loaded in the first lane as a negative control, to demonstrate the absence of Fn in the basal culture medium used in the experiment. **B)** Graphic representation of the densitometric analysis of the Fn bands detected in WB. **C)** Graphic representation of the mean of densitometric values from WB analysis of Fn bands in Exo-101-treated or control NHDF. Data is presented as the mean ± standard error of five independent experiments. Statistical analysis was performed by independent samples Mann-Whitney test (p=0.05; ns: p>0.05;). **D)** Graphic representation of the ratios of Fn intensity in Exo-101 samples compared to the respective PBS control samples (Exo-101/PBS).

The performed three different experimental replicates and corresponding densitometric analysis of Fn secretion (≈245kDa) are shown in Figure 38. The samples, and the controls, were loaded in the same gel. The results show that Exo-101 treated samples N1, N2 and N3 result in higher Fn secretion than the samples treated with PBS (control). When we compared the values resulting from densitometric analysis of both groups, the results suggest a non-significant increase in the secretion of Fn by fibroblasts, upon treatment with Exo-101 (Figure 38C).

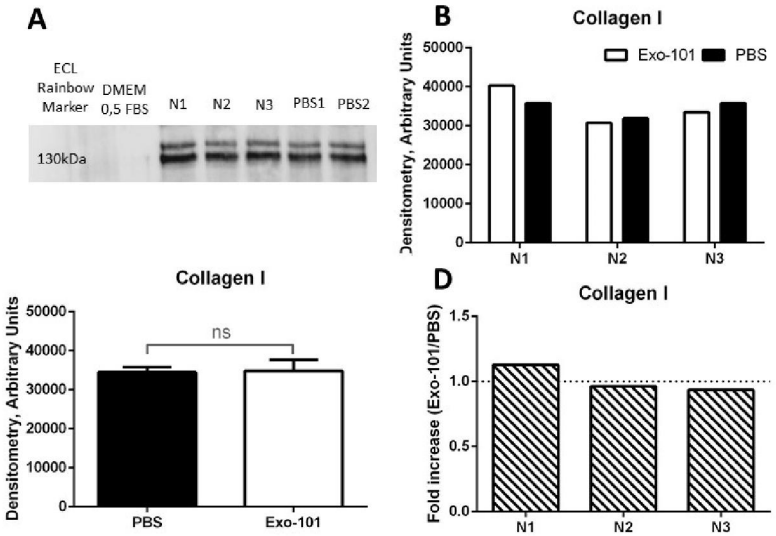

Figure 39 - WB analysis of collagen I (≈130kDa) secretion in NDHF after Exo-101 treatment.
A) Total protein (35µg) of CM collected from Exo-101-treated cells (n=3) and control cells (n=2) was loaded in a polyacrylamide gel and analysed by WB to detect collagen I. Additionally, a sample of culture medium (DMEM 0.5% FBS) was loaded in the first lane as a negative control, to demonstrate the absence of Col1 in the basal culture medium used in the experiment. **B)** Graphic representation of the densitometric analysis of the Col1 bands detected in WB. **C)** Graphic representation of the mean of densitometric values from WB analysis of Col1 bands in Exo-101-treated or control NHDF. Data is presented as the mean ± SEM of three independent experiments. Statistical analysis was performed by independent samples Mann-Whitney test (p=0.05; ns: p>0.05). **D)** Graphic representation of the ratios of Col1 intensity in Exo-101 samples compared to the respective PBS control samples (Exo-101/PBS).

The performed three independent biologic replicates and corresponding densitometric analysis for evaluating Col1 secretion (≈130kDa) are shown in Figure 39. All samples, treated and control, were loaded in the same gel. The results show that Exo-101 treated samples N1, N2 and N3 a similar Col1 presence relatively to control samples (PBS1 and PBS2). Thus, these results showed that Exo-101 does not significantly alter the secretion of Col1 by fibroblasts (Figure 39C).

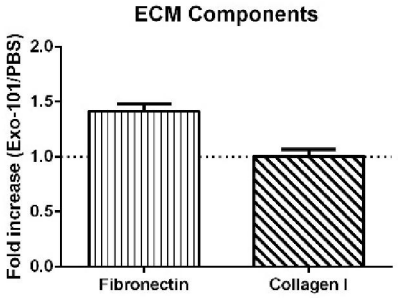

Figure 40 - Comparison between the effect of Exo-101 over fibronectin and collagen I secretion.
Graph includes the data represented in Figures 38D (fibronectin) and 39D (collagen I) represented as the mean ± SEM of three and five independent experiments, respectively.

When we compare directly the fold increase resulting from the treatment of fibroblasts with Exo-101, the results suggest a potential impact in the secretion of Fn, but not of Col1 (Figure 40).

The expression and production of ECM components by NHDF after treatment with Exo-101 was evaluated using RT-qPCR, WB and ICC. The RT-qPCR analysis showed no expressive

differences between groups, regarding expression of FN and COL3A1 genes. Nevertheless, COL3A1 gene is slightly downregulated upon treatment with Exo-101. Through WB analysis, the results show that relatively to the secretion of Col1 the differences between groups are not statistically significant and the resulting fold increase is approximately 1. However, this analysis to secretion of Fn suggests a non-significant increase in the secretion of this protein by fibroblasts, upon treatment with Exo-101. Likewise, the images acquired from ICC intracellular staining of Fn, Col1 and Col3 do not suggest meaningful differences between the groups. The corresponding MFI analysis suggests the same pattern of expression as analysed by RT-qPCR, where Fn and Col1 levels are not expressively influenced by Exo-101 treatment, while Col 3 appears to be less expressed in the Exo-101-treated cells.

Results from WB analysis suggest an increased in Fn secretion, but not Col1, by NHDF upon treatment with Exo-101. *In vitro*, fibroblasts secrete and assemble Fn to promote initial attachment and spreading. Given that in our experimental conditions the fibroblasts were still in initial attachment, it is conceivable that NHDF were more prompt to secrete Fn rather than Col1. Nevertheless, although it is not significant result, there is an increase of Fn secretion by fibroblasts treated with Exo-101, which may indicate an induction of the beginning of granulation tissue formation [128,129]. At early stages of wound healing, cellular Fn is deposited by fibroblast to form an immature ECM. The assembly of this ECM influence cell migration and the deposition of other molecules of ECM, such as collagen, which are processes related to granulation tissue formation. Thus, our results suggest that Exo-101 may increase Fn secretion by NHDF, potentially inducing processes related to the proliferative phase of wound healing.

Although the results presented do not show very well-defined differences, there is a tendency for decreased expression and production (RT-qPCR and ICC) of Col3, and expression of TGF-β1 (RT-qPCR). The down regulation of the expression or production of these proteins is interpreted in the literature as an antifibrotic effect [130–133]. Together with Col1, Col3 is one of the constituent components of the dermis ECM. Col3 is mostly produced by fibroblasts during the proliferative phase to form a still immature ECM along with Col1. As the healing process progresses and the dermal ECM becomes more mature, Col3 is replaced by Col1, which is the main constituent of normal skin. The researches that evaluate the antifibrotic effect study the collagens expression [132,133]. The decrease of collagen expression, namely Col3, is related with antifibrotic effect. TGF-β1 promotes collagen synthesis and contraction, and when at high levels, it may promote exaggerated effects and cause fibrosis [130,131]. Thus, the possible decrease in TGF-β1 expression and also the presumed decreased expression and production of Col3 by NHDF, upon treatment with Exo-101, suggests an antifibrotic effect in these cells.

- **Some considerations about NHDF culture and ECM assembly**

Analysing globally the results from the analysis of ECM components by WB and ICC we can observe that the assembly of an ECM composed of Fn, Col1 and Col3 may not be fully complete. The results from ICC and WB show that Fn is found deposited around cells and in CM. However, Col1 and Col3 is found in intracellular space and in CM from NHDF culture. As mentioned above, secretion of ECM components in CM by cells cultured *in vitro* is described in other works [119,120]. In these works, the secretion of proteins is evaluated by WB using samples of CM and cell lysates. The CM samples evaluated were collected with one week of culture and cells were collected with two or four weeks of culture. The time of culture influences the production and the assembly of ECM components. Similarly, the intracellular staining profile of Col1 and Col3 is in line with some other works which study the production of ECM by dermal or lung fibroblasts [131,134]. Researches which report the same intracellular staining profile describe a culture time of 24 hours or 3 days, in agreement with the one used in this work. A report published in 2014 which studied the assembly of ECM by fibroblasts in co-culture with endothelial and dendritic cells, and whose culture time reached 14 days, show an extracellular staining of Col1 [135]. From these evidences, it may be suggested that the intracellular staining of the collagens obtained in this work may be due to the short culture time of the NHDF. On the other hand, the fact that the culture used is a monoculture cultured directly on plastic of the well plate may be preventing the formation of a consistent ECM.

It is important to note that the NHDF used to assess the secretion and assembly of ECM components were cultured for more than 72 hours. The fibronectin and collagens identified by WB in CM could be molecules secreted by the NHDFs and which did not have the necessary conditions to be assembled into a stable extracellular matrix. Probably, the collagen molecules identified by ICC with intracellular staining may be the procollagen chains, before its secretion. This may mean that the culture time of the NHDF may not be sufficient for these cells to construct a consistent ECM. On the other hand, these cells may not have the necessary conditions to build an ECM as would be expected *in vivo*. These may explain the presence of matrix proteins in CM and collagen molecules in NHDF cytoplasm. Thus, the *in vitro* ECM assembly timeframe by NHDF should be evaluated, as well as some types of coating should be considered, in order to understand the optimal culture time and conditions for NHDF to begin assembling a more complex ECM.

Chapter 4:
Conclusion and Future Perspectives

4. Conclusion and Future Perspectives

The objective of this dissertation was to implement biomolecular techniques in Exogenus Therapeutics' laboratory to enable their use for the characterization of the mode of action of the lead product under development, Exo-Wound. This includes the evaluation of the expression or production of dermal ECM components and GFs essential for wound healing. For this, a literature review was first carried out in order to ascertain which molecules to evaluate and which methodologies would be most advantageous. Thus, it was concluded that the expression analysis and production of ECM components should be evaluated by analysing expression and secretion of proteins such as fibronectin, and the two most prevalent types of collagen in human skin, Collagen I and Collagen III. In addition, it was decided that the best approach to assess the involvement of GFs would be the analysis of the expression of several GFs in two cell lines of the skin. In accordance with the needs of the company, it was decided that RT-qPCR, WB and ICC would be the most advantageous methods to implement to achieve the proposed analyses.

To assess the expression of both ECM components and GFs, RT-qPCR was implemented successfully. This technique has gone through several optimization steps to obtain the best quality data. In addition, evaluation of the production of ECM components was also performed through the implementation of WB and ICC. Likewise, these techniques were used to characterize the profile of expression and secretion of the proteins of interest in order to obtain reliable data.

After the laboratory techniques were implemented and optimized, preliminary tests were carried out to validate the use of these techniques to evaluate the expression and production of the molecules of interest for this work. The results obtained through RT-qPCR showed that this technique is sensitive, replicative and quantitative. However, the fact that some genes did not have sufficient expression to be analysed, probably due to the lack of quality of the RNA samples, may indicate the need to optimize RNA extraction. The results obtained by WB and ICC suggest that these techniques enable good qualitative data on whether the proteins of interest are produced or not, but they are not optimal for obtaining quantitative data. From the data obtained by these techniques it is perceptible that there may be a need to better study the production and assembly of ECM by human fibroblasts *in vitro*, in order to obtain more robust results. Nevertheless, we attempted to quantify protein expression and secretion by means of using WB and ICC.

In NHEK, Exo-101 seems to increase the expression of TGFB1 and VEGFA, which may be related to the acceleration of the healing process in general and more specifically to the process of angiogenesis. It is important to note that these preliminary tests were not performed with the

necessary replicates to obtain robust and statistically significant results. Relatively to the effect of the Exo-101 product on the NHDF, we observe that Exo-101 seems to increase the secretion of Fn, while reducing the intracellular expression of Col3 and TGFB1. These evidences may correspond to a possible induction of granulation tissue formation in association with an antifibrotic effect.

As a future perspective, the implementation of more quantitative techniques for the evaluation of protein production, such as Enzyme-Linked Immunosorbent Assay (ELISA), may be imperative. Furthermore, we also recognize the need for implementing a comprehensive method of analysis of the production and assembly of ECM by NHDF *in vitro*, using optimal culture conditions to be defined. Regarding the potential modelling effects exerted by Exo-101 on the expression and production of the molecules evaluated, the data needs to be sustained by more biological replicates, including more controls, to confirm the tendencies observed in this work. Finally, this master's thesis constitutes an important technical and scientific contribution to the laboratory of Exogenus Therapeutics, by introducing methods that did not exist in the company's laboratory. In addition, it is expected that this work will serve as a basis for future research carried out within the scope of characterizing the mode of action of Exo-Wound product under development.

Chapter 5: Bibliography

5. Bibliography

1. Rani S, Ryan AE, Griffin MD, Ritter T. Mesenchymal Stem Cell-derived Extracellular Vesicles: Toward Cell-free Therapeutic Applications. *Mol. Ther*. 2015;23:812–23.
2. Kim JY, Song S-H, Kim KL, Ko J-J, Im J-E, Yie SW. Human Cord Blood-Derived Endothelial Progenitor Cells and Their Conditioned Media Exhibit Therapeutic Equivalence for Diabetic Wound Healing. *Cell Transplant*. 2010;19:1635–44.
3. Hacker S, Mittermayr R, Nickl S, Haider T, Lebherz-Eichinger D, Beer L, et al. Paracrine Factors from Irradiated Peripheral Blood Mononuclear Cells Improve Skin Regeneration and Angiogenesis in a Porcine Burn Model. *Sci. Rep*. 2016;6:25168.
4. Lazarus GS, Cooper DM, Knighton DR, Margolis DJ, Pecoraro RE, Rodeheaver G. Definitions and guidelines for assessment of wounds and evaluation of healing. *Arch. Dermatol.* 1994;130:489–93.
5. Satish L, Kathju S. Cellular and Molecular Characteristics of Scarless versus Fibrotic Wound Healing. Dermatol. *Res. Pract*. 2010;2010:1–11.
6. Albanna MZ. Skin tissue engineering and regenerative medicine. 1st ed. Boston, MA: *Elsevier*; 2016.
7. Werdin F, Tennenhaus M, Schaller H-E, Rennekampff H-O. Evidence-based Management Strategies for Treatment of Chronic Wounds. *Eplasty*; 2009
8. Sen CK, Gordillo GM, Roy S, Kirsner R, Lambert L, Hunt TK. Human skin wounds: A major and snowballing threat to public health and the economy. *Wound Repair Regen*. 2009;17:763–71.
9. Dreifke MB, Jayasuriya AA, Jayasuriya AC. Current wound healing procedures and potential care. Mater. *Sci. Eng*. C 2015;48:651–62.
10. MedMarket Diligence. Projected global wound prevalence by wound types. *Adv. Med. Technol.* Available from: http://blog.mediligence.com/2013/02/17/projected-global-wound-prevalence-by-wound-types/
11. Gottrup F, Apelqvist J, Price P, European Wound Management Association Patient Outcome Group. Outcomes in controlled and comparative studies on non-healing wounds: recommendations to improve the quality of evidence in wound management. *J. Wound Care* 2010;19:237–68.
12. Frykberg RG, Banks J. Challenges in the Treatment of Chronic Wounds. *Adv. Wound Care* 2015;4:560–82.
13. Bryant RA, Nix DP. Acute & chronic wounds: current management concepts. 5th ed. St Louis, Missouri: *Elsevier*; 2016.
14. VanPutte CL, Seeley RR. Seeley's anatomy & physiology. 10th ed. New York, NY: McGraw-Hill; 2014.
15. Baum CL, Arpey CJ. Normal cutaneous wound healing: clinical correlation with cellular and molecular events. Dermatol. Surg. Off. Publ. Am. *Soc. Dermatol. Surg*. Al 2005;31:674–686; discussion 686.
16. Tracy LE, Minasian RA, Caterson EJ. Extracellular Matrix and Dermal Fibroblast Function in the Healing Wound. *Adv. Wound Care* 2016;5:119–36.
17. Cichorek M, Wachulska M, Stasiewicz A, Tymińska A. Skin melanocytes: biology and development. *Adv. Dermatol. Allergol*. 2013;1:30–41.
18. Jaitley S, Saraswathi T. Pathophysiology of Langerhans cells. J. Oral Maxillofac. *Pathol*. 2012;16:239.

19. Woo S-H, Lumpkin EA, Patapoutian A. Merkel cells and neurons keep in touch. *Trends Cell Biol.* 2015;25:74–81.
20. Shetty S. Keratinization and its Disorders. *Oman Med. J*. 2012;27:348–57.
21. Shaw TJ, Martin P. Wound repair: a showcase for cell plasticity and migration. Curr. Opin. *Cell Biol*. 2016;42:29–37.
22. Osnovative Systems. Enluxtra. Non-Healling Wounds; 2016; Available from: http://www.enluxtrawoundcare.com/non-healing-wounds.html
23. Cho J, Degen JL, Coller BS, Mosher DF. Fibrin but Not Adsorbed Fibrinogen Supports Fibronectin Assembly by Spread Platelets: Effects of the interaction of αIIbβ3 with the c-terminusof fibrinogen γ-chain. *J. Biol. Chem*. 2005;280:35490–8.
24. Lenselink EA. Role of fibronectin in normal wound healing: Role of fibronectin in normal wound healing. *Int. Wound J*. 2015;12:313–6.
25. Pastar I, Stojadinovic O, Yin NC, Ramirez H, Nusbaum AG, Sawaya A. Epithelialization in Wound Healing: A Comprehensive Review. *Adv. Wound Care* 2014;3:445–64.
26. Frelinger III AL, Torres AS, Caiafa A, Morton CA, Berny-Lang MA, Gerrits AJ. Platelet-rich plasma stimulated by pulse electric fields: Platelet activation, procoagulant markers, growth factor release and cell proliferation. *Platelets* 2015;1–8.
27. Barrientos S, Stojadinovic O, Golinko MS, Brem H, Tomic-Canic M. Growth factors and cytokines in wound healing. Wound Repair Regen. Off. Publ. *Wound Heal. Soc. Eur. Tissue Repair Soc*. 2008;16:585–601.
28. Landén NX, Li D, Ståhle M. Transition from inflammation to proliferation: a critical step during wound healing. *Cell. Mol. Life Sci*. 2016;73:3861–85.
29. Willenborg S, Lucas T, van Loo G, Knipper JA, Krieg T, Haase I. CCR2 recruits an inflammatory macrophage subpopulation critical for angiogenesis in tissue repair. *Blood* 2012;120:613–25.
30. Russo VC, Andaloro E, Fornaro SA, Najdovska S, Newgreen DF, Bach LA. Fibroblast growth factor-2 over-rides insulin-like growth factor-I induced proliferation and cell survival in human neuroblastoma cells. *J. Cell. Physiol*. 2004;199:371–80.
31. Serini G, Bochaton-Piallat ML, Ropraz P, Geinoz A, Borsi L, Zardi L. The fibronectin domain ED-A is crucial for myofibroblastic phenotype induction by transforming growth factor-beta1. *J. Cell Biol*. 1998;142:873–81.
32. Rajkumar VS, Shiwen X, Bostrom M, Leoni P, Muddle J, Ivarsson M. Platelet-Derived Growth Factor-β Receptor Activation Is Essential for Fibroblast and Pericyte Recruitment during Cutaneous Wound Healing. *Am. J. Pathol*. 2006;169:2254–65.
33. Rohani MG, Parks WC. Matrix remodeling by MMPs during wound repair. *Matrix Biol.* 2015;44–46:113–21.
34. Lindner D, Zietsch C, Becher PM, Schulze K, Schultheiss H-P, Tschöpe C. Differential Expression of Matrix Metalloproteases in Human Fibroblasts with Different Origins. *Biochem. Res. Int.* 2012;2012:1–10.

35. Roh S-S, Lee M-H, Hwang Y-L, Song H-H, Jin MH, Park SG. Stimulation of the Extracellular Matrix Production in Dermal Fibroblasts by Velvet Antler Extract. *Ann. Dermatol.* 2010;22:173.
36. Quan T, Wang F, Shao Y, Rittié L, Xia W, Orringer JS. Enhancing Structural Support of the Dermal Microenvironment Activates Fibroblasts, Endothelial Cells, and Keratinocytes in Aged Human Skin In Vivo. *J. Invest. Dermatol*. 2013;133:658–67.
37. Rapraeger AC, Ell BJ, Roy M, Li X, Morrison OR, Thomas GM. Vascular endothelial-cadherin stimulates syndecan-1-coupled insulin-like growth factor-1 receptor and cross-talk between αVβ3 integrin and vascular endothelial growth factor receptor 2 at the onset of endothelial cell dissemination during angiogenesis. *FEBS J.* 2013;280:2194–206.
38. Martins VL, Caley M, O'Toole EA. Matrix metalloproteinases and epidermal wound repair. *Cell Tissue Res*. 2013;351:255–68.
39. Shinde AV, Humeres C, Frangogiannis NG. The role of α-smooth muscle actin in fibroblast-mediated matrix contraction and remodeling. *Biochim. Biophys*. Acta BBA - Mol. Basis Dis. 2017;1863:298–309.
40. Cheng W, Yan-hua R, Fang-gang N, Guo-an Z. The content and ratio of type I and III collagen in skin differ with age and injury. *Afr. J. Biotechnol.* 2011;10:2524–9.
41. Soo C, Shaw WW, Zhang X, Longaker MT, Howard EW, Ting K. Differential expression of matrix metalloproteinases and their tissue-derived inhibitors in cutaneous wound repair. *Plast. Reconstr. Surg*. 2000;105:638–47.
42. Madlener M, Parks WC, Werner S. Matrix Metalloproteinases (MMPs) and Their Physiological Inhibitors (TIMPs) Are Differentially Expressed during Excisional Skin Wound Repair. *Exp. Cell Res.* 1998;242:201–10.
43. Desmoulière A, Redard M, Darby I, Gabbiani G. Apoptosis mediates the decrease in cellularity during the transition between granulation tissue and scar. *Am. J. Pathol*. 1995;146:56–66.
44. Dinh T, Braunagel S, Rosenblum BI. Growth Factors in Wound Healing. *Clin. Podiatr. Med. Surg*. 2015;32:109–19.
45. Theocharis AD, Skandalis SS, Gialeli C, Karamanos NK. Extracellular matrix structure. *Adv. Drug Deliv. Rev*. 2016;97:4–27.
46. Eming SA, Koch M, Krieger A, Brachvogel B, Kreft S, Bruckner-Tuderman L. Differential Proteomic Analysis Distinguishes Tissue Repair Biomarker Signatures in Wound Exudates Obtained from Normal Healing and Chronic Wounds. *J. Proteome Res*. 2010;9:4758–66.
47. Robson MC. The role of growth factors in the healing of chronic wounds. Wound Repair Regen. Off. Publ. Wound Heal. *Soc. Eur. Tissue Repair Soc*. 1997;5:12–7.
48. Telgenhoff D, Shroot B. Cellular senescence mechanisms in chronic wound healing. *Cell Death Differ.* 2005;12:695–8.
49. Jiang L, Dai Y, Cui F, Pan Y, Zhang H, Xiao J. Expression of cytokines, growth factors and apoptosis-related signal molecules in chronic pressure ulcer wounds healing. *Spinal Cord* 2014;52:145–51.
50. Trengove NJ, Bielefeldt-Ohmann H, Stacey MC. Mitogenic activity and cytokine levels in non-healing and healing chronic leg ulcers. Wound Repair Regen. Off. Publ. *Wound Heal. Soc. Eur. Tissue Repair Soc*. 2000;8:13–25.

51. Rennert RC, Rodrigues M, Wong VW, Duscher D, Hu M, Maan Z. Biological therapies for the treatment of cutaneous wounds: Phase III and launched therapies. Expert Opin. *Biol. Ther.* 2013;13:1523–41.
52. Shankaran V, Brooks M, Mostow E. Advanced therapies for chronic wounds: NPWT, engineered skin, growth factors, extracellular matrices. *Dermatol. Ther*. 2013;26:215–21.
53. Margolis DJ, Bartus C, Hoffstad O, Malay S, Berlin JA. Effectiveness of recombinant human platelet-derived growth factor for the treatment of diabetic neuropathic foot ulcers. Wound Repair Regen. Off. Publ. *Wound Heal. Soc. Eur. Tissue Repair Soc.* 2005;13:531–6.
54. Wainwright D, Madden M, Luterman A, Hunt J, Monafo W, Heimbach D. Clinical evaluation of an acellular allograft dermal matrix in full-thickness burns. *J. Burn Care Rehabil.* 1996;17:124–36.
55. Mostow EN, Haraway GD, Dalsing M, Hodde JP, King D, OASIS Venus Ulcer Study Group. Effectiveness of an extracellular matrix graft (OASIS Wound Matrix) in the treatment of chronic leg ulcers: a randomized clinical trial. *J. Vasc. Surg*. 2005;41:837–43.
56. Hu L, Wang J, Zhou X, Xiong Z, Zhao J, Yu R. Exosomes derived from human adipose mensenchymal stem cells accelerates cutaneous wound healing via optimizing the characteristics of fibroblasts. *Sci. Rep*. 2016
57. Zhang J, Guan J, Niu X, Hu G, Guo S, Li Q. Exosomes released from human induced pluripotent stem cells-derived MSCs facilitate cutaneous wound healing by promoting collagen synthesis and angiogenesis. *J. Transl. Med*. 2015;13:49.
58. Zhao B, Zhang Y, Han S, Zhang W, Zhou Q, Guan H. Exosomes derived from human amniotic epithelial cells accelerate wound healing and inhibit scar formation. *J. Mol. Histol.* 2017;48:121–32.
59. Zhang J, Chen C, Hu B, Niu X, Liu X, Zhang G. Exosomes Derived from Human Endothelial Progenitor Cells Accelerate Cutaneous Wound Healing by Promoting Angiogenesis Through Erk1/2 Signaling. *Int. J. Biol. Sci*. 2016;12:1472–87.
60. Guo S-C, Tao S-C, Yin W-J, Qi X, Yuan T, Zhang C-Q. Exosomes derived from platelet-rich plasma promote the re-epithelization of chronic cutaneous wounds via activation of YAP in a diabetic rat model. *Theranostics* 2017;7:81–96.
61. Wang L, Hu L, Zhou X, Xiong Z, Zhang C, Shehada HMA. Exosomes secreted by human adipose mesenchymal stem cells promote scarless cutaneous repair by regulating extracellular matrix remodelling. *Sci. Rep*. 2017; 41598-017-12919-x
62. Frantz C, Stewart KM, Weaver VM. The extracellular matrix at a glance. *J. Cell Sci.* 2010;123:4195–200.
63. Clark RA. Fibronectin matrix deposition and fibronectin receptor expression in healing and normal skin. *J. Invest. Dermatol*. 1990;94:128S–134S.
64. Whitby DJ, Ferguson MW. The extracellular matrix of lip wounds in fetal, neonatal and adult mice. *Development* 1991;112:651–68.
65. Bielefeld KA, Amini-Nik S, Whetstone H, Poon R, Youn A, Wang J. Fibronectin and β-Catenin Act in a Regulatory Loop in Dermal Fibroblasts to Modulate Cutaneous Healing. *J. Biol. Chem.* 2011;286:27687–97.
66. Hughes OB, Rakosi A, Macquhae F, Herskovitz I, Fox JD, Kirsner RS. A Review of Cellular and Acellular Matrix Products: Indications, Techniques, and Outcomes. *Plast. Reconstr. Surg.* 2016;138:138S–147S.

67. Shinde AV, Kelsh R, Peters JH, Sekiguchi K, Van De Water L, McKeown-Longo PJ. The α4β1 integrin and the EDA domain of fibronectin regulate a profibrotic phenotype in dermal fibroblasts. *Matrix Biol.* 2015;41:26–35.
68. To WS, Midwood KS. Plasma and cellular fibronectin: distinct and independent functions during tissue repair. *Fibrogenesis Tissue Repair* 2011;4:21.
69. Obara M, Sakuma T, Fujikawa K. The third type III module of human fibronectin mediates cell adhesion and migration. *J. Biochem.* (Tokyo) 2010;147:327–35.
70. Lin F, Zhu J, Tonnesen MG, Taira BR, McClain SA, Singer AJ. Fibronectin Peptides that Bind PDGF-BB Enhance Survival of Cells and Tissue under Stress. *J. Invest. Dermatol.* 2014;134:1119–27.
71. Asaga H, Kikuchi S, Yoshizato K. Collagen gel contraction by fibroblasts requires cellular fibronectin but not plasma fibronectin. *Exp. Cell Res.* 1991;193:167–74.
72. Velling T, Risteli J, Wennerberg K, Mosher DF, Johansson S. Polymerization of Type I and III Collagens Is Dependent On Fibronectin and Enhanced By Integrins $\alpha_{11}\beta_1$ and $\alpha_2\beta_1$. *J. Biol. Chem*. 2002;277:37377–81.
73. Maqueda A, Moyano JV, Hernández Del Cerro M, Peters DM, Garcia-Pardo A. The heparin III-binding domain of fibronectin (III4-5 repeats) binds to fibronectin and inhibits fibronectin matrix assembly. *J. Int. Soc. Matrix Biol*. 2007;26:642–51.
74. Stepp MA, Daley WP, Bernstein AM, Pal-Ghosh S, Tadvalkar G, Shashurin A. Syndecan-1 regulates cell migration and fibronectin fibril assembly. *Exp. Cell Res*. 2010;316:2322–39.
75. Purohit T, Qin Z, Quan C, Lin Z, Quan T. Smad3-dependent CCN2 mediates fibronectin expression in human skin dermal fibroblasts. *PLOS ONE* 2017;12:e0173191.
76. Parkin JD, San Antonio JD, Persikov AV, Dagher H, Dalgleish R, Jensen ST. The collαgen III fibril has a "flexi-rod" structure of flexible sequences interspersed with rigid bioactive domains including two with hemostatic roles. PLoS ONE; 2017; PMC5509119
77. Ricard-Blum S. The Collagen Family. *Cold Spring Harb. Perspect. Biol*. 2011;3:a004978–a004978.
78. Ehrlich HP, Sun B, Saggers GC, Kromath F. Gap junction communications influence upon fibroblast synthesis of Type I collagen and fibronectin. *J. Cell. Biochem*. 2006;98:735–43.
79. Wu J, Reinhardt DP, Batmunkh C, Lindenmaier W, Far RK-K, Notbohm H. Functional diversity of lysyl hydroxylase 2 in collagen synthesis of human dermal fibroblasts. *Exp. Cell Res*. 2006;312:3485–94.
80. Zoppi N, Gardella R, De Paepe A, Barlati S, Colombi M. Human Fibroblasts with Mutations in *COL5A1* and *COL3A1* Genes Do Not Organize Collagens and Fibronectin in the Extracellular Matrix, Down-regulate $\alpha_2\beta_1$ Integrin, and Recruit $\alpha_v\beta_3$ Instead of $\alpha_5\beta_1$ Integrin. *J. Biol. Chem*. 2004;279:18157–68.
81. Zigrino P, Brinckmann J, Niehoff A, Lu Y, Giebeler N, Eckes B. Fibroblast-Derived MMP-14 Regulates Collagen Homeostasis in Adult Skin. *J. Invest. Dermatol.* 2016;136:1575–83.
82. Lichtman MK, Otero-Vinas M, Falanga V. Transforming growth factor beta (TGF-β) isoforms in wound healing and fibrosis: TGF-β and wound healing. *Wound Repair Regen*. 2016;24:215–22.
83. Morikawa M, Derynck R, Miyazono K. TGF-β and the TGF-β Family: Context-Dependent Roles in Cell and Tissue Physiology. *Cold Spring Harb. Perspect. Biol*. 2016;8:a021873.

84. Kim SK, Barron L, Hinck CS, Petrunak EM, Cano KE, Thangirala A. An engineered transforming growth factor β (TGF-β) monomer that functions as a dominant negative to block TGF-β signaling. *J. Biol. Chem*. 2017;292:7173–88.
85. Kim C-R, Kim Y-M, Lee M-K, Kim I-H, Choi Y-H, Nam T-J. Pyropia yezoensis peptide promotes collagen synthesis by activating the TGF-β/Smad signaling pathway in the human dermal fibroblast cell line Hs27. *Int. J. Mol. Med.* 2016
86. Pakyari M, Farrokhi A, Maharlooei MK, Ghahary A. Critical Role of Transforming Growth Factor Beta in Different Phases of Wound Healing. *Adv. Wound Care* 2013;2:215–24.
87. Le M, Naridze R, Morrison J, Biggs LC, Rhea L, Schutte BC. Transforming growth factor Beta 3 is required for excisional wound repair in vivo. *PLOS ONE* 2012;7:e48040.
88. Li X, Wang C, Xiao J, McKeehan WL, Wang F. Fibroblast growth factors, old kids on the new block. Semin. *Cell Dev. Biol.* 2016;53:155–67.
89. Steringer JP, Müller H-M, Nickel W. Unconventional Secretion of Fibroblast Growth Factor 2—A Novel Type of Protein Translocation across Membranes? *J. Mol. Biol.* 2015;427:1202–10.
90. Losi P, Briganti E, Errico C, Lisella A, Sanguinetti E, Chiellini F. Fibrin-based scaffold incorporating VEGF- and bFGF-loaded nanoparticles stimulates wound healing in diabetic mice. *Acta Biomater*. 2013;9:7814–21.
91. Shi H, Cheng Y, Ye J, Cai P, Zhang J, Li R. bFGF Promotes the Migration of Human Dermal Fibroblasts under Diabetic Conditions through Reactive Oxygen Species Production via the PI3K/Akt-Rac1- JNK Pathways. *Int. J. Biol. Sci*. 2015;11:845–59.
92. Kashpur O, LaPointe D, Ambady S, Ryder EF, Dominko T. FGF2-induced effects on transcriptome associated with regeneration competence in adult human fibroblasts. *BMC Genomics* 2013;14:656.
93. Xuan Y, Chi L, Tian H, Cai W, Sun C, Wang T. The activation of the NF-κB-JNK pathway is independent of the PI3K-Rac1-JNK pathway involved in the bFGF-regulated human fibroblast cell migration. *J. Dermatol. Sci*. 2016;82:28–37.
94. Zhu X-J, Liu Y, Dai Z-M, Zhang X, Yang X, Li Y. BMP-FGF Signaling Axis Mediates Wnt-Induced Epidermal Stratification in Developing Mammalian Skin. *PLoS Genet.* 2014;10:e1004687.
95. Andreadis ST, Hamoen KE, Yarmush ML, Morgan JR. Keratinocyte growth factor induces hyperproliferation and delays differentiation in a skin equivalent model system. FASEB J. Off. Publ. *Fed. Am. Soc. Exp. Biol*. 2001;15:898–906.
96. DiPietro LA. Angiogenesis and wound repair: when enough is enough. *J. Leukoc. Biol.* 2016;100:979–84.
97. Crafts TD, Jensen AR, Blocher-Smith EC, Markel TA. Vascular endothelial growth factor: Therapeutic possibilities and challenges for the treatment of ischemia. *Cytokine* 2015;71:385–93.
98. Ciarlillo D, Celeste C, Carmeliet P, Boerboom D, Theoret C. A hypoxia response element in the Vegfa promoter is required for basal Vegfa expression in skin and for optimal granulation tissue formation during wound healing in mice. *PLOS ONE* 2017;12:e0180586.

99. Wang N, Wu Y, Zeng N, Wang H, Deng P, Xu Y. E2F1 Hinders Skin Wound Healing by Repressing Vascular Endothelial Growth Factor (VEGF) Expression, Neovascularization, and Macrophage Recruitment. *PLOS ONE* 2016;11:e0160411.
100. Jiang Q. Moist exposed burn ointment promotes cutaneous excisional wound healing in rats involving VEGF and bFGF. *Mol. Med. Rep*. 2014
101. Mia MM, Bank RA. The pro-fibrotic properties of transforming growth factor on human fibroblasts are counteracted by caffeic acid by inhibiting myofibroblast formation and collagen synthesis. *Cell Tissue Res*. 2016;363:775–89.
102. Li Y, Kilani RT, Hartwell R, Ghahary A. MAP kinase mediates silica-induced fibrotic nodule formation and collagen accumulation in fibroblasts. *J. Cell. Physiol*. 2012;227:328–38.
103. Gibson UE, Heid CA, Williams PM. A novel method for real time quantitative RT-PCR. *Genome Res*. 1996;6:995–1001.
104. Nolan T, Hands RE, Bustin SA. Quantification of mRNA using real-time RT-PCR. *Nat. Protoc*. 2006;1:1559–82.
105. Schmittgen TD, Livak KJ. Analyzing real-time PCR data by the comparative CT method. *Nat. Protoc*. 2008;3:1101–8.
106. Chang C-M, Chang W-H, Wang C-H, Wang J-H, Mai JD, Lee G-B. Nucleic acid amplification using microfluidic systems. *Lab. Chip* 2013;13:1225–42.
107. Towbin H, Staehelin T, Gordon J. Electrophoretic transfer of proteins from polyacrylamide gels to nitrocellulose sheets: procedure and some applications. *Proc. Natl. Acad. Sci. U. S. A*. 1979;76:4350–4.
108. Liu X, Wang Y, Yang W, Guan Z, Yu W, Liao DJ. Protein multiplicity can lead to misconduct in western blotting and misinterpretation of immunohistochemical staining results, creating much conflicting data. *Prog. Histochem. Cytochem*. 2016;51:51–8.
109. Taylor SC, Posch A. The Design of a Quantitative Western Blot Experiment. *BioMed Res. Int.* 2014;2014:1–8.
110. Mattson DL, Bellehumeur TG. Comparison of three chemiluminescent horseradish peroxidase substrates for immunoblotting. *Anal. Biochem*. 1996;240:306–8.
111. Bio-Rad. Protein Blotting Guide. Available from: http://www.bio-rad.com/webroot/web/pdf/lsr/literature/Bulletin_2895.pdf
112. Smejkal G, Gallagher S. Determination of semidry protein transfer efficiency with transverse gradient gel electrophoresis. *BioTechniques* 1994;16:196–8, 200–2.
113. Pinheiro C, Roque R, Adriano A, Mendes P, Praça M, Reis I. Optimization of immunocytochemistry in cytology: comparison of two protocols for fixation and preservation on cytospin and smear preparations. *Cytopathology* 2015;26:38–43.
114. Glynn MW, McAllister AK. Immunocytochemistry and quantification of protein colocalization in cultured neurons. *Nat. Protoc*. 2006;1:1287–96.
115. Liu X, Wang Z, Wang R, Zhao F, Shi P, Jiang Y. Direct comparison of the potency of human mesenchymal stem cells derived from amnion tissue, bone marrow and adipose tissue at inducing dermal fibroblast responses to cutaneous wounds. *Int. J. Mol. Med*. 2013;31:407–15.

116. Maas-Szabowski N, Stark HJ, Fusenig NE. Keratinocyte growth regulation in defined organotypic cultures through IL-1-induced keratinocyte growth factor expression in resting fibroblasts. *J. Invest. Dermatol.* 2000;114:1075–84.

117. Hobro AJ, Smith NI. An evaluation of fixation methods: Spatial and compositional cellular changes observed by Raman imaging. *Vib. Spectrosc*. 2017;91:31–45.

118. Turoverova LV, Khotin MG, Yudintseva NM, Magnusson K-E, Blinova MI, Pinaev GP. Analysis of extracellular matrix proteins produced by cultured cells. *Cell Tissue Biol.* 2009;3:497–502.

119. McKay TB, Hjortdal J, Priyadarsini S, Karamichos D. Acute hypoxia influences collagen and matrix metalloproteinase expression by human keratoconus cells in vitro. *PLOS ONE* 2017;12:e0176017.

120. McKay TB, Lyon D, Sarker-Nag A, Priyadarsini S, Asara JM, Karamichos D. Quercetin Attenuates Lactate Production and Extracellular Matrix Secretion in Keratoconus. *Sci. Rep.* 2015

121. Romero-Calvo I, Ocón B, Martínez-Moya P, Suárez MD, Zarzuelo A, Martínez-Augustin O. Reversible Ponceau staining as a loading control alternative to actin in Western blots. *Anal. Biochem*. 2010;401:318–20.

122. Eaton SL, Roche SL, Llavero Hurtado M, Oldknow KJ, Farquharson C, Gillingwater TH. Total Protein Analysis as a Reliable Loading Control for Quantitative Fluorescent Western Blotting. *PLOS ONE* 2013;8:e72457.

123. Aldridge GM, Podrebarac DM, Greenough WT, Weiler IJ. The use of total protein stains as loading controls: an alternative to high-abundance single-protein controls in semi-quantitative immunoblotting. *J. Neurosci. Methods* 2008;172:250–4.

124. Negahdari S, Galehdari H, Kesmati M, Rezaie A, Shariati G, Sayfiabad Shapouri M. Analysis of VEGF AND TGFB1 proteins in normal and streptozotocin-induced diabetic rats, during treatment of formulations of Aloe Vera, Henna, Adiantum capillus-veneris, and Myrrha. *Wound Med*. 2017;16:22–8.

125. Frank S, Hübner G, Breier G, Longaker MT, Greenhalgh DG, Werner S. Regulation of vascular endothelial growth factor expression in cultured keratinocytes. Implications for normal and impaired wound healing. *J. Biol. Chem.* 1995;270:12607–13.

126. Yan X, Chen B, Lin Y, Li Y, Xiao Z, Hou X. Acceleration of diabetic wound healing by collagen-binding vascular endothelial growth factor in diabetic rat model. *Diabetes Res. Clin. Pract*. 2010;90:66–72.

127. Wilgus TA, Matthies AM, Radek KA, Dovi JV, Burns AL, Shankar R. Novel Function for Vascular Endothelial Growth Factor Receptor-1 on Epidermal Keratinocytes. *Am. J. Pathol.* 2005;167:1257–66.

128. Kubow KE, Vukmirovic R, Zhe L, Klotzsch E, Smith ML, Gourdon D. Mechanical forces regulate the interactions of fibronectin and collagen I in extracellular matrix. *Nat. Commun*. 2015

129. Rozario T, Dzamba B, Weber GF, Davidson LA, DeSimone DW. The Physical State of Fibronectin Matrix Differentially Regulates Morphogenetic Movements In Vivo. *Dev. Biol*. 2009;327:386–98.

130. Cao Y-L, Duan Y, Zhu L-X, Zhan Y-N, Min S-X, Jin A-M. TGF-β1, in association with the increased expression of connective tissue growth factor, induce the hypertrophy of the ligamentum flavum through the p38 MAPK pathway. *Int. J. Mol. Med.* 2016;38:391–8.

131. Yang Z, Sun Z, Liu H, Ren Y, Shao D, Zhang W. Connective tissue growth factor stimulates the proliferation, migration and differentiation of lung fibroblasts during paraquat-induced pulmonary fibrosis. *Mol. Med. Rep.* 2015;12:1091–7.

132. Park HJ, Cho DH, Kim HJ, Lee JY, Cho BK, Bang SI. Collagen Synthesis Is Suppressed in Dermal Fibroblasts by the Human Antimicrobial Peptide LL-37. J. *Invest. Dermatol.* 2009;129:843–50.

133. Song Y, Zhu L, Li M. Antifibrotic effects of crocetin in scleroderma fibroblasts and in bleomycin-induced sclerotic mice. *Clinics* 2013;68:1350–7.

134. Fang C-L, Huang L-H, Tsai H-Y, Chang H-I. Dermal Lipogenesis Inhibits Adiponectin Production in Human Dermal Fibroblasts while Exogenous Adiponectin Administration Prevents against UVA-Induced Dermal Matrix Degradation in Human Skin. *Int. J. Mol. Sci.* 2016;17:1129.

135. Harrington H, Cato P, Salazar F, Wilkinson M, Knox A, Haycock JW. Immunocompetent 3D Model of Human Upper Airway for Disease Modeling and In Vitro Drug Evaluation. *Mol. Pharm.* 2014;11:2082–91.